Title

SYNTHESIS AND CHARACTERIZATION OF (PENTAMErrHYLCYCLOPENTADIENYL) IRIDIUM POLYHYDRIDE AND POLYPHOSPHINE COMPLEXES

Author

Gilbert, T.M.

Publication Date

1985-07-01

Lawrence Berkeley Laboratory
UNIVERSITY OF CALIFORNIA

Materials & Molecular Research Division

SYNTHESIS AND CHARACTERIZATION OF (PENTAMETHYLCYCLOPENTADIENYL)IRIDIUM POLYHYDRIDE AND POLYPHOSPHINE COMPLEXES

T.M. Gilbert
(Ph.D. Thesis)

July 1985

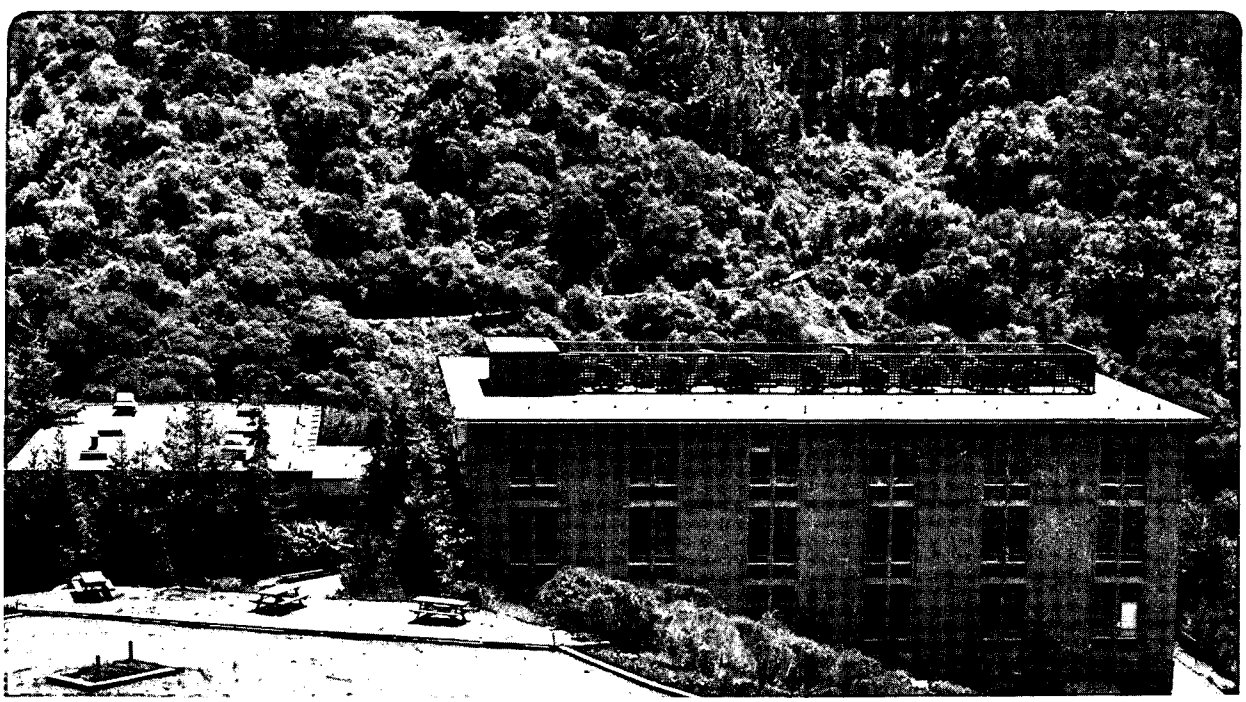

Prepared for the U.S. Department of Energy under Contract DE-AC03-76SF00098

DISCLAIMER

LBL-22535

Synthesis and Characterization of (Pentamethylcyclopentadienyl)iridium Polyhydride and Polyphosphine Complexes

Thomas M. Gilbert
(Ph.D. Thesis)

July 1985

Department of Chemistry
University of California
Berkeley, California 94720

and

Lawrence Berkeley Laboratory
Berkeley, California 94720

Synthesis and Characterization of (Pentamethylcyclopentadienyl)iridium Polyhydride and Polyphosphine Complexes

Thomas M. Gilbert

Abstract

Chapter 1. Trimethylphosphine reacts with $[(C_5(CH_3)_5)Ir]_2(\mu\text{-}H)_3PF_6$ producing $[(C_5(CH_3)_5)Ir(P(CH_3)_3)(H)]_2(\mu\text{-}H)PF_6$. $LiEt_3BH$ reduction of this dimer yields two equiv of $(C_5(CH_3)_5)Ir(P(CH_3)_3)H_2$.

Protonation of the dihydride with $HBF_4 \cdot OEt_2$ gives $(C_5(CH_3)_5)Ir(P(CH_3)_3)H_3BF_4$, the first isolated cationic iridium (V) complex. Low temperature ^1H NMR studies reveal a surprisingly large H-H coupling constant.

Deprotonation of the dihydride with t-BuLi affords "$(C_5(CH_3)_5)Ir(P(CH_3)_3)HLi$"; subsequent alkylation provides hydrido-(alkyl)iridium complexes $(C_5(CH_3)_5)Ir(P(CH_3)_3)(R)(H)$ in good yield.

Chapter 2. A series of (poly-trimethylphosphine)iridium complexes is reported. The coupling constants J_{PC}, $J_{P'C}$ and $J_{PP'}$ were determined for eighteen (poly-trimethylphosphine)rhenium, ruthenium and iridium compounds. The coupling values vary markedly from metal to metal, but are not affected significantly by the nature of the other ligands present.

Chapter 3. The novel iridium (V) complex $(C_5(CH_3)_5)IrH_4$ produces $(C_5(CH_3)_5)Ir(P(CH_3)_3)H_2$ on irradiation in the presence of $P(CH_3)_3$, affords $C_5(CH_3)_5$-substituted chloro- and hydrido-

(chloro)iridium dimers on treatment with CCl_4, and gives sequentially $(C_5(CH_3)_5)Ir(CO)H_2$ and $(C_5(CH_3)_5)Ir(CO)_2$ with CO. The tetrahydride undergoes thermal and photochemical H/D exchange in the presence of D_2 gas and deuteron-induced H/D exchange with CD_3OD.

Chapter 4. Treatment of $[(C_5(CH_3)_5)Ir]_2(\mu\text{-}H)_3PF_6$ with $LiBH_4$ yields $[(C_5(CH_3)_5)Ir]_2H_3BH_4$; the borohydride moiety bridges the metal centers in a unique fashion. Hydrolysis of this complex produces the formally iridium (IV) dimer $[(C_5(CH_3)_5)IrH_3]_2$.

Treatment of $[(C_5(CH_3)_5)Ir]_2(\mu\text{-}H)_3PF_6$ with the reducing agent $LiEt_3BH$ affords the mononuclear salt $(C_5(CH_3)_5)IrH_3[Li(THF)_x]$, which may be hydrolyzed to the iridium (V) complex $(C_5(CH_3)_5)IrH_4$. The overall mechanism of formation of the tetrahydride is discussed.

Deprotonation of $(C_5(CH_3)_5)IrH_4$ with t-BuLi/pmdeta yields $(C_5(CH_3)_5)IrH_3[Li(pmdeta)]$. The anion may be derivatized affording the new polyhydrides $(C_5(CH_3)_5)IrH_3SiMe_3$, $(C_5(CH_3)_5)IrH_3SnMe_3$, $(C_5(CH_3)_5)IrH_3SnPh_3$ and $(C_5(CH_3)_5)IrH_3((C_5H_5)_2ZrCl)$.

Chapter 5. The upfield hydride resonances in the ^1H NMR spectra of $(C_5(CH_3)_5)IrH_2Si(CH_3)_3Li(pmdeta)$ and $(C_5(CH_3)_5)IrH_3Li(pmdeta)$ appear as 1:1:1:1 quartets due to ^7Li-^1H coupling. This was confirmed by $^1H\{^7Li\}$, ^7Li, and $^7Li\{^1H\}$ NMR experiments. Variable temperature NMR studies of the quartet feature are described.

This thesis is joyfully dedicated to six people:

Carmen and Steve,

Betty Anne and Barrie,

and

My Mom and Dad.

There must be something about couples.

Acknowledgments.

I certainly wish to thank Bob Bergman, who probably spent a long time wishing I'd stayed on my original C-H activation project instead of getting involved in the less dramatic world of polyhydrides. To his credit, Bob never expressed the opinion that perhaps I should rein in a bit; he was continually willing to let me chase leprechauns and work in areas in which neither of us had any expertise. I shall always be grateful for that.

I also appreciate the contributions of the past and present members of the Bergman, Muetterties, Andersen and Streitweiser groups. A few special people stand out: Linda Newman, whose friendship helped during difficult times; Steve McKenna, whose knowledge astounds me (even if he is a Red Sox fan) and who was willing to teach me about DYNAMAR, the AM-500 NMR spectrometer and ORTEP, even if it meant staying up all night (it often did); and Mike Heinekey, who provided intelligence and perspective. I also want to thank, in no particular order, Mike Buchanan, Jeff Stryker, Mark Seidler, Tim Wenzel, Jeff Hayes, Bill McGhee, Bob Price, Mike Krause, Al DelPaggio, Steve Fine, E. J. Wucherer, Ron Wexler, Matt Kulzick, Carol Burns, Joanne Stewart, Dave Berg, Steve Stults, all the Dux on the Pond, and the Friday afternoon hoopsters. They made the bad times easier and the good times better.

May Gill probably made the largest contribution to my development by being kind enough to teach me Wordstar and to add Greek lettering to anything that needed it. For her kindness, and extraordinary secretarial skill, she gets her own paragraph.

Thanks are due to Drs. Andy Janowicz and Carol Kovac for their assistance in the preparation and characterization of $(C_5(CH_3)_5)Ir(P(CH_3)_3)_2ClPF_6$, to Dr. John Bercaw for a revealing discussion regarding $(C_5(CH_3)_5)Ir(P(CH_3)_3)H_3BF_4$, to Dr. Alex Pines for help with NMR coupling constants, to Steve McKenna for setting up the line shape analysis program DYNAMAR, to Dr. Gerhard Binsch for providing a copy of ACTPAR, to Dr. Richard Andersen for helpful discussions regarding $[(C_5(CH_3)_5)Ir]_2H_3BH_4$, and to Drs. William A. G. Graham and Peter Maitlis for discussions regarding $(C_5(CH_3)_5)IrH_4$. The interest of Dr. Earl Muetterties in early parts of this work is gratefully acknowledged.

This work was continually simplified by the incredibly talented people toiling in the shops and labs. I thank Dr. Fred Hollander for his patience as I struggled with single crystal X-ray diffraction, Rudi Nunlist and Rich Mazzarisi for letting me put the NMR spectrometers through arctic temperatures and weird nuclei, Leah Zebre, Arnie Falick, and Sherri Ogden in the UCB Mass Spectrometry Facility for letting me destroy a series of sources with iridium polyhydride goop, and Cathy Sigler in the glass shop for always sneaking my work in ahead of everyone else's.

Significant financial support of this work was provided by the Director, Office of Energy Research, Office of Basic Energy Sciences, Chemical Sciences Division of the U. S. Department of Energy under Contract DE-AC03-76SF00098. I have it on good authority that this man is four feet eight inches tall and seeks to compensate with long job titles.

Contents

Chapter 1. Trimethylphosphine-Substituted (Pentamethylcyclopentadienyl)iridium Complexes; Protonation and Deprotonation of $(C_5(CH_3)_5)Ir(P(CH_3)_3)H_2$.

Introduction

Strongly electron donating ligands promote a large range of interesting chemical transformations at transition metal centers.[1] Two donating ligands which have been prominent in recent efforts of this type are trimethylphosphine,[2-4] characterized by relatively small steric bulk,[5] and the much more sterically demanding pentamethylcyclopentadienyl group.[6-8] Both ligands have allowed the development of chemistry not accessible to complexes containing more commonly used ligands such as triphenylphosphine or the cyclopentadienyl (C_5H_5) group. Maitlis and coworkers, in particular, have extensively developed the chemistry of pentamethylcyclopentadienylrhodium and iridium compounds, aspects of which may be found in recent reviews.[9,10]

In 1982, workers from our laboratory reported[11] the insertion of a photogenerated trimethylphosphine(pentamethylcyclopentadienyl)-iridium (I) intermediate into the carbon-hydrogen bonds of various organic compounds, including the simple alkanes cyclohexane and neopentane, producing stable hydrido(alkyl)iridium complexes. Motivated by these results, we attempted to synthesize new trimethylphosphine(pentamethylcyclopentadienyl)iridium hydride species, with an eye toward preparing complexes of varied formal oxidation state of iridium. We report the synthesis of several such compounds, including $(C_5(CH_3)_5)Ir(P(CH_3)_3)H_3BF_4$, **5**, the first isolated example of a cation containing iridium in the formal +5 oxidation state, and "$(C_5(CH_3)_5)Ir(P(CH_3)_3)HLi$", **6**, which allows the high yield preparation of numerous hydrido(alkyl)iridium complexes.

Experimental

General. Unless otherwise noted, all reactions and manipulations were performed in dried glassware under inert atmosphere using either standard Schlenk techniques or a nitrogen-filled Vacuum Atmospheres 553-2 drybox equipped with a MO-40-1 inert gas purifier. Reagent THF, benzene, toluene, and diethyl ether were distilled from Na/benzophenone under nitrogen. Acetone was distilled from anhydrous $CaSO_4$/4 Å molecular sieves. Spectral grade hexane and pentane were distilled from $LiAlH_4$; dichloromethane was distilled from CaH_2. Chloroform was distilled from Na/Pb alloy (Dri-Na) onto 4 Å molecular sieves and purged with nitrogen before use. Methanol was vacuum distilled from $Mg(OMe)_2$. $LiEt_3BH$ (Super-Hydride, 1 M in THF), $HBF_4 \cdot OEt_2$, and t-BuLi (1.7-1.9 M in pentane) were obtained from Aldrich and stored in the drybox at appropriate temperatures. $P(CH_3)_3$ (Strem Chemical) was vacuum transferred from sodium and handled using known volume bulb techniques. N,N,N',N'',N''-pentamethyldiethylenetriamine (pmdeta, Alfa) was distilled in vacuo from sodium and stored on 4 Å molecular sieves in the drybox. Alkyl trifluoromethylsulfonates (triflates) were prepared by methods described in a review,[12] distilled under vacuum, and confirmed as pure by ^1H and $^{13}C\{^1H\}$ NMR spectroscopies. All other reagents were purified in an appropriate fashion or were used as received from suppliers.

^1H, ^{13}C, ^{19}F, and ^{31}P NMR spectra were recorded on the 180, 200, 250, 300 and 500 MHz instruments at the UCB NMR facility, and are reported as ppm downfield of TMS (^1H, ^{13}C), $CFCl_3$ in $CDCl_3$ (^{19}F), or

85% H_3PO_4 (^{31}P). Elemental analyses were performed by V. Tashinian at the UCB Microanalysis Facility. IR spectra were recorded either on a Perkin Elmer 283 Spectrometer or on a Perkin-Elmer 1550 Fourier Transform Infrared Spectrometer. Mass spectra were recorded at the UCB Mass Spectrometry Facility under the conditions noted. Melting points and decomposition ranges were determined in sealed nitrogen-filled capillaries on a Thomas UniMelt apparatus and are uncorrected.

$[(C_5(CH_3)_5)Ir]_2(\mu\text{-}H)_3PF_6$, (1·$PF_6$). The method of Maitlis[13] was used with slight modification. A slurry of $[(C_5(CH_3)_5)IrCl_2]_2$[6] (10.38 g, 13.0 mmol) in 2:2:1 isopropanol/acetone/water (750 mL) was warmed to 40 °C as H_2 was bubbled through the solution. The orange slurry became a black, homogeneous solution over 3 to 5 h; fresh solvent was added periodically to replace evaporation losses. After 24 h, the solution was cooled to room temperature, and approximately half the solvent removed on a rotary evaporator. Addition of an aqueous solution of NH_4PF_6 (5.0 g, 27 mmol) resulted in the immediate precipitation of air-stable yellow powder, which was filtered, washed with water, recrystallized from $CHCl_3$/octane and dried in a vacuum desiccator to give 8.44 g (10.5 mmol, 80%) of bright yellow **1·PF_6**. The ^1H NMR spectrum of this material agrees with that reported by Maitlis; we have collected the following additional data on this compound: $^{13}C\{^1H\}$ NMR (CD_2Cl_2): δ 94.4 (s, $\underline{C}_5Me_5$); 11.2 (s, $C_5\underline{Me}_5$).

1·BF_4 was prepared in the same manner using $NaBF_4$ in 80% yield. Anal. Calcd for $C_{20}H_{33}IrBF_4$: C, 32.25; H, 4.47; Cl, 0. Found: C, 32.48; H, 4.53; Cl, 0.55.

$[(C_5(CH_3)_5)Ir(P(CH_3)_3)(H)]_2(\mu\text{-}H)PF_6$, (2·$PF_6$). $P(CH_3)_3$ (0.700 mmol) was expanded into a known volume bulb at room temperature and condensed into a degassed acetonitrile solution of **1·PF_6** (245 mg, 0.305 mmol) at liquid nitrogen temperature. The solution was warmed to room temperature and stirred two days. Removal of solvent in vacuo gave an orange-yellow solid, which was recrystallized from acetone/ether yielding 249 mg (0.261 mmol, 86%) of air-stable yellow crystals. A crystal of **2·PF_6** suitable for X-ray diffraction study was grown from saturated THF solution.[14]

^1H NMR (CD_2Cl_2, 60 °C): δ 2.06 (d, J_{PH}=1.5, 30H, C_5Me_5); 1.66 (d, J_{PH}=10.2, 18H, PMe_3); -20.49 (t, J_{PH}=18.3, 3H, Ir-H). ^1H NMR (CD_2Cl_2, -80 °C): δ 1.95 (d, J_{PH}=1.2, 30H, C_5Me_5); 1.52 (d, J_{PH}=10.2, 18H, PMe_3); -19.16 (dd, J_{PH}=33.2, J_{HH}=5.4, 2H, Ir-H_t); -23.02 (tt, J_{PH}=20.9, J_{HH}=5.4, 1H, Ir-H_{bridg}). $^{13}C\{^1H\}$ NMR (CD_3CN): δ 95.72 (s, $\underline{C}_5Me_5$); 21.74 (d, J_{PC}=40.8, PMe_3); 11.57 (s, $C_5\underline{Me}_5$). $^{31}P\{^1H\}$ NMR (CD_2Cl_2): δ -47.03 (s, PMe_3); -144.03 (septet, J_{PF}=710, PF_6). IR (KBr): ν_{Ir-H} 2165 cm^{-1}; (CH_2Cl_2) 2170 cm^{-1}. Anal. Calcd for $C_{26}H_{51}P_3IrF_6$: C, 32.70; H, 5.38; P, 9.73. Found: C, 32.61; H, 4.85; P, 9.38.

The BF_4 salt, **2·BF_4**, was prepared from **1·BF_4** in 85% yield. $^{31}P\{^1H\}$ NMR (CD_2Cl_2): δ -46.92 (s). FAB MS (1:1 glycerol/thioglycerol): m/e 875/873 (M^+-F); 811/809 (M^+-BF_4). Anal. Calcd for $C_{26}H_{51}P_2IrBF_4$: C, 34.82; H, 5.73. Found: C, 34.92; H, 5.97. Solid state decomposition temperature: 230-240 °C.

Reaction of $2\cdot PF_6$ with $LiEt_3BH$. $2\cdot PF_6$ (46 mg, 0.048 mmol) was slurried in THF and treated with $LiEt_3BH$ (0.050 mmol). The yellow solution slowly decolorized over 24 h of stirring. Removal of solvent and workup of the residue as described previously[11b] gave 31 mg (0.076 mmol, 80%) of $(C_5(CH_3)_5)Ir(P(CH_3)_3)H_2$, 4, shown to be pure by ^1H NMR spectroscopy.

$(C_5(CH_3)_5)Ir(P(CH_3)_3)H_3BF_4$, (5). Treatment of $HBF_4\cdot OEt_2$ (0.700 mmol in 30 mL ether) with an ethereal solution of $(C_5(CH_3)_5)Ir(P(CH_3)_3)H_2$ (240 mg, 0.592 mmol) at -78 °C resulted in the precipitation of air-sensitive, off-white powder (274 mg, 0.555 mmol, 94%), which was filtered, washed with ether and dried under nitrogen. ^1H NMR (CD_2Cl_2, RT): δ 2.28 (d, J_{PH}=1.6, 15H, C_5Me_5); 1.82 (d, J_{PH}=11.8, 9H, PMe_3); -13.51 (d, J_{PH}=10.0, 3H, Ir-H). ^1H NMR (CD_2Cl_2, -90 °C, 500 MHz): δ 2.18 (br s, 15H, C_5Me_5); 1.73 (d, J_{PH}=11.8, 9H, PMe_3); -12.71 (dt, $|J_{PH}|$=12.6, J_{HH}=56.3, 1H, Ir-H_{tr}); -14.12 (dd, $|J_{PH}|$=21.4, J_{HH}=56.3, 2H, Ir-H_{cis}). $^{13}C\{^1H\}$ NMR (CD_2Cl_2): δ 103.0 (s, $\underline{C}_5Me_5$); 21.7 (d, J_{PC}=47.0, PMe_3); 10.49 (s, $C_5\underline{Me}_5$). ^{19}F NMR (CD_2Cl_2): δ -153.15 (s). $^{31}P\{^1H\}$ NMR (CD_2Cl_2): δ -37.8 (s). IR(KBr): ν_{Ir-H} 2140 (sh), 2090 (vs), 2065 (sh) cm^{-1}. FAB MS (tetraglyme): m/e 407/405 (M^+). Anal. Calcd for $C_{13}H_{27}IrBF_4$: C, 31.65; H, 5.52. Found: C, 31.55; H, 5.49.

"$(C_5(CH_3)_5)Ir(P(CH_3)_3)HLi$", (6). t-Butyl lithium (0.350 mmol) was added dropwise to a solution of dihydride 4 (126 mg, 0.310 mmol) in pentane (1 mL) at -40 °C. The reaction was allowed to proceed at this temperature for 24 h, at which time the precipitated yellow solid was filtered and dried to give 58 mg (0.14 mmol, 45%) of

material.

The NMR spectra of this material demonstrate the presence of two products, possibly different oligomers, in a 9:1 ratio. However, the analytical data as well as the derivative chemistry of this material (see below) indicate the empirical formula to be $[(C_5(CH_3)_5)Ir(P(CH_3)_3)HLi]_x$. ^1H NMR (C_6D_6): δ 2.35 (very br s, C_5Me_5 of major product); 2.23 (s, C_5Me_5 of minor product); 1.82 (br, PMe_3 of major product); 1.69 (d, J_{PH}=8.4, PMe_3 of minor product); -18.3 (very br, Ir-H). $^{31}P\{^1H\}$ NMR (C_6D_6): δ -57.6 (s, minor product); -58.9 (br s, major product). IR (silicone oil): ν_{Ir-H} 1980 cm^{-1} (br). Anal. Calcd for $C_{13}H_{25}PIrLi$: C, 37.95; H, 6.12. Found: C, 38.34; H, 6.21.

$(C_5(CH_3)_5)Ir(P(CH_3)_3)H[Li(pmdeta)_x]$, [6·$(pmdeta)_x$]. A pentane solution of dihydride **4** (379 mg, 0.935 mmol) and pmdeta (200 mg, 1.15 mmol) was cooled to -40 °C, then treated dropwise with t-BuLi (1.4 mmol) while warming slowly to ambient temperature. A yellow precipitate was observed to form as the solution stirred for 16 h. After cooling to -40 °C, the pale yellow solid was filtered and washed with pentane to give an air-sensitive powder as product (338 mg). Elemental analyses of the product demonstrated the amount of pmdeta present to vary from run to run, with values of x between 0.5 and 0.05. The product in all cases proved insoluble in inert solvents, and in general was characterized by further reaction, as described below. IR (silicone oil): ν_{Ir-H} 1950 (br) cm^{-1}.

In order to chemically characterize this material, a pentane slurry of **[6·$(pmdeta)_x$]** (9.3 mg, x ~ 0.5 by elemental analysis) was

treated with excess MeOD (50 μL). Immediate evaporation of solvent gave pmdeta and $(C_5(CH_3)_5)Ir(P(CH_3)_3)(H)(D)$, the monodeuterated analogue of **4** (0.0134 mmol by integration vs. internal $(Me_3Si)_2O$, 56% based on **4**). ^1H NMR (C_6D_6): δ 2.11 (d, J_{PH}=1.6, 15H, C_5Me_5); 1.32 (d, J_{PH}=9.8, 9H, PMe_3); -17.43 (d, J_{PH}=32.1, 1H, Ir-H). ^2H NMR (C_6H_6): δ -17.22 (d, J_{PD}=5.4, Ir-D).

$(C_5(CH_3)_5)Ir(P(CH_3)_3)(CH_3)(H)$. A solution/slurry of **6** was prepared by the dropwise addition of t-BuLi (0.300 mmol) to a pentane solution of dihydride **4** (103 mg, 0.254 mmol). The reagent was stirred for 24 h at ambient temperature, then added dropwise over 10 min to a pentane solution of $CH_3O_3SCF_3$ (51 mg, 0.31 mmol) at 0 °C with external light excluded by wrapping the reaction flask with aluminum foil, giving a pale yellow solution and a dark precipitate. After stirring 1 h at this temperature, the solvent was evaporated and the residue taken up in pentane. The pentane solution was filtered through celite packed in a frit into a foiled-wrapped flask, whereupon the solvent was evaporated to give a pale yellow oil (83 mg). Integration of the resonances in the ^1H NMR spectrum demonstrated the material to be 81% hydrido(methyl) complex, 14% dihydride **4**, and 5% $(C_5(CH_3)_5)Ir(P(CH_3)_3)(CH_3)_2$.[15] Complete purification of the material has been reported.[15]

^1H NMR (C_6D_6): δ 1.87 (d, J_{PH}=1.5, 15H, C_5Me_5); 1.22 (d, J_{PH}=10.0, 9H, PMe_3); 0.70 (d, J_{PH}=6.0, 3H, Ir-CH_3); -17.23 (d, J_{PH}=37.9, 1H, Ir-H). ^{13}C NMR (C_6D_6): δ 91.1 (d, J_{PC}=3.9, $\underline{C}_5Me_5$); 19.0 (dq, J_{PC}=36.3, J_{CH}=127.3, PMe_3); 10.1 (q, J_{CH}=126.3, $C_5\underline{Me}_5$); 1.38 (q, J_{CH}=117.7, Ir-CH_3). $^{31}P\{^1H\}$ NMR (C_6D_6): δ -43.7 (s).

$(C_5(CH_3)_5)Ir(P(CH_3)_3)(CH_2CH_3)H$. A solution/slurry of **6** was prepared by the dropwise addition of t-BuLi (0.300 mmol) to dihydride **4** (108 mg, 0.266 mmol) in pentane (1 mL) at -40 °C. The reaction was allowed to proceed for 24 h, at which time the solution/slurry was added dropwise to neat ethyl triflate (0.600 mmol) at -40 °C. After 4 h, the solvent was evaporated to give a yellow-white solid. This was extracted with pentane; the extracts were then filtered through celite. The solvent was evaporated to give an orange oil, which was combined with another batch of product prepared similarly from dihydride **4** (0.266 mmol).

The material was chromatographed on alumina III under air-free conditions at -50 ± 10 °C. A pale yellow band eluted with 5% Et_2O/hexane; evaporation of the solvent from this fraction gave the pure hydrido(ethyl)iridium complex as a yellow oil (71 mg, 0.17 mmol, 32%). ^1H NMR (C_6D_6): δ 1.88 (d, J_{PH}=1.4, 15H, C_5Me_5); 1.76 (complex, overlapping, 5H, Ir-CH_2CH_3); 1.24 (d, J_{PH}=9.6, 9H, PMe_3); -17.90 (d, J_{PH}=37.2, 1H, Ir-H). $^{13}C\{^1H\}$ NMR (C_6D_6): δ 91.4 (d, J_{PC}=3.0, $\underline{C}_5Me_5$); 25.2 (s, Ir-$CH_2\underline{C}H_3$); 18.9 (d, J_{PC}=36.4, PMe_3); 10.0 (s, $C_5\underline{Me}_5$); -21.3 (d, J_{PC}=7.7, Ir-$\underline{C}H_2CH_3$). $^{31}P\{^1H\}$ NMR (C_6D_6): δ -43.0 (s). IR (neat oil): ν_{Ir-H} 2095 cm^{-1}. EIMS (50 °C, 70 eV): m/e 434, 432. Anal. Calcd for $C_{15}H_{30}IrP$: C, 41.55; H, 6.97. Found: C, 41.97; H, 7.12.

Further elution of the chromatography column with 20% Et_2O/hexane gave a colorless fraction; evaporation of the solvent gave a colorless oil (20 mg), shown to be mostly dihydride **4** by ^1H NMR spectroscopy.

$(C_5(CH_3)_5)Ir(P(CH_3)_3)(CH_2CH_2CH_2CH_2CH_3)(H)$. A solution/slurry of **6** was prepared by the dropwise addition of t-BuLi (0.250 mmol) to a pentane solution of dihydride **4** (97 mg, 0.24 mmol). After stirring 20 h at ambient temperature, the reagent was added dropwise over 20 min to a pentane solution of n-pentyl triflate (55 mg, 0.25 mmol). The solution became cloudy and darkened to orange during the addition; stirring was continued for 22 h. The solvent was evaporated, and the orange residue extracted with pentane. The extracts were filtered through celite, whereupon evaporation of the solvent gave a yellow-white semisolid.

The semisolid was chromatographed on neutral alumina III at a column temperature of -55 ± 10 °C. A pale yellow band eluted with 5% Et_2O/hexane; evaporation of the solvent from this fraction gave the hydrido(n-pentyl)iridium complex as a yellow-white semisolid (61 mg, 0.14 mmol, 54%). This material was shown to be pure by ^1H NMR spectroscopy, and was spectroscopically identical to a sample isolated and fully characterized in C-H activation studies.[11,19d] Further elution of the column with 10% Et_2O/hexane gave a colorless fraction; evaporation of solvent gave a colorless semisolid (10 mg). Inspection of the ^1H NMR spectrum showed the major component of this fraction to be dihydride **4**.

$(C_5(CH_3)_5)Ir(P(CH_3)_3)(CH_2C(CH_3)_3)(H)$. A solution/slurry of **6** was prepared by the dropwise addition of t-BuLi (0.300 mmol) to a pentane solution of dihydride **4** (100 mg, 0.247 mmol). After stirring 24 h at ambient temperature, the reagent was added dropwise over 30 min to a pentane solution of neopentyl triflate (66 mg, 0.30 mmol) at

-78 °C. The resulting yellow solution was stirred 2 h at this temperature, then slowly warmed to room temperature. Evaporation of solvent gave a yellow-white solid, which was extracted with pentane. The pentane extracts were filtered through celite, whereupon evaporation of the solvent gave yellow-white semisolid.

This material was combined with another batch of product prepared similarly from dihydride **4** (0.200 mmol). Chromatography on neutral alumina III at -55 ± 10 °C, eluting with 5% Et_2O/hexane gave a pale yellow solution, from which the solvent was evaporated to give the hydrido(neopentyl)iridium complex (44 mg, 0.093 mmol, 21%), as a white semisolid. This material was shown to be pure by ^1H NMR spectroscopy, and was identical to a sample isolated and fully characterized in C-H activation studies.[11,19d] Further elution of the chromatography column with 20% Et_2O/hexane gave a pale yellow solution, from which evaporation of solvent gave dihydride **4** (35 mg).

$(C_5(CH_3)_5)Ir(P(CH_3)_3)(Si(CH_3)_3)(H)$. A concentrated solution/slurry of **6** was prepared by the dropwise addition of t-BuLi (0.380 mmol) to a solution of dihydride **4** (107 mg, 0.264 mmol) in 1 mL pentane at -40 °C. The solution/slurry was maintained at this temperature for 24 h, then added dropwise to neat $(CH_3)_3SiO_3SCF_3$ (0.575 g, 2.59 mmol) at -40 °C. After 3 h at this temperature, the solvent and excess triflate were evaporated to give a white solid. The solid was extracted with pentane, and the extracts filtered through celite. Evaporation of solvent gave the white, air-sensitive hydrido(trimethylsilyl)iridium complex (95 mg, 0.20 mmol, 75%), which was dried under high vacuum overnight. This method gave material

sufficiently pure for elemental analysis and further study; the complex may be recrystallized from pentane/$(Me_3Si)_2O$, but recovery of material is low. ^1H NMR (C_6D_6): δ 1.89 (d, J_{PH}=1.1, 15H, C_5Me_5); 1.29 (d, J_{PH}=9.6, 9H, PMe_3); 0.67 (s, 9H, $SiMe_3$); -18.50 (d, J_{PH}=28.4, 1H, Ir-H). $^{13}C\{^1H\}$ NMR (C_6D_6): δ 94.3 (s, $\underline{C}_5Me_5$); 23.2 (d, J_{PC}=39.3, PMe_3); 11.2 (s, $C_5\underline{Me}_5$); 9.6 (s, $SiMe_3$). $^{31}P\{^1H\}$ NMR (C_6D_6): δ -50.3 (s). IR (C_6H_6): ν_{Ir-H} 2115 cm^{-1}. Exact Ion MS: Calcd 478.1796, 476.1779. Found 478.1803, 476.1762. Anal. Calcd for $C_{16}H_{34}IrPSi$: C, 40.23; H, 7.17. Found: C, 40.04; H, 7.44.

Results and Discussion

Synthesis and Characterization of $[(C_5(CH_3)_5)Ir(P(CH_3)_3)(H)]_2(\mu\text{-}H)A$

Treatment of an acetone solution of trihydride $[(C_5(CH_3)_5)Ir]_2(\mu\text{-}H)_3A$ (A = PF_6 or BF_4), **1**, with $P(CH_3)_3$ rapidly yields the bisphosphine dimer $[(C_5(CH_3)_5)Ir(P(CH_3)_3)(H)]_2(\mu\text{-}H)A$, **2** (Scheme 1). The yellow salt crystallizes in analytical purity from acetone/ether, or, in the case of **2**·PF_6, from hot THF. Isolated yields are typically 85%, and air has no effect on solutions of the pure compound. Interestingly, use of less than two equivalents of phosphine yields a mixture of **2** and unchanged **1**; no complex containing only one phosphine ligand proved isolable. We suspect that the monophosphine complex reacts more quickly with $P(CH_3)_3$ than **1** does, and thus this intermediate never builds up during the reaction.

While the alkyl region of the ^1H NMR spectrum of **2** varies little with temperature, the hydride region shows dynamic behavior over a fairly large temperature range. At 60 °C, the hydride signal (δ -20.5) appears as an apparent binomial triplet, with J_{PH} = 18.3 Hz, a somewhat low value compared to J_{PH} = 32 Hz observed for $(C_5(CH_3)_5)Ir(P(CH_3)_3)H_2$.[11b] The coupling constant represents an average of three static ^{31}P-^1H coupling constants (see below).

At room temperature (23 °C), the resonance broadens to a structureless lump just above the baseline. Upon cooling the sample to -80 °C, two well-resolved patterns are observed, a downfield doublet of doublets (δ -19.2) integrating as two equivalent hydrogens and an upfield triplet of triplets (δ -23.0) integrating as one

Scheme I

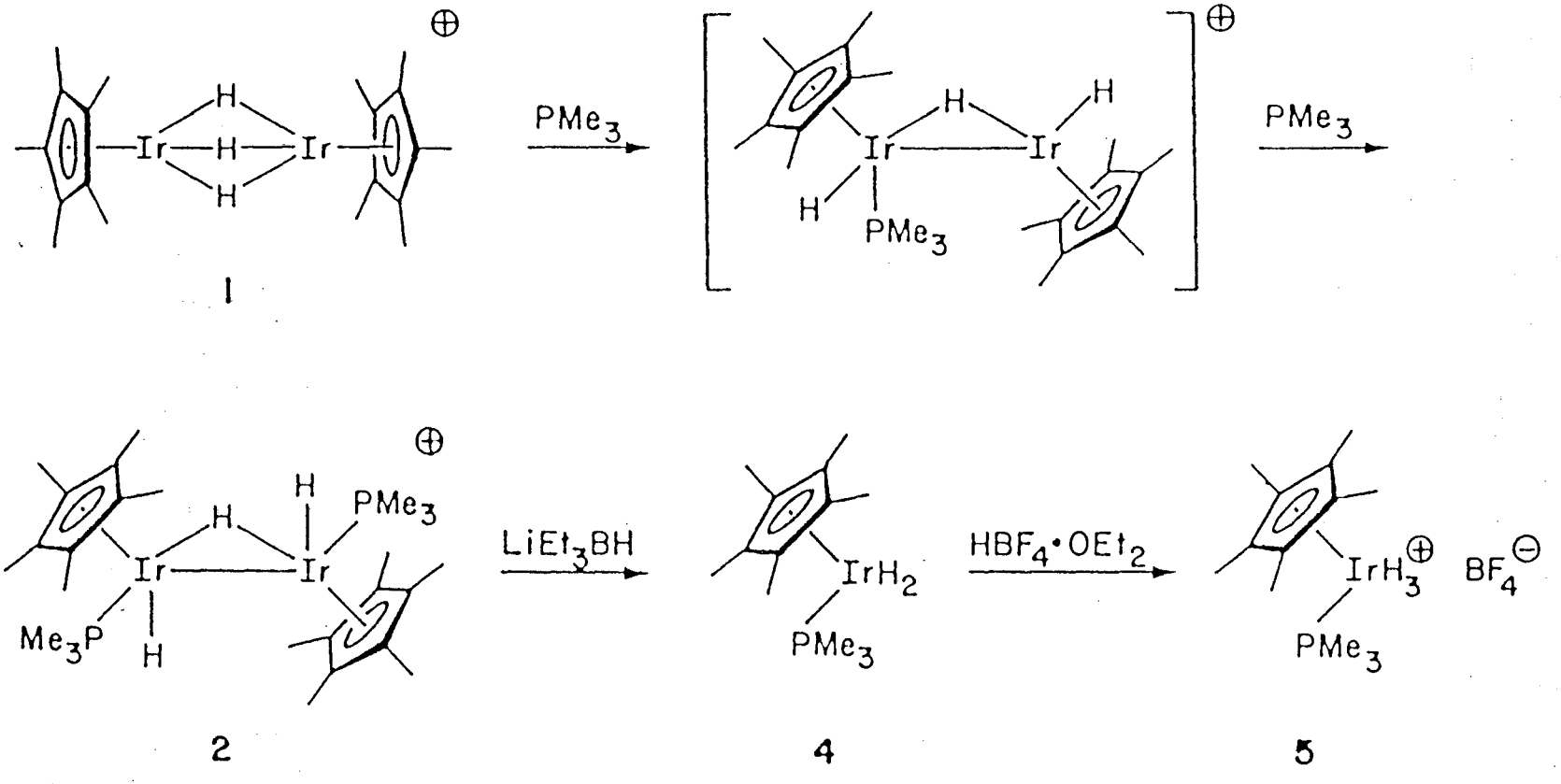

1 2 4 5

hydrogen. A $^{1}H\{^{31}P\}$ NMR experiment demonstrated the largest coupling in each case to be due to the phosphorus in the phosphine ligand, with a larger $^{31}P-^{1}H$ coupling (33.2 Hz) observed for the downfield peak and a smaller coupling (20.9 Hz) for the upfield peak. The three-bond $^{31}P-^{1}H$ coupling of a terminal hydrogen attached to one iridium center to the phosphorus attached to the other iridium center could not be resolved, and we therefore assume the value of this $J_{PH} \sim 0$ Hz. The $^{1}H\{^{31}P\}$ NMR experiment plus the data from the undecoupled ^{1}H NMR spectrum showed that the smallest coupling (5.4 Hz) is due to the two sets of hydrogens coupling to each other.

In total, the spectrometric evidence suggests a static structure for **2** with two terminal iridium-bound hydrides and one hydride bridging the metals, with one phosphine datively bound to each center. Line shape analysis based on the variable temperature ^{1}H NMR data (see Appendix), assuming, (a) that exchange occurs through a terminal-bridge-terminal mode, (b) that no more than one hydrogen is terminally bound to a particular iridium at any time, and (c) that no more than two hydrogens occupy sites bridging the metal centers at any moment (two exchange permutations total), yields the activation parameters $\Delta H^{\ddagger} = 9.1(3)$ kcal, $\Delta S^{\ddagger} = -6.4(1.2)$ e.u., k_{298} (extrapolated) = $3.0(2) \times 10^{4}$ s^{-1}, and $\Delta G^{\ddagger}_{298} = 10.96(4)$ kcal for the "exchange" of the hydride ligands.

In order to conclusively determine the static structure of dimer **2**, a single crystal X-ray diffraction study was performed. The details of the study will be reported;[14] Figure 1 shows the ORTEP of the determined structure and gives some important bond lengths and

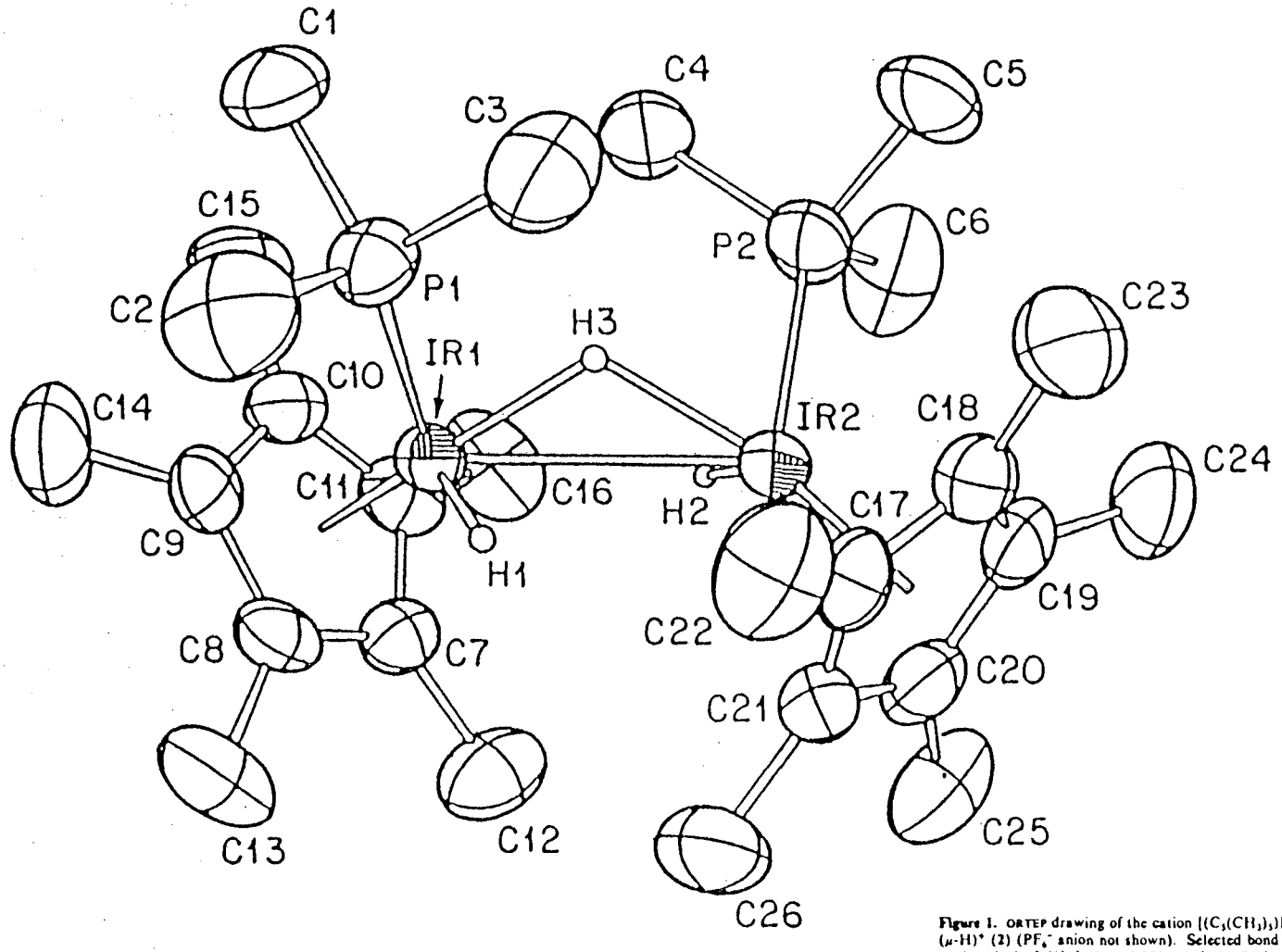

Figure 1. ORTEP drawing of the cation $[(C_5(CH_3)_5)Ir(P(CH_3)_3)(H)]_2(\mu\text{-}H)^+$ (2) (PF_6^- anion not shown). Selected bond distances (Å) and angles (deg): Ir(1)-Ir(2) = 2.983 (1); Ir(1)-P(1) = 2.248 (1); Ir(2)-P(2) = 2.246 (1); Ir(1)-Cp*(1) centroid = 1.896 (1); Ir(2)-Cp*(2) centroid = 1.891 (1); Ir(1)-H(1) = 1.47 (5); Ir(2)-H(2) = 1.52 (6); Ir(1)-H(3) = 1.69 (4); Ir(2)-H(3) = 1.80 (4); Ir(2)-Ir(1)-H(1) = 73.4 (17); Ir(1)-Ir(2)-H(2) = 70.9 (19); Ir(2)-Ir(1)-P(1) = 101.51 (3); Ir(2)-Ir(1)-P(2) = 101.28 (3).

angles. Of note is the rather long Ir-Ir distance (2.981(1) Å), possibly suggestive of a somewhat weak metal-metal interaction.

The formation of **2** without detection of an intermediate monophosphine complex allows us to suggest an answer to a reported result. Maitlis and coworkers[13] noted that trihydride dimer **1** underwent H/D exchange with deuterium gas only in the presence of NEt_3. We propose that this result is due to the formation of a weakly bound monoamine adduct analogous to our unisolable monophosphine adduct, which then oxidatively adds D_2 and reductively eliminates HD. This proposal obviates the need to suggest either binuclear reductive elimination or oxidative addition across the metal-metal bond.

Dimer **2** reacts with one equivalent of $LiEt_3BH$ in ether at room temperature to give $(C_5(CH_3)_5)Ir(P(CH_3)_3)H_2$ in 80% isolated yield (Scheme 1). The reaction requires approximately 18 h to go to completion, curiously slow given our experience[11b] with such reductions. Solubility effects may cause this; the sparing solubility of $\mathbf{2}\cdot PF_6$ in THF probably limits the reaction rate to a value smaller than a reduction run under purely homogeneous conditions.

Protonation of $(C_5(CH_3)_5)Ir(P(CH_3)_3)H_2$

Several workers have protonated metal hydride complexes in order to prepare either monomeric salts of metals in higher formal oxidation states,[16a-g] or in at least one instance a hydride bridged dimer analogous to **2**.[16h] Prompted by the latter result, we attempted

to prepare **2** by treating dihydride **4** with $HBF_4 \cdot OEt_2$, both at low and ambient temperature using normal and reverse addition techniques. In all cases, the interesting iridium (V) monomer $(C_5(CH_3)_5)Ir(P(CH_3)_3)H_3BF_4$, **5**, precipitated and proved to be stable toward the hydrogen loss necessary to generate **2** (Scheme 1). Complex **5** thus represents the first example of an isolated organometallic cation containing iridium in the formal +5 oxidation state.[16g] Spectral and analytical data agree completely with this formulation.

The most interesting aspect of the characterization of **5** stems from the dynamic behavior of the hydride resonance in the ^1H NMR spectrum. At room temperature and above, a simple first order doublet (δ -13.5) with J_{PH} = 10 Hz is observed. As has been noted previously for cationic trihydride complexes,[16b,d] the resonance shifts strongly downfield from that in dihydride **4** (δ -17.4), indicating a significant deshielding of the hydride ligands upon protonation. The remarkably small ^{31}P-^1H coupling, as compared with dihydride **4** (J_{PH}=32.1 Hz), results from the fact that the static couplings of the phosphorus to the two different types of iridium-bound hydrogens (see below) are of opposite sign. Verification of this hypothesis resulted from line shape analysis of the variable temperature ^1H NMR data (Figure 2), assuming the smaller J_{PH} to be negative, which mimicked the "fast limit" result accurately. An Eyring plot of the data (see Appendix and Figure 3), assuming exchange only between the sets of hydrogens and not between members of a set (two exchange permutations total), yielded the activation parameters $\Delta H^{\ddagger}$ = 12.0(4) kcal, $\Delta S^{\ddagger}$ = 3.7(1.6) e.u., k_{298}

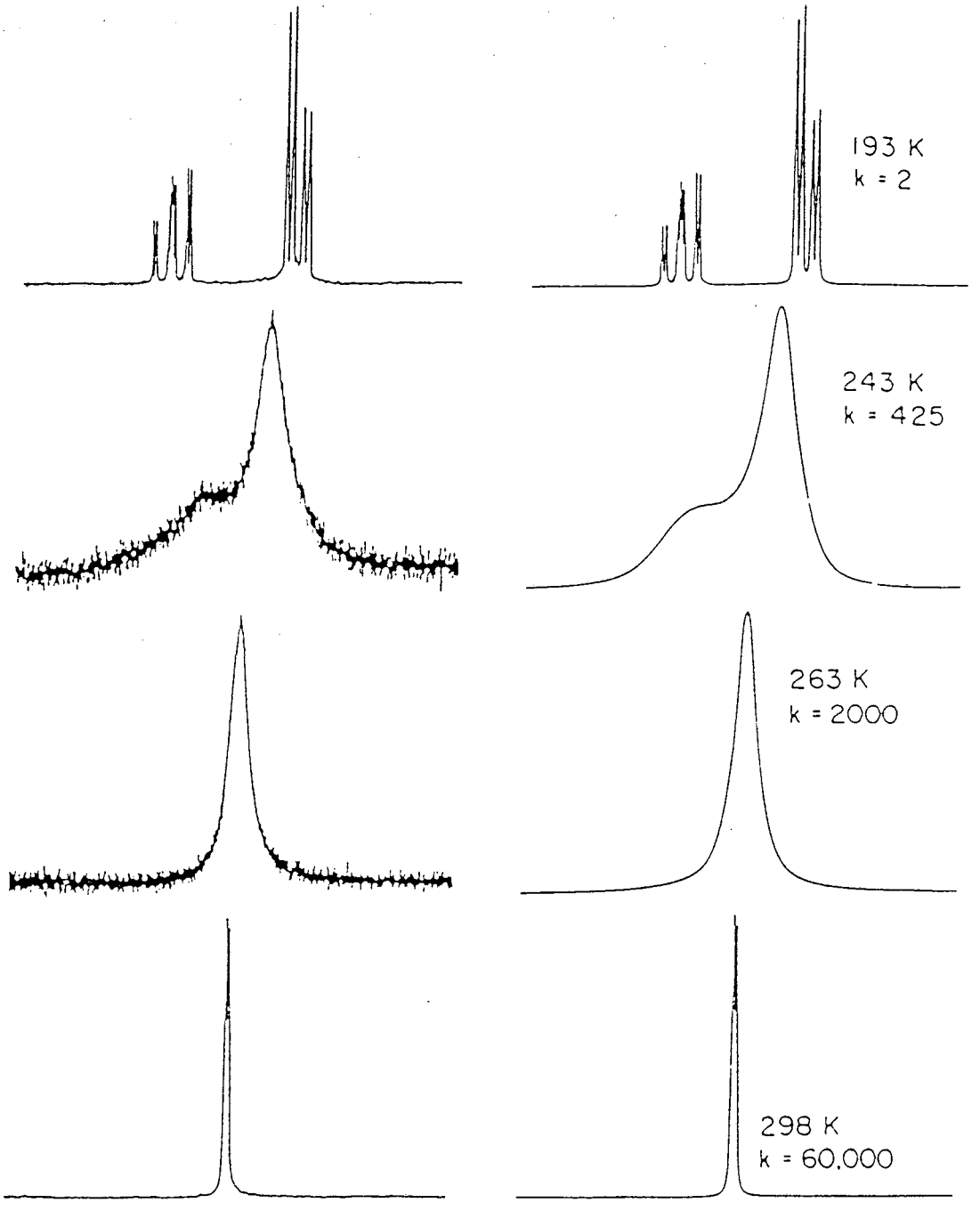

Figure 2. Experimental and calculated ^1H NMR spectra (300 MHz) for **5** at various temperatures. The region shown is that between δ −11 and −16.

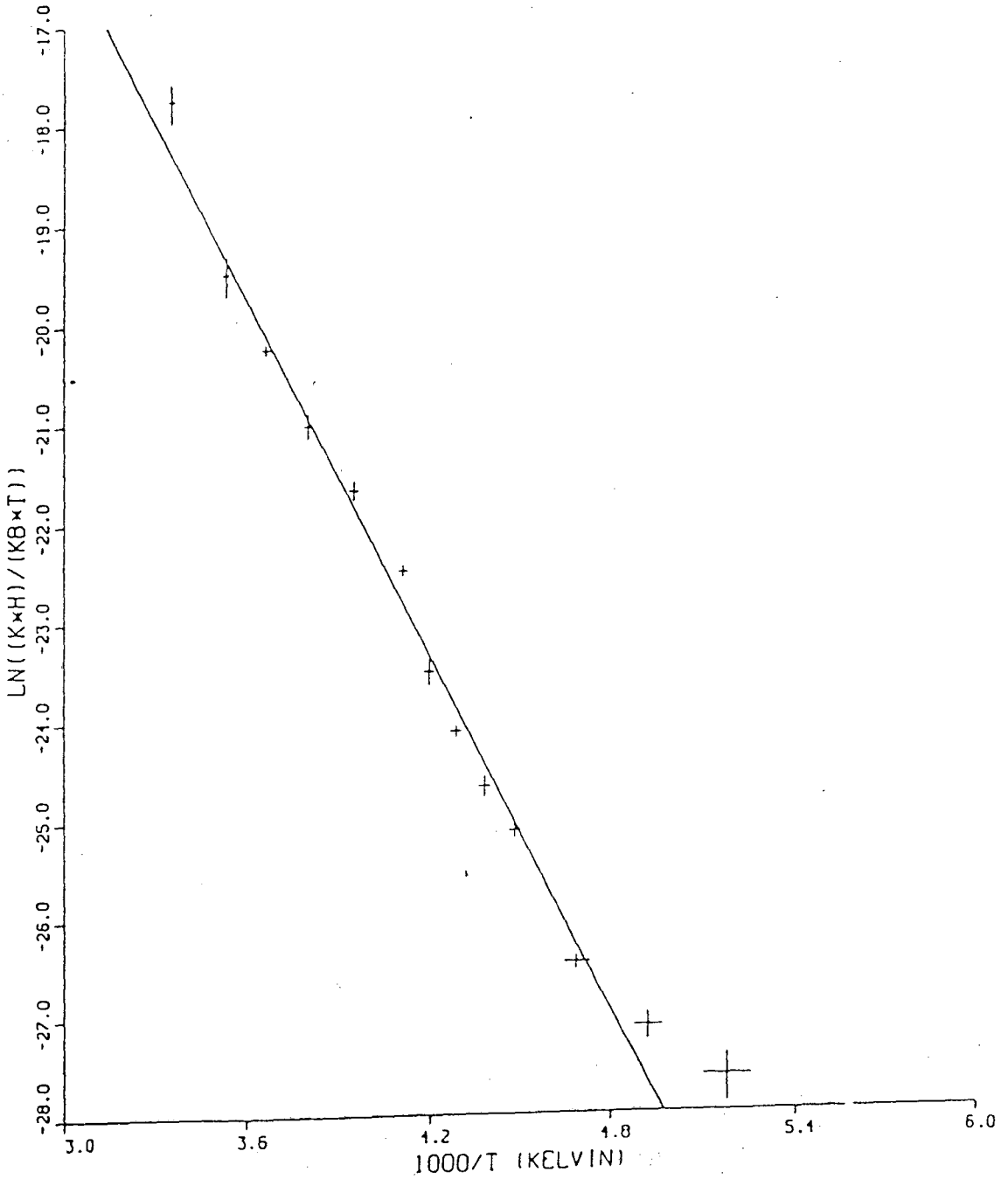

Figure 3. Eyring plot (from ACTPAR) for 5.

(extrapolated) = 3.7(6) x 10^4 s^{-1}, and $\Delta G^{\ddagger}_{298}$= 10.84(8) kcal for the hydride ligand exchange process.

Decoalescence of the hydride signal into two different resonances occurs at -30 °C. At -90 °C and a field strength of 300 MHz, a second order pattern appears, seemingly a downfield doublet of doublets of doublets (δ -12.7) integrating as one hydrogen, and an upfield doublet of doublets (δ -14.1) integrating as two equivalent hydrogens. However, at -90 °C with a field strength of 500 MHz, a first order pattern is observed, consisting of a downfield triplet of doublets (δ -12.7), integrating as one hydrogen, and an upfield doublet of doublets (δ -14.1), integrating as two hydrogens. Surprisingly, a $^1H\{^{31}P\}$ NMR experiment demonstrated the smallest coupling to each set of hydrides to be due to ^{31}P-^1H splitting, with the larger value (21.5 Hz) representing the coupling to the two equivalent hydrogens and the smaller value (12.6 Hz) representing the coupling to the unique hydrogen. This left the larger coupling to be due to the different hydrogen atoms coupling to each other, with the remarkably large value of J_{HH} = 56.3 Hz! We found this value difficult to accept in view of data for similar complexes (Ref. 17 and Chapter 4), but accurate computer simulations of both the first and second order spectra using the Bruker simulation program PANIC each yielded this value. Given that the HH coupling in free H_2 is approximately 280 Hz,[18] and that for $(C_5(CH_3)_5)IrH_3L$ complexes typical values of J_{HH} = 5-8 Hz obtain (Chapter 4), the hydrogen atoms in 5 must either sit quite near each other, or must occupy sites different from those of the "four-legged piano stool".

Deprotonation and Alkylation of $(C_5(CH_3)_5)Ir(P(CH_3)_3)H_2$.

Deprotonation of $(C_5(CH_3)_5)Ir(P(CH_3)_3)H_2$, **4**, with t-BuLi leads to a solution/slurry containing some form of "$(C_5(CH_3)_5)Ir(P(CH_3)_3)HLi$", **6**, as confirmed by further reaction with alkylating agents (Scheme 2).[19a] The yellow material may be isolated from the reaction mixture by filtration; however, yields are invariably low, as the complex is highly soluble. Removal of the solvent from the reaction mixture seems to regenerate impure dihydride **4** in low yield.

While proper analytical data were obtained for **6**, interpretation of the ^1H NMR spectrum of a solution of this material proved difficult as two products are seen, possibly an equilibrium mixture of oligomers. The only resonance in the upfield hydride region is a structureless lump. This feature may be due to peak overlap, to unresolved coupling between the hydrogen, the phosphorus, and the lithium atoms, to a combination of these, or to some unknown factor. A significant upfield shift is observed for the resonances in the $^{31}P\{^1H\}$ NMR spectrum (δ -57.6, -58.9) compared to that for **4** (δ -46.8), indicating an increase in shielding of the phosphorus upon deprotonation. Of interest also is the significant low-energy shift of the Ir-H stretch in the IR spectrum (see **[6·(pmdeta)$_x$]** below).

A pentane solution/slurry of the salt **6** reacts with $CH_3O_3SCF_3$ (methyl triflate) to generate the photosensitive alkyl hydride $(C_5(CH_3)_5)Ir(P(CH_3)_3)(CH_3)(H)$,[15] in good yield on a large scale, although slightly contaminated with dihydride **4** and $(C_5(CH_3)_5)Ir(P(CH_3)_3)(CH_3)_2$. This complex was previously isolated

Scheme 2

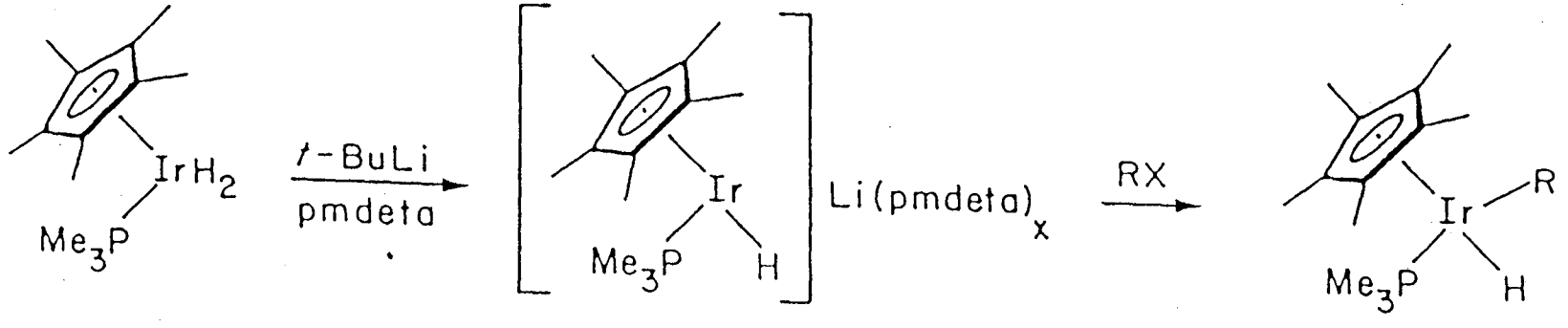

4

[6 · (pmdeta)$_x$]

from the reaction of $(C_5(CH_3)_5)Ir(P(CH_3)_3)(CH_3)Cl$ with $LiBH_4$, and, more importantly, by the thermal C-H activation of methane by the proposed intermediate "$(C_5(CH_3)_5)Ir(P(CH_3)_3)$".

Synthesis of alkyl hydride complexes through this method (Scheme 2) has proved useful in determining components of photolytic C-H activation reaction mixtures.[11] We have prepared the complete series of hydrido(n-alkyl)iridium compounds for ethyl through n-pentyl, as well as $(C_5(CH_3)_5)Ir(P(CH_3)_3)$(neopentyl)(H) and $(C_5(CH_3)_5)Ir(P(CH_3)_3)(\eta^1$-allyl)(H),[19b] on either NMR tube or preparative scale. Until recently, only primary alkylating agents reacted to give alkyl hydrides in general; secondary and tertiary agents usually resulted in production of dihydride 4 by an undetermined (although probably elimination-based) mechanism. Recently, however, the synthesis of $(C_5(CH_3)_5)Ir(P(CH_3)_3)$(s-butyl)(H) from a solution of 6 and s-butyl chloride[19c] has renewed our hope of making this a general synthetic method.

Another interesting complex synthesized by the reaction of a solution of 6 with $Me_3SiO_3SCF_3$ is the silyl hydride $(C_5(CH_3)_5)Ir(P(CH_3)_3)(Si(CH_3)_3)(H)$. Further chemistry of this surprisingly air-sensitive material is described in Chapter 5.

When the sequestering agent pentamethyldiethylenetriamine, pmdeta, is added to the t-BuLi deprotonation reaction, precipitation of yellow solid is significant and rapid; the isolated material has been characterized as the salt $(C_5(CH_3)_5)Ir(P(CH_3)_3)H[Li(pmdeta)_x]$, **$[6\cdot(pmdeta)_x]$** (Scheme 2). Unfortunately, the amount of pmdeta present in the isolated product varies between 0.5 and 0.05, as

determined by elemental analysis. The effect of adding the sequestering agent is clearly a significant acceleration in reaction rate; quantitative deprotonation of dihydride **4** requires minutes when pmdeta is used, while approximately twelve hours are necessary for similar results when no pmdeta is present. We do not understand why pmdeta does not sequester the lithium atom in this complex, especially in light of the reproducible preparation of $(C_5(CH_3)_5)IrH_3[Li(pmdeta)]$ (Chapter 4); a reasonable hypothesis might be that the molecule adopts a structure (possibly oligomeric) in which steric constraints dictate that certain lithium atoms be in positions where stable sequestering is impossible. A single crystal X-ray diffraction study might answer this question.

Regardless of the amount of pmdeta present in isolated **[6·(pmdeta)$_x$]**, the salt proved completely insoluble in inert solvents at ambient temperature, thus limiting spectral characterization. Upon attempted dissolution in non-hydrocarbon solvents, **[6·(pmdeta)$_x$]** often scavenges a proton to regenerate dihydride **4**. Surprisingly, solid **[6·(pmdeta)$_x$]** decomposes relatively slowly in air compared to $(C_5(CH_3)_5)IrH_3Li$ and $(C_5(CH_3)_5)IrH_3[Li(pmdeta)]$, requiring minutes rather than seconds to darken completely; possibly this result indicates a closer iridium-lithium contact in **[6·(pmdeta)$_x$]**, or a different degree of oligomerization in the solid state. Of interest is the significant low-frequency shift of the iridium-terminal hydrogen stretching mode in the IR spectrum of **[6·(pmdeta)$_x$]**; for dihydride **4**, the band appears at 2099 cm^{-1} (C_6H_{12}), while for monohydride **[6·(pmdeta)$_x$]** the band appears at 1950 cm^{-1} (silicone

oil). Unfortunately, not enough data exist to indicate the significance of this result, especially in light of the fact that the stretch for trihydride cation 5 occurs at essentially the same frequency (2090 cm^{-1}, KBr) as for 4; however, the direction of the shift agrees with previous data.[20,21]

Possibly due to the insolubility of this material, or because the sequestering agent presents another substrate with which the anion can react, significant amounts of side products are formed upon attempted alkylation (Scheme 2). Foremost among these side products is dihydride 4, usually comprising the major proportion of material isolated from the reaction. Normally the desired iridium alkyl hydride constitutes the second most abundant product; minor unidentified iridium hydride species account for the balance of the organometallic material. Therefore we commonly generate the anionic reagent in situ without the addition of pmdeta, in spite of the additional time required.

Conclusion

We have shown that a number of trimethylphosphine-substituted pentamethylcyclopentadienyl iridium complexes may be prepared, with the metal centers in varied formal oxidation states. The stability and reactions of these materials suggest a rich synthetic chemistry for the $(C_5(CH_3)_5)Ir(P(CH_3)_3)$ fragment.

As expected for polyhydride complexes, those described here show fluxional behavior. Line shape analysis has allowed the determination of the activation parameters for the hydride ligand site exchange process; as more data become available, these values

should provide insight into the nature of such exchange.[22,23]

The most synthetically useful reaction is that of the deprotonation of dihydride 4 followed by alkylation, a method first developed for molybdenum and tungsten complexes by Green and coworkers.[20,21] Few examples of stable organometallic alkyl hydride complexes exist; in our group, the use of this method to prepare independently products observed in photolysis reactions of 4[11] has proved a boon to further research. At this point, the scope of the reaction is somewhat limited, but recent work suggests that variation of the leaving group may allow considerable range in the type of products accessible.

The complexes $(C_5(CH_3)_5)Ir(P(CH_3)_3)_3(BF_4)_2$, $(C_5(CH_3)_5)Ir(P(CH_3)_3)_2HBF_4$ (both described in the following Chapter), $(C_5(CH_3)_5)Ir(P(CH_3)_3)H_2$, and $(C_5(CH_3)_5)IrH_3Li$ (Chapter 4) represent an isoelectronic series of (pentamethylcyclopentadienyl)iridium compounds, successively substituting hydride anions (H^-) for trimethylphosphine. We point this out to preface our idea that the hydride anion and trimethylphosphine, being sterically undemanding strong sigma donor ligands, may be formally, if not necessarily chemically, substituted for each other in certain cases. Such formal substitution of H^- for $P(CH_3)_3$ in organometallic complexes has led us to new chemistry, which is discussed in Chapter 4. Along these lines, we note that, in total, Scheme 1 may be thought of as describing a step by step mechanism for the oxidation of dimer cation 1 to two equivalents of a monomeric iridium (V) complex.

Appendix

Line shape simulations were performed at the UCB Computer Center, using the program DYNAMAR, a locally modified version of a program described by Meakin and Jesson.[23] ^{1}H NMR chemical shifts were assumed to vary linearly with temperature, while coupling constants were maintained at values derived from experimental spectra taken at or near the low temperature static limit. The number and type of permutations required to define exchange were derived from consideration of possible simplified exchange modes, as described in the text. All permutations were assumed to occur at the same rate at a given temperature. A line broadening parameter (typically 4-6 Hz) was included based on the static limit experimental spectra and was not varied with temperature.

Values of the exchange rate constant k were determined by comparison of calculated spectra with experimental spectra collected at various temperatures; k values used were estimated to be accurate to +/- 25% or better. The data were plotted to the form of the Eyring[24] equation $\ln(nhk/k_bT) = -\Delta H^{\ddagger}/RT + \Delta S^{\ddagger}/R$, where n is the number of permutations, h is Planck's constant, k_b is Boltzmann's constant, and the transmission coefficient has been set equal to 1. From a weighted least-squares fit using a locally modified version of the program ACTPAR,[25] the values of $\Delta H^{\ddagger}$, $\Delta S^{\ddagger}$, $\sigma(\Delta H^{\ddagger})$, and $\sigma(\Delta S^{\ddagger})$ were determined, and used to calculate $\Delta G^{\ddagger}_{298}$ and $\sigma(\Delta G^{\ddagger}_{298})$.[25] Correlation coefficients for the least-squares line were typically 0.99 or better.

Following are two listings of ACTPAR: an IBM BASIC version

appropriate for a PC without graphics capability, and a TEKTRONIX BASIC version with graphics capability modified for the Professor Andrew Streitweiser, Jr. system at the University of California, Berkeley.

IBM BASIC Version of ACTPAR

```
100 CLS
110 PRINT "********** ACTPAR - A Program for NMR Band Shape Analysis **********"
120 PRINT
130 PRINT "This program is written in IBM Basic based on a Tektronix Basic"
140 PRINT "program written by K. L. Park, August, 1983, which in turn is based"
150 PRINT "on a Fortran program written by Dr. Gerhard Binsch, Institute of"
160 PRINT "Organic Chemistry, University of Munich.  IBM rewriting at the"
170 PRINT "University of California, Berkeley, was done by Tom Gilbert, who"
180 PRINT "is solely responsible for editorial content."
190 PRINT
200 PRINT "The program solves for the Eyring Parameters using a least-squares"
210 PRINT "method based on an algorithm published by W. E. Deming"
220 PRINT "(Statistical Adjustment of Data 1943, ch9, 18-p178, ex4)"
230 PRINT "In order to run the program, the following data are needed:"
240 PRINT
250 PRINT "1. The number of lines you wish to calculate (1-5);"
260 PRINT "2. The number of points in the M-th line (1-25);"
270 PRINT "3. The values of T(K), sigma(T), k(1/s), and sigma(k)."
280 PRINT
290 PRINT "Data must be input stepwise (as if there were any other way). The"
300 PRINT "program will output activation parameter data in tabular form, either"
310 PRINT "on the screen or on a line printer, but will not draw a plot."
320 PRINT
330 PRINT "When you're ready to go, hit the g key."
340 INPUT A$
350 IF A$<>"g" THEN 100
360 PRINT "How many lines do you want to calculate (1-5) ?"
370 INPUT M
380 DIM N(5)
390 DIM X(5,25),S1(5,25),Y(5,25),S2(5,25),V1(5,25),V2(5,25)
400 DIM P1(5,25),P2(5,25),Q1(5,25),Q2(5,25),T(5,25),R(5,25)
410 DIM F0(25),W(25)
420 FOR I=1 TO M
430 CLS
440 PRINT "How many data points are there in Line ";I;" (up to 25) ?"
450 INPUT N(I)
460 PRINT
470 PRINT "Enter your data"
480 PRINT "(I),T(K),sigma(T),k(1/s),sigma(k)"
490 PRINT
500 REM K2(Boltzmann)=cal/mole, h(Planck)=cal*s, R1(gas constant)=cal/mole*K
510 K2=3.2996E-24
520 H=1.5835E-34
530 FOR J=1 TO N(I)
540 PRINT "(";J;")";
550 INPUT T(I,J),S1(I,J),R(I,J),S2(I,J)
560 X(I,J)=1/T(I,J)
570 Y(I,J)=LOG(R(I,J)*H/(K2*T(I,J)))
580 V1(I,J)=S1(I,J)^2*X(I,J)^4
590 V2(I,J)=(S2(I,J)/R(I,J))^2+(S1(I,J)/T(I,J))^2
600 NEXT J
610 NEXT I
620 CLS
630 DIM A9(5),B9(5),S8(5),S9(5),C8(5),C9(5)
640 PRINT
650 PRINT "Hang on,already ! I'm busy"
660 PRINT
670 R1=1.9872
680 FOR I=1 TO M
690 REM --Subroutine for the Least-Squares Calculation--
```

```
700 GOSUB 1190
710 REM --Defining the Final Parameters--
720 REM entropy of activation
730 A9(I)=A*R1
740 REM enthalpy of activation
750 B9(I)=-R1*B/1000
760 REM covariance = (correlation coefficient)*(sigma d-H)*(sigma d-S)
770 C8(I)=-C4*R1^2*(S3*S4)
780 REM correlation coefficient
790 C9(I)=-C4
800 REM sigma(enthalpy of activation)
810 S8(I)=S3*R1/1000
820 REM sigma(entropy of activation)
830 S9(I)=S4*R1
840 NEXT I
850 PRINT "How do you want your data output ?"
860 PRINT
870 PRINT "If you want to see it on the screen, hit b (for Bildschirm)"
880 PRINT "If you want to send the data to the printer, hit p"
890 PRINT "If you've gotten everything you want, hit d"
900 INPUT B$
910 CLS
920 IF B$="b" THEN 1970
930 IF B$="p" THEN 960
940 IF B$="d" THEN 2120
950 GOTO 850
960 PRINT "Want to title your output (y or n) ?"
970 INPUT T$
980 IF T$="n" THEN 1050
990 IF T$<>"y" THEN 960
1000 PRINT "Title ?"
1010 INPUT Q$
1020 LPRINT Q$
1030 LPRINT
1040 LPRINT
1050 LPRINT "M"SPC(10)"d-H (kcal/mole)"SPC(9)"sigma(d-H)"
1060 FOR I=1 TO M
1070 LPRINT I;SPC(10)B9(I);SPC(12)S8(I)
1080 NEXT I
1090 LPRINT "M"SPC(12)"d-S (e. u.)"SPC(11)"sigma(d-S)"
1100 FOR I=1 TO M
1110 LPRINT I;SPC(10)A9(I);SPC(12)S9(I)
1120 NEXT I
1130 LPRINT "M"SPC(8)"Cov((cal/mole)^2/K)"SPC(6)"Corre. Coeff."
1140 FOR I=1 TO M
1150 LPRINT I;SPC(10)C8(I);SPC(12)C9(I)
1160 NEXT I
1170 INPUT Z$
1180 GOTO 850
1190 REM -Subroutine for Least Squares-
1200 REM -"Systematic Computation for Fitting Curves by Least Squares"-
1210 REM -W. E. Deming, Chapter 9-
1220 X1=0
1230 Y1=0
1240 X2=0
1250 Y2=0
1260 A=0
1270 B=0
1280 G0=N(I)-INT(N(I)/2)*2
1290 IF G0=1 THEN 1420
1300 REM N = even
1310 N2=N(I)/2
1320 FOR I1=1 TO N2
1330 J=N(I)-I1+1
1340 X1=X1+X(I,I1)
1350 Y1=Y1+Y(I,I1)
```

```
1360 X2=X2+X(I,J)
1370 Y2=Y2+Y(I,J)
1380 NEXT I1
1390 B=B+(Y2-Y1)/(X2-X1)
1400 A=A+(Y2-B*X2)/N2
1410 GOTO 1550
1420 REM N = odd
1430 N2=INT(N(I)/2)
1440 FOR I1=1 TO N2
1450 J=N(I)-I1
1460 X1=X1+X(I,I1)
1470 Y1=Y1+Y(I,I1)
1480 X2=X2+X(I,J)
1490 Y2=Y2+Y(I,J)
1500 NEXT I1
1510 X2=X2+X(I,N(I))
1520 Y2=Y2+Y(I,N(I))
1530 B=B+(Y2-Y1)/(X2-X1)
1540 A=A+(Y2-B*X2)/(N2+1)
1550 REM --Iteration Sequence--
1560 FOR K1=1 TO 20
1570 FOR I1=1 TO N(I)
1580 F0(I1)=Y(I,I1)-A-B*X(I,I1)
1590 W(I1)=1/(B^2*V1(I,I1)+V2(I,I1))
1600 NEXT I1
1610 A1=0
1620 A2=0
1630 B1=0
1640 A0=0
1650 B0=0
1660 O0=0
1670 FOR I1=1 TO N(I)
1680 A1=A1+W(I1)
1690 A2=A2+X(I,I1)*W(I1)
1700 B1=B1+X(I,I1)^2*W(I1)
1710 A0=A0-F0(I1)*W(I1)
1720 B0=B0-X(I,I1)*F0(I1)*W(I1)
1730 O0=O0+F0(I1)^2*W(I1)
1740 NEXT I1
1750 REM -Normal Equation-
1760 D=A1*B1-A2^2
1770 B3=(A1*B0-A2*A0)/D
1780 B=B-B3
1790 A3=(A0-A2*B3)/A1
1800 A=A-A3
1810 S=(O0-A0*A3-B0*B3)/(N(I)-2)
1820 IF K1=1 THEN 1850
1830 REM -Value Tests for A and B-
1840 IF ABS((S5-SQR(S))/S5)<.000001 THEN 1880
1850 S5=SQR(S)
1860 PRINT S5
1870 NEXT K1
1880 V4=B1*S/D
1890 PRINT S5
1900 V3=A1*S/D
1910 S4=SQR(V4)
1920 S3=SQR(V3)
1930 C0=-A2*S/D
1940 C4=-A2/SQR(A1*B1)
1950 REM -End or Least Squares Routine-
1960 RETURN
1970 PRINT "M"SPC(10)"d-H (kcal/mole)"SPC(9)"sigma(d-H)"
1980 FOR I=1 TO M
1990 PRINT I;SPC(10)B9(I);SPC(12)S8(I)
2000 NEXT I
2010 PRINT "M"SPC(12)"d-S (e. u.)"SPC(11)"sigma(d-S)"
```

```
2020 FOR I=1 TO M
2030 PRINT I;SPC(10)A9(I);SPC(12)S9(I)
2040 NEXT I
2050 PRINT "M"SPC(8)"Cov((cal/mole)*2/K)"SPC(6)"Corre. Coeff."
2060 FOR I=1 TO M
2070 PRINT I;SPC(10)C8(I);SPC(12)C9(I)
2080 NEXT I
2090 INPUT X$
2100 CLS
2110 GOTO 850
2120 CLS
2130 PRINT "***** After You're Done *****"
2140 PRINT
2150 PRINT
2160 PRINT "Anything else you want to do ?"
2170 PRINT
2180 PRINT "If you want another hard copy or another screen copy, hit c"
2190 PRINT
2200 PRINT "For another problem, hit r (remember that you'll be kissing your"
2210 PRINT "data goodbye !"
2220 PRINT
2230 PRINT "If you want to quit, hit q"
2240 INPUT X$
2250 IF X$="c" THEN 850
2260 ERASE N,X,S1,Y,S2,V1,V2,P1,P2,Q1,Q2,T,R,F0,W,A9,B9,S8,S9,C8,C9
2270 IF X$="r" THEN 100
2280 IF X$<>"q" THEN 2120
2290 END
Ok
```

Tektronix BASIC Version of ACTPAR

```
100 PAGE
110 INIT
120 PRINT "********** ACTPAR - A PROGRAM FOR NMR BAND SHAPE ANALYSIS **"
130 PRINT
140 PRINT "THIS PROGRAM WAS WRITTEN BY K.L. PARK, AUGUST 1983, AND IS"
150 PRINT "BASED ON A FORTRAN PROGRAM WRITTEN BY DR. G. BINSCH,"
160 PRINT "INSTITUTE OF ORGANIC CHEMISTRY, UNIVERSITY OF MUNICH. "
170 PRINT "MODIFICATION FOR THE AS,JR SYSTEM BY TOM GILBERT, WHO IS"
180 PRINT "SOLELY RESPONSIBLE FOR EDITORIAL CONTENT"
190 PRINT
200 PRINT "THE PROGRAM SOLVES FOR THE EYRING PARAMETERS USING A"
210 PRINT "LEAST SQUARES METHOD BASED ON A ALGORITHM PUBLISHED BY"
220 PRINT "W.E. DEMING (STATISTICAL ADJUSTMENT OF DATA 1943, CH9"
230 PRINT "18-P178, EX4)"
240 PRINT
250 PRINT "IN ORDER TO RUN THE PROGRAM, THE FOLLOWING DATA ARE NEEDED:"
260 PRINT "1. THE NUMBER OF LINES YOU WISH TO CALCULATE (1-5);"
270 PRINT "2. THE NUMBER OF POINTS IN THE M-TH LINE (1-25);"
280 PRINT "3. THE VALUES OF T(K), SIGMA(T), K(1/S), AND SIGMA(K)."
290 PRINT
300 PRINT "THE DATA MUST BE INPUT STEPWISE (AS IF THERE WERE ANY OTHER"
310 PRINT "WAY).  WHEN YOU'RE READY TO GO, HIT THE L KEY.";
320 INPUT A$
330 IF A$<>"L" THEN 90
340 PRINT
350 PRINT "     HOW MANY LINES DO YOU WANT TO CALCULATE (UP TO 5) ?";
360 INPUT M
370 DIM N(M)
380 DIM X(5,25),S1(5,25),Y(5,25),S2(5,25),V1(5,25),V2(5,25)
390 DIM P1(5,25),P2(5,25),Q1(5,25),Q2(5,25),T(5,25),R(5,25)
400 DIM F0(25),W(25)
410 FOR I=1 TO M
420    PAGE
430    PRINT "HOW MANY DATA POINTS ARE THERE IN LINE ";I;" (UP TO 25)?";
440    INPUT N(I)
450    PRINT
460    PRINT "ENTER YOUR DATA"
470    PRINT USING 480:"(I) ","T(K)","SIGMA(T)","K(1/S)","SIGMA(K)"
480    IMAGE 4A,8X,5A,6X,11A,10X,8A,9X,10A
490    PRINT
500    REM K2(BOLTZMANN)=CAL/MOLE; H(PLANCK)=CAL*S; R1(GAS)=CAL/MOLE*K
510    K2=3.2996E-24
520    H=1.5835E-34
530    FOR J=1 TO N(I)
540       PRINT "(";J;")";
550       INPUT T(I,J),S1(I,J),R(I,J),S2(I,J)
560       X(I,J)=1/T(I,J)
570       Y(I,J)=LOG(R(I,J)*H/(K2*T(I,J)))
580       V1(I,J)=S1(I,J)^2*X(I,J)^4
590       V2(I,J)=(S2(I,J)/R(I,J))^2+(S1(I,J)/T(I,J))^2
600    NEXT J
610 NEXT I
620 PAGE
630 DIM A9(5),B9(5),S8(5),S9(5),C8(5),C9(5),G8(5),G9(5)
640 PRINT
650 PRINT "HANG ON A SECOND ! I'M BUSY, FOR CRISSAKES !";
660 PRINT
670 R9=1.9872
680 FOR I=1 TO M
690    REM -- SUBROUTINE FOR LEAST-SQUARE CALCULATION --
```

```
700     GOSUB 1560
710     REM -- DEFINING THE FINAL PARAMETERS --
720     REM ENTROPY OF ACTIVATION (D-S)
730     A9(I)=A*R9
740     REM ENTHALPY OF ACTIVATION (D-H)
750     B9(I)=-R9*B/1000
760     REM COVARIANCE (=(CORR. COEFF.)*(SIGMA D-H)*(SIGMA D-S))
770     C8(I)=-C4*R9^2*(S3*S4)
780     REM CORR. COEFF.
790     C9(I)=-C4
800     REM SIGMA (D-H)
810     S8(I)=S3*R9/1000
820     REM SIGMA (D-S)
830     S9(I)=S4*R9
840     REM FREE ENERGY OF ACTIVATION (D-G)
850     G8(I)=(-R9*B-298.15*(A*R9))/1000
860     REM SIGMA (D-G)
870     G9(I)=ABS(S3*R9-298.15*(S4*R9))/1000
880 NEXT I
890 PAGE
900 PRINT
910 PRINT "CHOOSE HOW YOU WANT YOUR DATA OUTPUT"
920 PRINT
930 PRINT "      ON THE SCREEN (WITH B, FOR BILDSCHIRM)"
940 PRINT "      ON THE PRINTER (WITH P)"
950 INPUT B$
960 PAGE
970 IF B$="B" THEN 1000
980 IF B$="P" THEN 1020
990 GO TO 910
1000 D1=32
1010 GO TO 1030
1020 D1=40
1030 PRINT @D1: USING 1040:"T","SIGMA(T)","K","SIGMA(K)"
1040 IMAGE 2X,1A,7X,8A,15X,1A,16X,9A
1050 FOR I=1 TO M
1060    FOR J=1 TO N(I)
1070       PRINT @D1: USING 1080:T(I,J),S1(I,J),R(I,J),S2(I,J)
1080       IMAGE 3D.1D,7X,1D.1D,11X,10D.2D,7X,10D.2D
1090    NEXT J
1100    PRINT @D1:
1110    PRINT @D1: USING 1120:"(1/T)*1000","LN (K*H)/(KB*T)"
1120    IMAGE 3X,10A,10X,18A
1130    FOR J=1 TO N(I)
1140       PRINT @D1: USING 1150:X(I,J)*1000,Y(I,J)
1150       IMAGE 5X,2D.3D,12X,5D.5D
1160    NEXT J
1170    PRINT @D1:
1180    PRINT @D1:
1190    PRINT @D1:"***** EYRING PARAMETERS *****"
1200    PRINT @D1:"-----------------------------"
1210    PRINT @D1:
1220    PRINT @D1: USING 1230:"M","D-H(KCAL/MOLE)","SIGMA(D-H)"
1230    IMAGE 1A,14X,14A,5X,12A
1240    PRINT @D1: USING 1250:I,B9(I),S8(I)
1250    IMAGE 1D,14X,6D.5D,5X,6D.5D
1260    PRINT @D1:
1270    PRINT @D1: USING 1280:"M","D-S(E.U.)","SIGMA(D-S)"
1280    IMAGE 1A,14X,13A,5X,12A
1290    PRINT @D1: USING 1300:I,A9(I),S9(I)
```

```
1300     IMAGE 1D,14X,6D.5D,5X,6D.5D
1310     PRINT @D1:
1320     PRINT @D1: USING 1330:"M","D-G(KCAL/MOLE)","SIGMA(D-G)"
1330     IMAGE 1A,14X,14A,5X,12A
1340     PRINT @D1: USING 1350:I,G8(I),G9(I)
1350     IMAGE 1D,14X,6D.5D,5X,6D.5D
1360     PRINT @D1:
1370     PRINT @D1: USING 1380:"M","COV((CAL/MOL)^2/K)","CORRE.COEFF."
1380     IMAGE 1A,10X,18A,4X,12A
1390     PRINT @D1: USING 1400:I,C8(I),C9(I)
1400     IMAGE 1D,11X,6D.8D,5X,6D.5D
1410 NEXT I
1420 D1=32
1430 PRINT "DO YOU WANT TO RESELECT A DATA OUTPUT SCHEME (Y OR N) ?"
1440 INPUT Q$
1450 IF Q$="Y" THEN 890
1460 IF Q$="N" THEN 1480
1470 GO TO 1430
1480 PRINT "-------------------------------------------------------"
1490 PRINT "IF YOU WANT TO SEE YOUR GRAPH ON THE SCREEN, HIT P."
1500 PRINT "IF NOT, HIT ANY OTHER KEY."
1510 D1=32
1520 INPUT C$
1530 PAGE
1540 IF C$<>"P" THEN 890
1550 GO TO 2310
1560 REM -- SUBROUTINE FOR LEAST-SQUARES CALCULATION --
1570 REM -- "SYSTEMATIC COMPUTUATION FOR FITTING CURVES BY LEAST SQUARES
1580 REM -- W.E. DEMING, CHAPTER 9 --
1590 X1=0
1600 Y1=0
1610 X2=0
1620 Y2=0
1630 A=0
1640 B=0
1650 G0=N(I)-INT(N(I)/2)*2
1660 IF G0=1 THEN 1790
1670 REM N IS EVEN
1680 N2=N(I)/2
1690 FOR I1=1 TO N2
1700     J=N(I)-I1+1
1710     X1=X1+X(I,I1)
1720     Y1=Y1+Y(I,I1)
1730     X2=X2+X(I,J)
1740     Y2=Y2+Y(I,J)
1750 NEXT I1
1760 B=B+(Y2-Y1)/(X2-X1)
1770 A=A+(Y2-B*X2)/N2
1780 GO TO 1920
1790 REM N IS ODD
1800 N2=INT(N(I)/2)
1810 FOR I1=1 TO N2
1820     J=N(I)-I1
1830     X1=X1+X(I,I1)
1840     Y1=Y1+Y(I,I1)
1850     X2=X2+X(I,J)
1860     Y2=Y2+Y(I,J)
1870 NEXT I1
1880 X2=X2+X(I,N(I))
1890 Y2=Y2+Y(I,N(I))
```

```
1900 B=B+(Y2-Y1)/(X2-X1)
1910 A=A+(Y2-B*X2)/(N2+1)
1920 REM -- ITERATION SUBROUTINE --
1930 FOR K1=1 TO 20
1940    FOR I1=1 TO N(I)
1950       F0(I1)=Y(I,I1)-A-B*X(I,I1)
1960       W(I1)=1/(B^2*V1(I,I1)+V2(I,I1))
1970    NEXT I1
1980    A1=0
1990    A2=0
2000    B1=0
2010    A0=0
2020    B0=0
2030    O0=0
2040    FOR I1=1 TO N(I)
2050       A1=A1+W(I1)
2060       A2=A2+X(I,I1)*W(I1)
2070       B1=B1+X(I,I1)^2*W(I1)
2080       A0=A0-F0(I1)*W(I1)
2090       B0=B0-X(I,I1)*F0(I1)*W(I1)
2100       O0=O0+F0(I1)^2*W(I1)
2110    NEXT I1
2120    REM -- NORMAL EQUATION --
2130    D=A1*B1-A2^2
2140    B3=(A1*B0-A2*A0)/D
2150    B=B-B3
2160    A3=(A0-A2*B3)/A1
2170    A=A-A3
2180    S=(O0-A0*A3-B0*B3)/(N(I)-2)
2190    IF K1=1 THEN 2220
2200    REM -- VALUE TESTS FOR A AND B
2210    IF (S5-SQR(S))/S5<1.0E-4 THEN 2240
2220    S5=SQR(S)
2230 NEXT K1
2240 V4=B1*S/D
2250 V3=A1*S/D
2260 S4=SQR(V4)
2270 S3=SQR(V3)
2280 C4=-A2/SQR(A1*B1)
2290 REM -- END OF LEAST SQUARES --
2300 RETURN
2310 REM -- PLOTTING SUBROUTINE --
2320 DIM Z$(1),X$(1)
2330 Z$="A"
2340 M1=1.0E+300
2350 M2=-1.0E+300
2360 L1=1.0E+300
2370 L2=-1.0E+300
2380 REM M1,M2 ARE THE MINIMUM AND MAXIMUM VALUES OF Y
2390 REM L1,L2 ARE THE MINIMUM AND MAXIMUM VALUES OF X
2400 FOR J=1 TO M
2410    FOR I=1 TO N(J)
2420       M1=Y(J,I) MIN M1
2430       M2=Y(J,I) MAX M2
2440       L1=X(J,I)*1000 MIN L1
2450       L2=X(J,I)*1000 MAX L2
2460    NEXT I
2470 NEXT J
2480 L3=L2-L1
2490 PRINT
```

```
2500 PRINT "--- MIN (X,Y)"
2510 PRINT USING "5D.3D,A,5D.3D":L1,",",M1
2520 PRINT
2530 PRINT "--- MAX (X,Y)"
2540 PRINT USING "5D.3D,A,5D.3D":L2,",",M2
2550 PRINT
2560 PRINT "--- INTERVAL (X,Y)"
2570 PRINT "--- 00.100, 01.000"
2580 IF Z$="Z" OR Z$="B" THEN 2630
2590 VIEWPORT 35,128,20,95
2600 WINDOW L1,L2,M1,M2
2610 AXIS 0.1,1
2620 GO TO 2660
2630 VIEWPORT 45,130,20,85
2640 WINDOW N9,N7,N8,N6
2650 AXIS @D1:N5,N4
2660 REM -- ERROR BARS --
2670 IF Z$="Z" THEN 2760
2680 FOR J=1 TO M
2690    FOR I=1 TO N(J)
2700       P1(J,I)=1/(T(J,I)-S1(J,I))
2710       P2(J,I)=1/(T(J,I)+S1(J,I))
2720       Q1(J,I)=LOG((R(J,I)+S2(J,I))*H/(K2*T(J,I)))
2730       Q2(J,I)=LOG((R(J,I)-S2(J,I))*H/(K2*T(J,I)))
2740    NEXT I
2750 NEXT J
2760 FOR J=1 TO M
2770    FOR I=1 TO N(J)
2780       MOVE @D1:X(J,I)*1000,Y(J,I)
2790       RMOVE @D1:(P1(J,I)-X(J,I))*1000,0
2800       RDRAW @D1:-(P1(J,I)-P2(J,I))*1000,0
2810       RMOVE @D1:(X(J,I)-P2(J,I))*1000,Q1(J,I)-Y(J,I)
2820       RDRAW @D1:0,-(Q1(J,I)-Q2(J,I))
2830    NEXT I
2840    REM -- CORRELATION LINE --
2850    MOVE @D1:L2+L3,A9(J)/R9-(L2+L3)*B9(J)/R9
2860    DRAW @D1:L1-L3,A9(J)/R9-(L1-L3)*B9(J)/R9
2870    DRAW @D1:L2+L3,A9(J)/R9-(L2+L3)*B9(J)/R9
2880 NEXT J
2890 IF Z$="Z" THEN 3460
2900 HOME
2910 PRINT "JJJJJJJJJJ"
2920 PRINT "CORRECT YOUR AXIS PARAMETERS BY HITTING Y."
2930 PRINT "IF YOU'VE CORRECTED ALREADY, HIT N."
2940 INPUT P$
2950 IF P$="Y" THEN 2990
2960 IF P$="N" THEN 3120
2970 GO TO 2920
2980 PRINT
2990 PRINT
3000 PRINT "PARAMETER CORRECTION"
3010 PRINT
3020 PRINT "MIN (X,Y) ?";
3030 INPUT N9,N8
3040 PRINT
3050 PRINT "MAX (X,Y) ?";
3060 INPUT N7,N6
3070 IF P$="N" THEN 3120
3080 PRINT
3090 PRINT "TIC INTERVAL ?";
```

```
3100 INPUT N5,N4
3110 PRINT
3120 PRINT "================================================="
3130 PRINT "IF YOU WANT TO CHECK YOUR PLOT ON THE SCREEN, HIT B"
3140 PRINT "IF YOU WANT A HARD COPY PLOT FROM THE PLOTTER, HIT Z"
3150 PRINT "IF YOU WANT TO FORGET THE WHOLE THING, HIT N"
3160 INPUT Z$
3170 IF Z$="N" THEN 3470
3180 IF Z$="B" THEN 3210
3190 D1=8
3200 GO TO 3230
3210 D1=32
3220 PAGE
3230 WINDOW 0,130,0,100
3240 VIEWPORT 33,130,20,85
3250 MOVE @D1:0,100
3260 PRINT @D1: USING "4D.1D":N6;
3270 MOVE @D1:0,0
3280 PRINT @D1: USING "4D.1D":N8;
3290 VIEWPORT 43,130,17,85
3300 MOVE @D1:0,0
3310 PRINT @D1: USING "1D.1D":N9;
3320 MOVE @D1:125,0
3330 PRINT @D1: USING "1D.1D":N7;
3340 VIEWPORT 43,130,14,85
3350 MOVE @D1:50,0
3360 PRINT @D1:"X = (1/T)*1000";
3370 VIEWPORT 43,130,5,87
3380 MOVE @D1:0,30
3390 IF D1=32 THEN 3440
3400 PRINT @D1,25:90
3410 PRINT @D1:"Y = LN[(K*H)/(KB*T)]";
3420 PRINT @D1,25:0
3430 GO TO 3450
3440 PRINT @D1:"Y = LN[(K*H)/(KB*T)]";
3450 GO TO 2580
3460 PAGE
3470 PRINT "***** AFTER YOU'RE DONE *****"
3480 PRINT
3490 PRINT "WHAT DO YOU WANT TO DO NEXT ?"
3500 PRINT
3510 PRINT "TO PUT A TITLE ON YOUR PLOT, HIT T"
3520 PRINT "FOR ANOTHER PLOT, HIT B"
3530 PRINT "FOR CORRECTIONS IN AXIS PARAMETERS AND A NEW PLOT, HIT K"
3540 PRINT "FOR THE NEXT SET OF CALCULATIONS, HIT R (BUT REMEMBER,"
3550 PRINT "YOU'LL BE KISSING THE PREVIOUS DATA GOODBYE !"
3560 PRINT
3570 PRINT "OR TO QUIT THE PROGRAM, HIT H"
3580 PRINT
3590 INPUT X$
3600 IF X$="B" THEN 3230
3610 IF X$="T" THEN 3700
3620 IF X$="K" THEN 3640
3630 GO TO 3660
3640 PAGE
3650 GO TO 2900
3660 IF X$="R" THEN 90
3670 PAGE
3680 IF X$<>"H" THEN 3480
3690 END
```

```
3700 PRINT "INPUT YOUR TITLE"
3710 WINDOW 0,130,0,100
3720 VIEWPORT 43,130,90,85
3730 MOVE @D1:50,0
3740 INPUT T$
3750 PRINT @D1:T$
3760 GO TO 3470
```

References.

(1) Werner, H. Angew. Chem., Intl. Ed. Engl. **1983**, 22, 927, and references therein.

(2) Thorn, D. L. Organometallics **1982**, 1, 197.

(3) Milstein, D. J. Am. Chem. Soc. **1982**, 104, 5227.

(4) Gibson, V. C.; Grebenik, P. D.; Green, M. L. H. J. Chem. Soc., Chem. Commun. **1983**, 1101.

(5) Tolman, C. A. Chem. Rev. **1977**, 313.

(6) Kang, J. W.; Moseley, K.; Maitlis, P. M. J. Am. Chem. Soc. **1969**, 91, 5970.

(7) Wolczanski, P. T.; Bercaw, J. E. Acc. Chem. Res. **1980**, 13, 121.

(8) Watson, P. L. J. Chem. Soc., Chem. Commun. **1983**, 276.

(9) Maitlis, P. M. Acc. Chem. Res. **1978**, 11, 301.

(10) Maitlis, P. M. Chem. Soc. Rev. **1981**, 10, 1.

(11) (a) Janowicz, A. H.; Bergman, R. G. J. Am. Chem. Soc. **1982**, 104, 351. (b) Janowicz, A. H.; Bergman, R. G. J. Am. Chem. Soc. **1983**, 105, 3929.

(12) Stang, P. J.; Hanack, M.; Subramanian, L. R. Synthesis **1982**, 85.

(13) White, C.; Oliver, A. J.; Maitlis, P. M. J. Chem. Soc., Dalton Trans. **1973**, 1901.

(14) Burns, C. J.; Rutherford, N. M.; Berg, D. J. Acta Crystallographica, Section C: Crystal Struc. Commun., submitted.

(15) Wax, M. J.; Stryker, J. M.; Buchanan, J. M.; Kovac, C. A.; Bergman, R. G. J. Am. Chem. Soc. **1984**, 106, 1121. Further data for $(C_5(CH_3)_5)Ir(P(CH_3)_3)(CH_3)(H)$ have been obtained for a sample prepared by the independent method described in the

reference. IR (C_6D_6): ν_{Ir-H} 2090 cm^{-1}. Anal. Calcd for $C_{14}H_{28}IrP$: C, 40.08; H, 6.73. Found: C, 39.68; H, 6.46.

(16) (a) Wilkinson, G.; Birmingham, J. M. J. Am. Chem. Soc. 1955, 77, 3421. (b) Green, M. L. H.; Pratt, L.; Wilkinson, G. J. Chem. Soc. 1958, 3916. (c) Rosenblum, M.; Santer, J. O. J. Am. Chem. Soc. 1959, 81, 5517. (d) Davison, A.; McCleverty, J. A.; Wilkinson, G. J. Chem. Soc. 1963, 1133. (e) Fischer, E. O.; Schmidt, M. W. Angew. Chem. 1967, 79, 99. (f) Werner, H.; Kletzin, H. J. Organomet. Chem. 1983, 243, C59. (g) Rhodes, L. F.; Caulton, K. G. J. Am. Chem. Soc. 1985, 107, 259. (h) Werner, H.; Wolf, J. Angew. Chem., Int. Ed. Eng. 1982, 21, 296.

(17) Graham, W. A. G.; Hoyano, J. K. J. Am. Chem. Soc. 1982, 104, 3722.

(18) (a) Kubas, G. J.; Ryan, R. R.; Swanson, B. I.; Vergamini, P. J.; Wasserman, H. J. J. Am. Chem. Soc. 1984, 106, 451, gives for free HD the value of J_{HD}=43.2 Hz (Nageswara Rao, B. D.; Anders, L. R. Phys. Rev. 1965, 140, A112). Since $J_{HX} \sim 6.51(J_{DX})$,[18b] then for free H_2, $J_{HH} \sim 280$ Hz. (b) Brevard, C.; Kintzinger, J. P. in "NMR and the Periodic Table", R. K. Harris and B. E. Mann, Eds. Academic Press: London, 1978, 110.

(19) (a) Addition of $(CH_3)_3CCH_2Li$ to $(C_5(CH_3)_5)Ir(P(C_6H_5)_3)H_2$ in THF results in a red solution. Treatment of this solution with MeI yields methane; no $(C_5(CH_3)_5)Ir(P(C_6H_5)_3)(CH_3)(H)$ (which may be synthesized independently from $(C_5(CH_3)_5)Ir(P(C_6H_5)_3)(CH_3)(I)$

and $NaBH_4$ in isopropanol) is observed by ^1H NMR spectroscopy. Janowicz, A. H.; Bergman, R. G., unpublished work. (b) McGhee, W. D.; Bergman, R. G., unpublished work. (c) Stryker, J. M.; Bergman, R. G., unpublished work. (d) Buchanan, J. M.; Bergman, R. G., unpublished work.

(20) $Cp_2MoH_2/(Cp_2MoHLi)_4$: D'Aniello, M. J.; Barefield, E. K. J. Organomet. Chem. **1974**, 76, C50.; Francis, B. R.; Green, M. L. H.; Luong-Thi, T.; Moser, G. A. J. Chem. Soc., Dalton Trans. **1976**, 1339.

(21) $Cp_2WH_2/[Cp_2WHLi(pmdeta)]_x$: Cooper, R. L.; Green, M. L. H.; Moelwyn-Hughes, J. T. J. Organomet. Chem. **1965**, 3, 261.; Johnson, M. D.; Shriver, D. F. J. Am. Chem. Soc. **1966**, 88, 301.; Mink, R. I. Ph. D. Dissertation, University of Illinois, Champaign-Urbana, Ill., 1977.

(22) Meakin, P.; Guggenberger, L. J.; Peet, W. G.; Muetterties, E. L.; Jesson, J. P. J. Am. Chem. Soc. **1973**, 95, 1467.

(23) (a) Meakin, P.; Muetterties, E. L.; Tebbe, F. N.; Jesson, J. P. J. Am. Chem. Soc. **1971**, 93, 4701. (b) Jesson, J. P.; Meakin, P. Acc. Chem. Res. **1973**, 6, 269.

(24) Glasstone, S.; Laidler, K. J.; Eyring, H. "The Theory of Rate Processes"; McGraw-Hill: New York, 1941.

(25) Binsch, G.; Kessler, H. Angew. Chem., Intl. Ed. Engl. **1980**, 19, 411.

Chapter 2. Synthesis and Characterization of Poly-Trimethylphosphine(pentamethylcyclopentadienyl)iridium Complexes. Simulation of "Virtually Coupled" ^{13}C NMR Spectra of $(C_5R_5)M(P(CH_3)_3)_xL^{n+}$ Species.

Introduction.

A number of multiply-trimethylphosphine-substituted organometallic compounds have been prepared.[1-7] These show promise as "metal bases";[1] that is, due to the strong electron-donating properties of the trimethylphosphine ligand, the complexes exhibit reactivity characteristic of a very electron-rich center, such as the oxygen atom in hydroxide ion.

As the ^{1}H and $^{13}C\{^{1}H\}$ NMR spectra of these complexes were investigated, interesting patterns were noted for the resonances corresponding to the trimethylphosphine ligand. Depending upon the number of such ligands, the patterns varied from binomial doublets through complex multiple order spectra to broad singlets. The ^{1}H NMR patterns were theoretically and experimentally analyzed as $A_nXX'A'_n$-type spectra by Harris,[8] and recently Verkade and coworkers showed examples of experimental spectra for organometallic compounds which could be simulated using Harris' method to calculate J_{PH}, $J_{P'H}$ and $J_{PP'}$.[9] Unfortunately, only in rare cases can the necessary lines be properly resolved in experimental ^{1}H NMR spectra; in most cases the middle of the complex "goalpost" pattern exhibits inadequate fine structure.

When $^{13}C\{^{1}H\}$ NMR spectra are considered, the situation changes. Since the small isotopic abundance of carbon-13 (1.1%, s = 1/2) requires in a statistical sense that only one phosphorus-bound carbon of the possible six per molecule be NMR-active, the $A_nXX'A'_n$ system is simplified to AXX'. If the phosphorus bound to the labeled carbon resonates at a significantly different frequency than the other

phosphorus (i.e. if the "isotope shift" is significant), the spectra are more appropriately analyzed as AXY. The AXX' analysis predicts a five-line pattern, which appears to be more common, while the AXY pattern predicts a six-line pattern. Obviously, these results depend on the applied magnetic field, but this does not present a problem in spectral analysis.

Nelson and coworkers have given the formulae required to calculate the coupling constants necessary to simulate "virtually coupled" $^{13}C\{^{1}H\}$ NMR spectra of the AXX'-type,[10] in essence rewriting the well-known equations[11] for a specific instance. Gunther[12] gives the formulae for the somewhat more complex AXY-type spectra in a monograph. However, in part because experimental observation of the outermost resonances in the $^{13}C\{^{1}H\}$ NMR spectrum is infrequent,[8,10] the coupling constants J_{PC}, $J_{P'C}$ and $J_{PP'}$ are not routinely determined by workers in the field.

In this Chapter, we report the synthesis of three (pentamethylcyclopentadienyl)iridium polyphosphine complexes, and the determination of J_{PC}, $J_{P'C}$ and $J_{PP'}$ for a series of $(C_5R_5)M(P(CH_3)_3)_xL^{n+}$ compounds. The values of these constants suggest unexpected electronic differences between structurally similar species.

Experimental

General. General experimental and characterization procedures were described in Chapter 1. $(C_5H_5)Ir(P(CH_3)_3)_2$ was prepared by the method of Buchanan and Bergman.[13]

$(C_5(CH_3)_5)Ir(P(CH_3)_3)_2ClPF_6$, (1). Trimethylphosphine (10.0 g, 0.132 mol) was added dropwise to a chloroform solution (350 mL) of $[(C_5(CH_3)_5)IrCl_2]_2$[14] (30.0 g, 0.0377 mol) in the drybox. After stirring 2 h, volatile materials were evaporated until approximately 10 mL of liquid remained. Ether was added, and the precipitated yellow solid filtered (35.25 g). This material, presumably $[(C_5(CH_3)_5)Ir(P(CH_3)_3)_2Cl]Cl$, could not be obtained in analytical purity. ^1H NMR ($CDCl_3$): δ 1.85 (t, J_{PH}=2.2, C_5Me_5); 1.86 (virtual t, N=10.9, PMe_3).

A sample of this material (550 mg) was slurried in isopropanol in air with KPF_6 (200 mg, 1.09 mmol). The solution was warmed to 45 °C and stirred vigorously for 12 h. Removal of solvent gave yellow-white solid, which was taken up in CH_2Cl_2. The solution was filtered through a frit to remove insoluble material, then treated with an equal volume of toluene. Slow evaporation of CH_2Cl_2 on a rotary evaporator precipitated yellow, air-stable microcrystals of $(C_5(CH_3)_5)Ir(P(CH_3)_3)_2ClPF_6$ in analytically pure form (654 mg, 0.991 mmol, 84% based on $[(C_5(CH_3)_5)IrCl_2]_2$). A single crystal of **1** suitable for an X-ray diffraction study[15] was grown by slow evaporation of CH_2Cl_2 from a 1:1 CH_2Cl_2/toluene solution. ^1H NMR ($CDCl_3$): δ 1.80 (t, J_{PH}=2.1, 15H, C_5Me_5); 1.72 (virtual t, N=10.7, 18H, PMe_3). $^{13}C\{^1H\}$ NMR ($CDCl_3$): δ 98.9 (s, $\underline{C}_5Me_5$); 16.9 (complex,

N=40.9, PMe_3); 9.5 (s, $C_5\underline{Me}_5$). $^{31}P\{^1H\}$ NMR ($CDCl_3$): δ -36.4 (s, PMe_3); -143.8 (septet, J_{PF}=712, PF_6). FAB MS (thioglycerol): m/e 515/513 (M^+-PF_6). Anal. Calcd for $C_{16}H_{33}P_3ClIrF_6$: C, 29.12; H, 5.04; Cl, 5.37; P, 14.08. Found: C, 29.23; H, 5.04; Cl, 5.41; P, 13.97.

$(C_5(CH_3)_5)Ir(P(CH_3)_3)_2HBF_4$, (2). $P(CH_3)_3$ (0.130 mmol) was expanded into a known volume bulb at room temperature and condensed into a degassed acetone solution of $[(C_5(CH_3)_5)Ir(P(CH_3)_3)(H)]_2(\mu$-H)$BF_4$ (Chapter 1) (105 mg, 0.117 mmol) in a glass bomb capped with a high vacuum Teflon stopcock at liquid nitrogen temperature. The yellow solution was heated to 90 °C for 20 h, at which point no color remained. The solvent was removed and the solid white residue extracted with 2 x 3 mL ether. The ether was evaporated to give $(C_5(CH_3)_5)Ir(P(CH_3)_3)H_2$[16] (43 mg, 0.11 mmol, 91% based on half the available iridium), shown to be pure by ^1H NMR spectroscopy.

The remaining white solid was recrystallized from acetone/ether, yielding two crops of white, slightly air-sensitive **2** (40 mg, 0.070 mmol, 60% based on half the available iridium). ^1H NMR (acetone-d_6): δ 2.09 (t, J_{PH}=2.0, 15H, C_5Me_5); 1.80 (virtual t, N=10.1, 9H, PMe_3); -17.78 (t, J_{PH}=30.1, 1H, Ir-H). $^{13}C\{^1H\}$ NMR (acetone-d_6): δ 98.4 (s, $\underline{C}_5Me_5$); 21.4 (complex, N=41.6, PMe_3); 10.7 (s, $C_5\underline{Me}_5$). $^{31}P\{^1H\}$ NMR (acetone-d_6): δ -47.3 (s). IR (silicone oil): ν_{Ir-H} 2104 cm^{-1}. Anal. Calcd for $C_{16}H_{34}IrBF_4$: C, 33.87; H, 6.04. Found: C, 33.57; H, 6.23. MP: 145-150 °C dec.

$(C_5(CH_3)_5)Ir(P(CH_3)_3)_3(BF_4)_2$, (3). $(C_5(CH_3)_5)Ir(acetone)_3(BF_4)_2$ was prepared in situ from $[(C_5(CH_3)_5)IrCl_2]_2$ (2.00 g, 2.51 mmol) by the method of Maitlis.[17] $P(CH_3)_3$ (16 mmol) was expanded into a known

volume bulb at room temperature, then added to this solution at liquid nitrogen temperature. Warming to room temperature and stirring 10 h resulted in the precipitation of white solid. Removal of solvent and recrystallization from water/THF gave 2.39 g (3.28 mmol, 65%) of white, air-stable product. ^1H NMR (D_2O): δ 1.87 (q, J_{PH}=2.0, 15H, C_5Me_5); 1.74 (virtual quartet, N=9.6, 27H, PMe_3). $^{13}C\{^1H\}$ NMR (D_2O): δ 104.6 (s, $\underline{C}_5Me_5$); 18.04 (complex, N=41.6, PMe_3); 9.39 (s, $C_5\underline{Me}_5$). $^{31}P\{^1H\}$ NMR (D_2O): δ -49.6 (s). Anal. Calcd for $C_{19}H_{42}P_3IrB_2F_8$: C, 31.29; H, 5.81. Found: C, 31.28; H, 5.73.

$(C_5H_5)Ir(P(CH_3)_3)_2HBF_4$. An ethereal solution of $(C_5H_5)Ir(P(CH_3)_3)_2$ (105 mg, 0.256 mmol) was cooled to -40 °C and treated with $HBF_4 \cdot OEt_2$ (0.30 mmol). A white solid precipitated instantly. After 30 min, the solid was filtered, washed with ether and dried to give the pure salt (101 mg, 0.203 mmol, 79%). ^1H NMR (acetone-d_6): δ 5.68 (s, 5H, Cp); 1.92 (virtual t, N=11.0, 18H, PMe_3); -17.14 (t, J_{PH}=28.8, 1H, Ir-H). $^{13}C\{^1H\}$ NMR (acetone-d_6): δ 89.0 (s, Cp); 26.6 (complex, N=43.0, PMe_3). $^{31}P\{^1H\}$ NMR (acetone-d_6): δ -42.1 (s). IR (silicone oil): ν_{Ir-H} 2163 cm^{-1}. Anal. Calcd for $C_{11}H_{24}P_2IrBF_4$: C, 26.57; H, 4.86. Found: C, 26.26; H, 5.07.

$(C_5H_5)Ir(P(CH_3)_3)_2(CH_3)(O_3SCF_3)$. An ethereal solution of $(C_5H_5)Ir(P(CH_3)_3)_2$ (99 mg, 0.242 mmol) was cooled to -40 °C and treated with $CH_3O_3SCF_3$ (0.30 mmol). A white solid precipitated. After 30 min, the solid was filtered, washed with ether and dried to give the pure salt (91 mg, 0.159 mmol, 65%). ^1H NMR (acetone-d_6): δ 5.66 (t, J_{PH}=1.0, 5H, Cp); 1.80 (virtual t, N=11.0, 18H, PMe_3);

0.68 (t, J_{PH}=6.1, 3H, Ir-CH_3). $^{13}C\{^1H\}$ NMR (acetone-d_6): δ 91.5 (s, Cp); 22.4 (complex, N=41.2, PMe_3); -37.4 (t, J_{PC}=8.2, Ir-CH_3). $^{31}P\{^1H\}$ NMR (acetone-d_6): δ -38.9 (s). Anal. Calcd for $C_{13}H_{26}P_2IrO_3SF_3$: C, 27.22; H, 4.57. Found: C,27.29; H, 4.67.

(1,5-c-C_8H_{12})Ir($P(CH_3)_3$)$_3$Cl. A toluene solution of [(1,5-c-C_8H_{12})IrCl]$_2$[18] (231 mg, 0.343 mmol) was degassed with three freeze/pump/thaw cycles. $P(CH_3)_3$ (3.00 mmol) was condensed onto the solution at 77 K. Upon warming to ambient temperature, white solid precipitated. The reaction was stirred three days. The solid was filtered, washed with hexane and dried to give the pure, air-stable product (325 mg, 0.576 mmol, 84%). ^1H NMR (D_2O): δ 3.13 (br s, 4H, ligand alkene); 2.28 (m, 4H, ligand alkyl); 2.05 (m, 4H, ligand alkyl); 1.41 (virtual q, N=8.0, 27H, PMe_3). $^{13}C\{^1H\}$ NMR (D_2O): δ 67.6 (q, J_{PC}=5.2, ligand alkene); 33.0 (s, ligand alkyl); 18.4 (complex, PMe_3). $^{31}P\{^1H\}$ NMR (D_2O): δ -54.4 (s). Anal. Calcd for $C_{17}H_{39}ClP_3Ir$: C, 36.20; H, 6.97. Found: C, 36.40; H, 6.69.

Spectral Simulations. The resonances of the $^{13}C\{^1H\}$ NMR spectra due to the trimethylphosphine ligands were simulated and refined through use of the Bruker NMR simulation program PANIC. Frequencies of the ^{13}C nuclei were determined from experimental spectra; frequencies for the coupled ^{31}P nuclei were assigned arbitrarily large values. Trial values for the required coupling constants (J_{PC}, $J_{P'C}$, $J_{PP'}$) were determined by the methods of either Nelson[10] or Gunther.[11] As the $^{31}P\{^1H\}$ NMR spectra for all complexes were invariably singlets, no checks could be made on these trial values.

An infinite number of equally correct spectral parameters exist

if only the frequency data and coupling constants are refined; the relative intensities of the individual lines are required to determine a unique solution. These intensities were taken from the experimental spectra; however, as the values are probably correct only to ca. 5 - 10%, we induce an automatic error in the coupling constants. Since PANIC does not take intensity errors into account in its error analysis, we estimated the effect of these on the coupling constants based on spectra simulated with slightly different values for each parameter in order. This method indicates a typical potential error of 2 Hz in J_{PC} and $J_{P'C}$ and 1 Hz for $J_{PP'}$. We feel these represent maximum errors; the real errors are probably smaller. Errors in chemical shift frequency proved to be essentially negligible.

Results and Discussion

Preparation of Monomeric (Polyphosphine)iridium Complexes

During the preparation of $(C_5(CH_3)_5)Ir(P(CH_3)_3)Cl_2$ from $[(C_5(CH_3)_5)IrCl_2]_2$,[16] we often noted the presence of a persistent impurity when excess $P(CH_3)_3$ was used. Suspecting this impurity was the salt $[(C_5(CH_3)_5)Ir(P(CH_3)_3)_2Cl]Cl$, we treated a sample of the dichloroiridium dimer with excess $P(CH_3)_3$, followed by KPF_6. This allowed the isolation of $(C_5(CH_3)_5)Ir(P(CH_3)_3)_2ClPF_6$, **1**, as yellow microcrystals in analytical purity (Scheme 1). The air-stable material was characterized analytically and spectroscopically; the most interesting features of its NMR spectra involve the resonances due to the $P(CH_3)_3$ ligands. In the ^1H NMR spectrum, a virtual triplet[19] appears (δ 1.72), with a separation between the taller side peaks of 10.9 Hz; a complex pattern, somewhat like a quintet with the outermost peaks pushed nearer the center, obtains for the phosphine methyl carbon resonance (δ 16.9) in the $^{13}C\{^1H\}$ NMR spectrum (Figure 1). However, only one line is seen in the $^{31}P\{^1H\}$ NMR spectrum (δ -36.4); thus the ^1H NMR spectrum is an example of a virtually coupled $X_nAA'X'_n$ system, and the $^{13}C\{^1H\}$ NMR spectrum corresponds to the AXX' type. In agreement with this view, the virtual triplet in the ^1H NMR spectrum collapses to a singlet in the $^1H\{^{31}P\}$ NMR spectrum.

The isolation of this bisphosphine monomer suggested that other, similar complexes might be isolable. Indeed, the addition of $P(CH_3)_3$ at elevated temperature splits $[(C_5(CH_3)_5)Ir(P(CH_3)_3)(H)]_2(\mu\text{-}H)BF_4$ (Chapter 1) into interesting monomeric species. The reaction cleanly

Scheme I

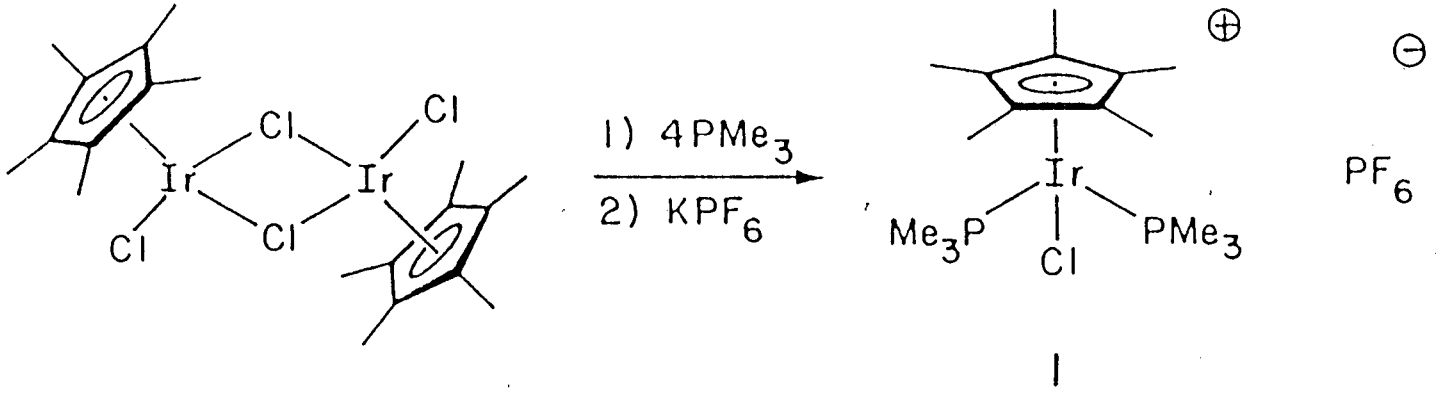

I

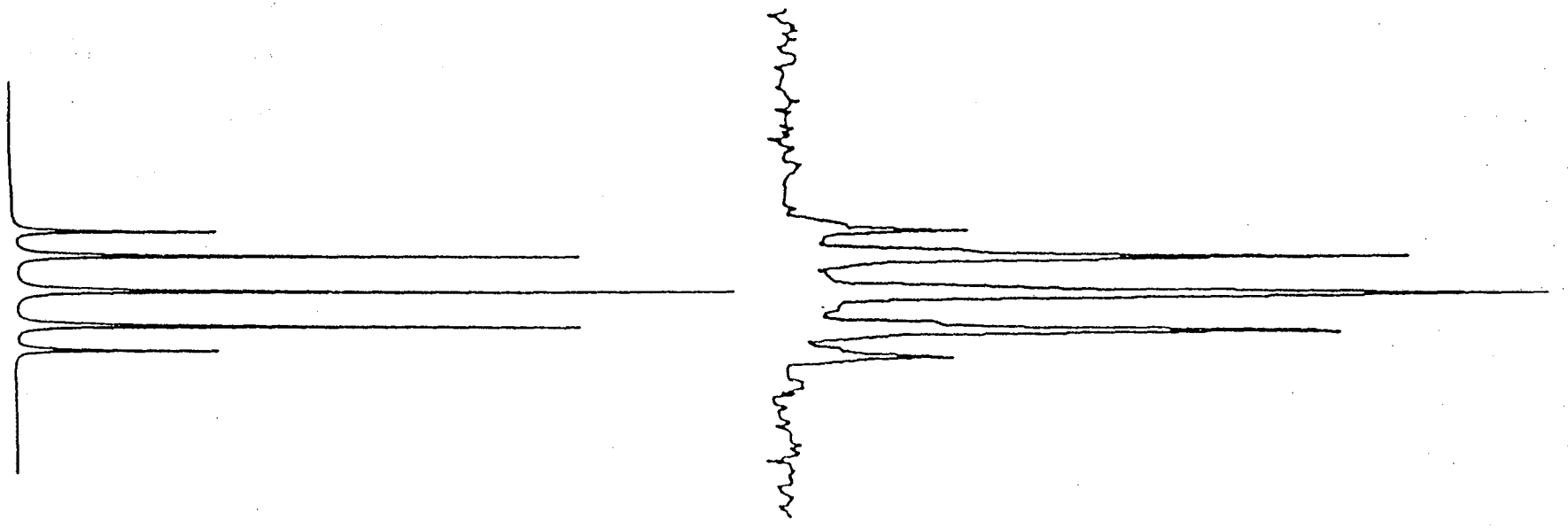

Figure 1. Experimental and calculated $^{13}C\{^{1}H\}$ NMR resonances due to the $P(CH_3)_3$ ligands for $(C_5(CH_3)_5)Ir(P(CH_3)_3)_2ClPF_6$, 1.

forms the new complex $(C_5(CH_3)_5)Ir(P(CH_3)_3)_2HBF_4$, **2**, along with one equivalent of $(C_5(CH_3)_5)Ir(P(CH_3)_3)H_2$ to account for all the iridium (Scheme 2). The product is a crystalline, colorless salt stable to air for reasonable periods in the solid state; acetone solutions of 2 decompose in air over days. In general, the compound exhibits spectral properties similar to $(C_5(CH_3)_5)Ir(P(CH_3)_3)_2ClPF_6$: virtual triplets are observed in both the ^1H and $^{13}C\{^1H\}$ NMR spectra for the $P(CH_3)_3$ fragment, while the $C_5(CH_3)_5$ and Ir-H resonances in the ^1H NMR spectrum appear as binomial triplets with ^{31}P-^1H couplings within the normal range.

Maitlis and coworkers reported the synthesis of the unstable solvent complex $(C_5(CH_3)_5)Ir(acetone)_3^{2+}$, prepared by the silver-induced loss of chloride from $[(C_5(CH_3)_5)IrCl_2]_2$.[17] We have found that replacement of the solvent ligands with $P(CH_3)_3$ occurs at room temperature, yielding the very stable trisphosphine salt $(C_5(CH_3)_5)Ir(P(CH_3)_3)_3(BF_4)_2$, **3** (Scheme 3). The dicationic salt does not decompose in water or air (in fact, water is by far the best solvent for the complex), and may be heated to 280 °C in the solid state without noticable decomposition. Presumably, the cation adopts a "three-legged piano stool" structure, with the anions well-separated in aqueous solution; the $^{31}P\{^1H\}$ NMR spectrum shows a single resonance, implying that the phosphine ligands are equivalent. Solubility problems and the complexity of the room temperature ^1H and $^{13}C\{^1H\}$ NMR spectra due to virtual coupling of the phosphorus atoms to the phosphine methyl hydrogen and carbon atoms discouraged us from attempting low temperature NMR experiments.

Scheme 2

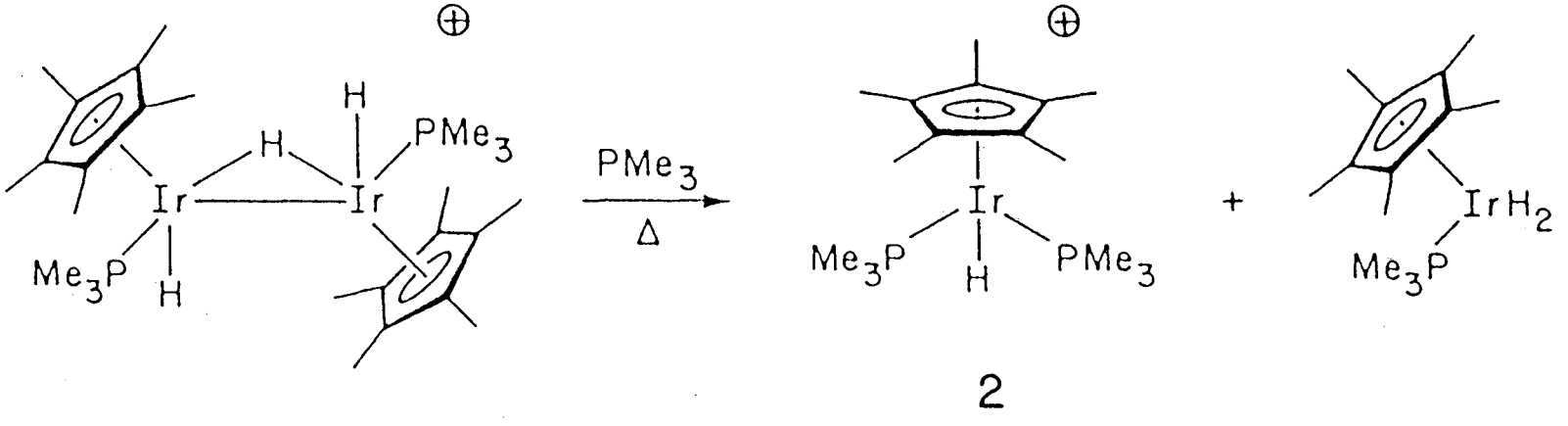

2

Scheme 3

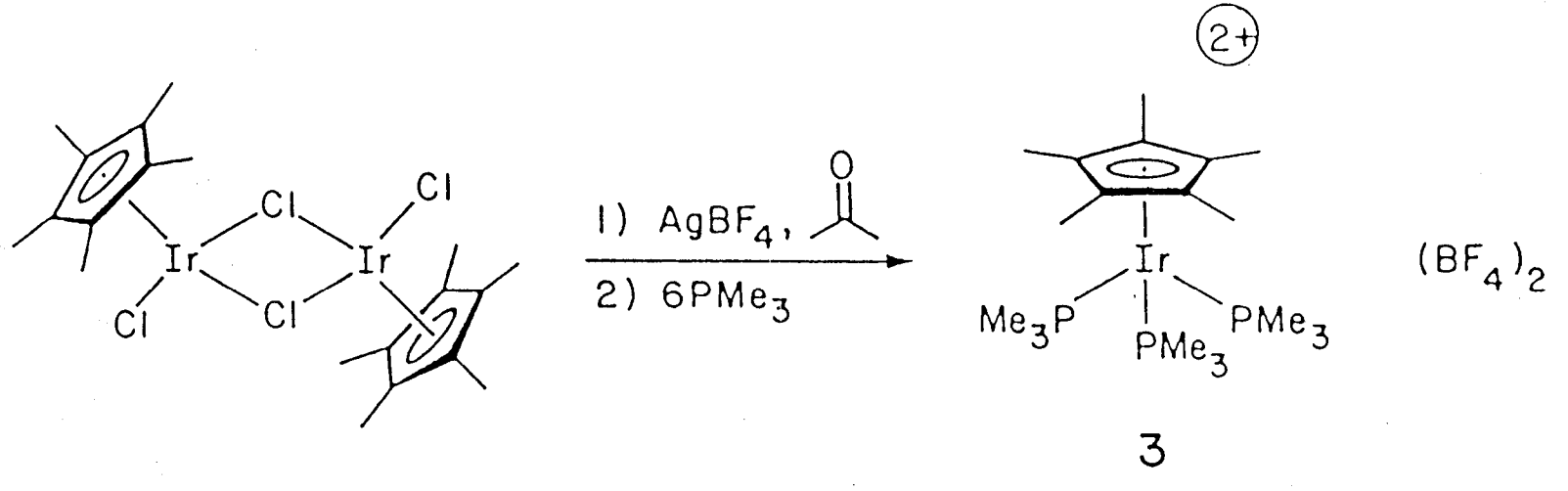

3

We have prepared the new organometallic salts $(C_5H_5)Ir(P(CH_3)_3)_2HBF_4$ and $(C_5H_5)Ir(P(CH_3)_3)_2(CH_3)(O_3SCF_3)$ by treating the metal base $(C_5H_5)Ir(P(CH_3)_3)_2$[13] with the strong electrophiles HBF_4 and $CH_3O_3SCF_3$ in the manner of Werner and coworkers.[1] The white, crystalline complexes are easy to handle, being quite air-stable in the solid state, stable to and soluble in acetone, and insoluble in ether. Like the analogous $C_5(CH_3)_5$-substituted iridium compounds, the phosphine ligands give rise to complex patterns in the ^1H and $^{13}C\{^1H\}$ NMR spectra.

As a check of the generality of our results, we have also prepared the (1,5-cyclooctadienyl)iridium (1,5-cyclooctadienyl = cod) salt $(cod)Ir(P(CH_3)_3)_3Cl$. This appears to be an unknown material, although numerous phosphine and phosphite analogues have been synthesized.[20] The complex almost certainly exists in a pseudo-trigonal bipyramidal form, with the cod ligand and one phosphine ligand occupying the equatorial sites and the other two phosphines the axial sites; however, the complex (and nearly all its analogues) is evidently quite fluxional at ambient temperature, as the ^1H, $^{13}C\{^1H\}$, and $^{31}P\{^1H\}$ NMR spectra all indicate the phosphine ligands to be equivalent. A Berry-type pseudorotation process probably equilibrates the ligands.[20] Interestingly, this salt is the only iridium-containing material we prepared to show the effect of a significant isotope shift in the $^{13}C\{^1H\}$ NMR spectrum; the pattern corresponding to the phosphine ligands is far more complex than that for $(C_5(CH_3)_5)Ir(P(CH_3)_3)_3^{2+}$, and shows the asymmetry characteristic of AXY_2 systems as observed for $(C_5H_5)Re(P(CH_3)_3)_3$.[21]

Structural Features of $(C_5(CH_3)_5)Ir(P(CH_3)_3)_2ClPF_6$.

The full report of the single-crystal X-ray diffraction study will appear in Acta Crystallographica, Section C.[15] Therefore, only a short description is given.

The complex crystallizes as well-separated cations and anions in the space group $P2_1/n$. The PF_6^- anion is either thermally "moving" or slightly disordered, but appears essentially octahedral, with the average P-F distance 1.559[22] Å.[22]

The organometallic cation crystallizes as a pseudo-octahedron, with the pentamethylcyclopentadienyl ring occupying an octahedral face (Figure 2). The centroid of the ring is 1.875 Å from the iridium center, and the ring methyl groups are bent slightly "away" from the metal. In order to minimize steric interactions, the phosphine ligands are bent away from each other (P-Ir-P = 96.40(5)°), thereby closing the phosphorus atoms in toward the chlorine atom (average P-Ir-Cl = 86.3[6]°). The bond distances appear normal, although surprisingly, the Ir-Cl distance (2.410(1) Å) is significantly longer than the average Ir-P distance (2.295[8] Å), the opposite of what one would expect based on covalent bonding radii.[23]

Calculation of J_{PC}, $J_{P'C}$ and $J_{PP'}$ for Polyphosphine Complexes.

Typically, the complexes containing phosphine ligands bound to iridium or ruthenium investigated in this study give rise to five-line AXX' patterns in the $^{13}C\{^1H\}$ NMR spectrum (Figure 1), while the rhenium complexes exhibit six-line AXY patterns. This observation indicates that for some reason, the "isotope shift" is consistently larger for rhenium complexes than for iridium or ruthenium complexes.

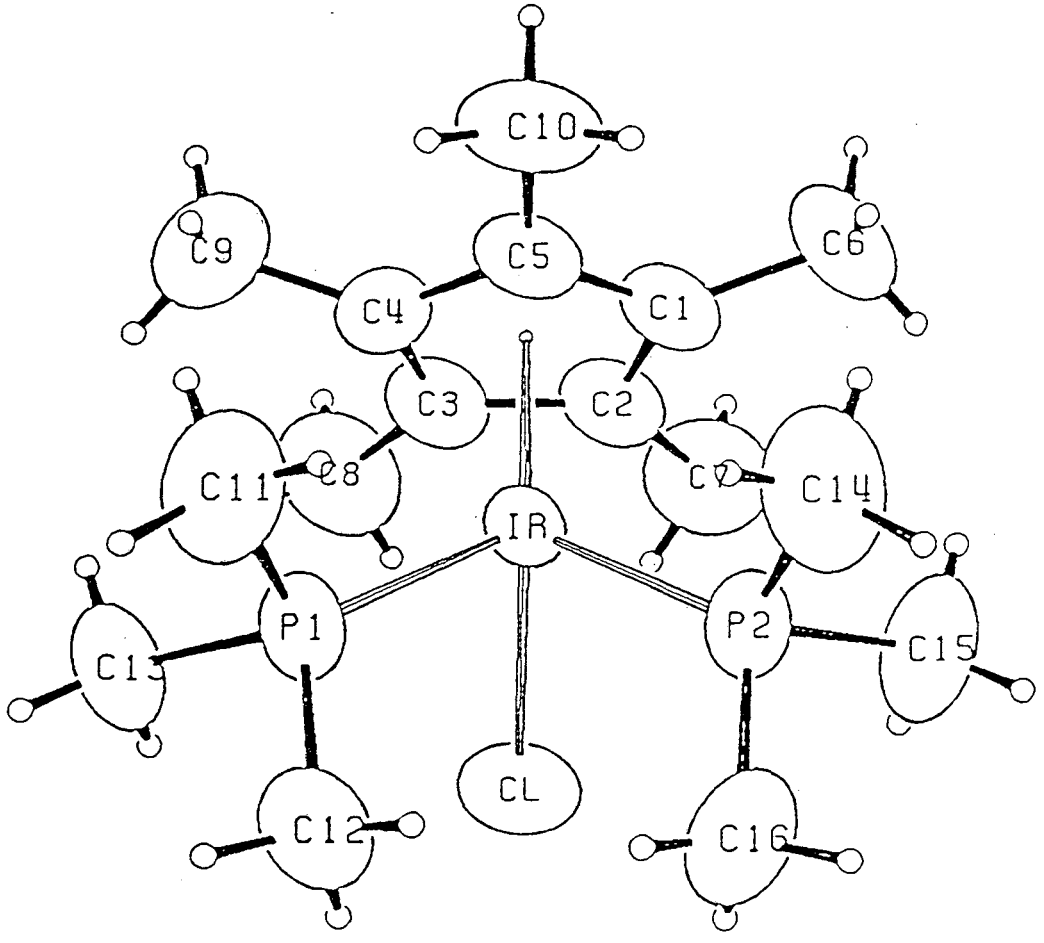

Figure 2. ORTEP drawing of $(C_5(CH_3)_5)Ir(P(CH_3)_3)_2ClPF_6$, **1** ($PF_6$ anion not shown).

Employing the formulae[10,12] as required by the system, we have determined the three coupling constants J_{PC}, $J_{P'C}$ and $J_{PP'}$ for eighteen compounds (Table 1). Though this data set is too small to allow demonstration of the effects of all possible factors, some conclusions may be drawn.

Statistically,[24] the type of cyclopentadiene ring appears to have no effect on the coupling constants. Overall, J_{PC} = 33[4] Hz and $J_{PP'}$ = 23[4] Hz for $(C_5H_5)M$ species, while the values are 38[5] Hz and 28[10] Hz respectively for $(C_5(CH_3)_5)M$ species. No significant difference exists between these sets of values. A more strict comparison may be made between $(C_5H_5)Ir$ and $(C_5(CH_3)_5)Ir$ complexes; the former exhibit J_{PC} = 38[4] Hz and $J_{PP'}$ = 24[5] Hz, while the latter show J_{PC} = 41[3] Hz and $J_{PP'}$ = 22[3] Hz. These averages are clearly indistinguishable statistically.

This result is surprising on both steric and electronic bases. The $C_5(CH_3)_5$ ligand is certainly more bulky than the C_5H_5 ligand, and thus complexes containing the former ring would be expected to have more "pushed-in" phosphine ligands, and therefore smaller P-M-P bond angles, than those containing the latter ring. Apparently $J_{PP'}$ is not sensitive to this angle. Electronically, the $C_5(CH_3)_5$ ligand is felt to be more electron-donating to a metal center than the C_5H_5 ligand; evidently the effect of a more electron-rich metal center is not reflected in the ligand couplings.

We can study in part the variation in coupling constants vs. the number of nonphosphine "piano-stool leg" ligands L. All rhenium complexes for which the values were determined have L = 2, and thus

Table 1.

Complex[a]	N[b]	$\lvert J_{PC} \rvert$[c]	$\lvert J_{P'C} \rvert$[c]	$\lvert J_{PP'} \rvert$[d]	Ref.
$CpReL_2(C_2H_4)$	31.2	29	2	26	e
$CpReL_2H_2$	30.8	31	1	17	e
$CpReL_2(CH_3)(H)$	29.2	31	2	17	e
$CpReL_2(C_2H_3)(H)$	31.5	31	0	16	e
$CpReL_2(c\text{-}C_3H_5)(H)$	29.4	31	1	18	e
$CpReL_2(C_6H_5)(H)$	31.0	32	1	18	e
$CpReL_2(n\text{-}C_6H_{13})(H)$	29.5	30	0	16	e
$Cp^*RuL_2(CN)$	28.7	31	3	40	f,j
$Cp^*RuL_2(NCCH_3)^+$	29.2	33	4	42	f,j
$CpIrL_2$	35.6	34	1	28	g,j
$CpIrL_2(H)^+$	43.0	41	2	19	j
$CpIrL_2(CH_3)^+$	41.2	40	2	24	j
Cp^*IrL_2	33.9	37	3	21	h,j
$Cp^*IrL_2H^+$	41.6	41	1	18	j
$Cp^*IrL_2Cl^+$	40.9	42	1	28	j
$Cp^*IrL_2(CH_3)^+$	39.6	41	1	21	h,j
$Cp^*IrL_3^{2+}$	-	42	0	23	j
$(cod)IrL_3^+$	-	32	3	21	j

a) Cp = C_5H_5; Cp^* = $C_5(CH_3)_5$; cod = 1,5-c-C_8H_{12}; L = $P(CH_3)_3$
b) $N = \lvert J_{PC} + J_{P'C} \rvert$
c) Values $\pm$ 2 Hz; see Experimental.
d) Values $\pm$ 1 Hz; see Experimental.
e) Wenzel, T. T.; Bergman, R. G.; unpublished work.
f) Seidler, M. D.; Bergman, R. G.; unpublished work.
g) Buchanan, J. M.; Bergman, R. G.; unpublished work.
h) McGhee, W. D.; Bergman, R. G. J. Am. Chem. Soc. 1985, 107, 3388.
j) This work.

are not amenable to study. Focusing on the iridium compounds in Table 1, we find, for N = 0, J_{PC} = 35[2] Hz and $J_{PP'}$ = 25[5] Hz, while for N = 1, J_{PC} = 40[4] Hz and $J_{PP'}$ = 22[3] Hz. Again, no significant difference exists between these sets of values, demonstrating that the orbital distinctions between the two types of complexes are not reflected in the coupling constants. Also, evidently the formal oxidation state of the metal is unimportant, as no difference exists between the coupling constants for neutral iridium (I) species and cationic iridium (III) species.

The only obvious distinction which can be made is that different metal centers give rise to complexes with markedly different coupling constants. In general, the scatter of values for a particular metal center is gratifyingly small, and quite different from those for other metal centers. For iridium complexes, J_{PC} = 39[4] Hz and $J_{PP'}$ = 23[4] Hz, while for ruthenium complexes the values are 32[2] Hz and 41[2] Hz respectively, and for rhenium complexes the values are 31[1] Hz and 18[4] Hz respectively. Clearly J_{PC} is largest for iridium compounds and essentially equal for ruthenium and rhenium compounds, while $J_{PP'}$ is smallest for rhenium compounds, followed closely by iridium compounds. Both $J_{PP'}$ values are very different from the large value for ruthenium compounds. Since the types of rings and the coordination number of the metal centers appear to be unimportant, this result suggests that subtle, metal-based electronic factors lie at the heart of the coupling constant variations. The data are insufficient to properly define these factors; however, it is clear that any attempt to understand these results on a

theoretical basis must explain the coupling constants based on the metal centers involved.

Conclusion

Of note in this Chapter is the presumably significant electron density forced on the iridium center by the strongly donating $C_5(CH_3)_5$ and $P(CH_3)_3$ ligands. One would predict that at some point the metal center would become too electron-rich to support all the ligands; clearly this point is not reached in any of the complexes described. The fact that in most cases the iridium center is formally cationic certainly contributes to the stability of these species; however, comparison with the related complexes $(C_5(CH_3)_5)Co(P(CH_3)_3)_2$,[5a] $(C_5(CH_3)_5)Rh(P(CH_3)_3)_2$,[5b] and $(C_5(CH_3)_5)Ir(P(CH_3)_3)_2$,[25] as well as $Co(P(CH_3)_3)_4$[6] and the $M(P(CH_3)_3)_4Cl$ series (M = Rh,[7] Ir[2]), indicates a remarkable ability of cobalt family metals to accept electron density. Undoubtably, the use of such complexes as metal bases will continue to be an important area of study.

References.

(1) Werner, H. Angew. Chem., Intl. Ed. Engl. **1983**, 22, 927, and references therein.

(2) Thorn, D. L. Organometallics **1982**, 1, 197.

(3) Milstein, D. J. Am. Chem. Soc. **1982**, 104, 5227.

(4) Gibson, V. C.; Grebenik, P. D.; Green, M. L. H. J. Chem. Soc., Chem. Commun. **1983**, 1101.

(5) (a) Werner, H.; Heiser, B.; Klingert, B.; Dolfel, R. J. Organomet. Chem. **1982**, 240, 179. (b) Klingert, B.; Werner, H. Chem. Ber. **1983**, 116, 1450.

(6) Rakowski, M. C.; Muetterties, E. L. J. Am. Chem. Soc. **1977**, 99, 739.

(7) Jones, R. A.; Mayor Real, F.; Wilkinson, G.; Galas, A. M. R.; Hursthouse, M. B.; Abdul Malik, K. M. J. Chem. Soc., Dalton Trans. **1980**, 511.

(8) (a) Harris, R. K. Can. J. Chem. **1964**, 42, 2275. (b) Aime, S.; Harris, R. K.; McVicker, E. M.; Fild, M. J. Chem. Soc., Dalton Trans. **1976**, 2144.

(9) (a) Bertrand, R. D.; Ogilvie, F. B.; Verkade, J. G. J. Am. Chem. Soc. **1970**, 92, 1908. (b) Ogilvie, F. B.; Jenkins, J. M.; Verkade, J. G. J. Am. Chem. Soc. **1970**, 92, 1916.

(10) Redfield, D. A.; Nelson, J. H.; Cary, L. W. Inorg. Nucl. Chem. Lett. **1974**, 10, 727.

(11) Becker, E. D. "High Resolution NMR: Theory and Chemical Applications"; Academic Press: New York, 1980. Chapter 7.17.

(12) Gunther, H. "NMR Spectroscopy: An Introduction"; John Wiley and Sons: New York, 1980. Section 5.2.3

(13) Buchanan, J. M.; Bergman, R. G., unpublished work.

(14) Kang, J. W.; Moseley, K.; Maitlis, P. M. J. Am. Chem. Soc. 1969, 91, 5970.

(15) Kaner, R. B.; Kouvetakis, J.; Mayorga, S. G. Acta Crystallographica, Sec. C: Crystal Struc. Commun., submitted.

(16) (a) Janowicz, A. H.; Bergman, R. G. J. Am. Chem. Soc. 1982, 104, 351. (b) Janowicz, A. H.; Bergman, R. G. J. Am. Chem. Soc. 1983, 105, 3929.

(17) White, C.; Thompson, S. J.; Maitlis, P. M. J. Organomet. Chem. 1977, 127, 415.

(18) Herde, J. L.; Lambert, J. C.; Senoff, C. V. Inorg. Syn. 1974, 15, 18.

(19) While not precisely a three line pattern, the term "virtual triplet" has been used to describe $X_nAA'X'_n$ spectra. See: (a) Tilley, T. D.; Grubbs, R. H.; Bercaw, J. E. Organometallics 1984, 3, 274. (b) Seidler, M. D.; Bergman, R. G. J. Am. Chem. Soc. 1984, 106, 6110.

(20) Haines, L. M.; Singleton, E. J. Chem. Soc., Dalton Trans. 1972, 1891.

(21) Bergman, R. G.; Seidler, P. F.; Wenzel, T. T. J. Am. Chem. Soc., in press.

(22) Throughout this thesis, esds for average values are given in brackets, and are calculated from the scatter formula:

$$[\sigma] = [(\Sigma (x_i - \bar{x})^2)/ N - 1]^{1/2}$$

Esds for individual values will be given as usual in parentheses.

(23) Huheey, J. E. "Inorganic Chemistry"; Harper and Row: New York, 1978. Chapter 6.

(24) Statistical significance of differences was determined employing the null hypothesis with at least a 95% confidence level. See: Skoog, D. A.; West, D. M. "Fundamentals of Analytical Chemistry"; Holt, Rinehart and Winston: New York, 1976. Chap. 4.

(25) McGhee, W. D.; Bergman, R. G. J. Am. Chem. Soc. 1985, 107, 3388.

Chapter 3. Preparation and Reactions of Tetrahydrido(pentamethylcyclopentadienyl)iridium: A Novel Iridium (V) Polyhydride.

Introduction

Few examples exist of organometallic complexes of late transition metals in high oxidation states. Comparison with high-valent complexes of early transition metals suggests that such compounds, especially those of group 8B, might be expected to possess unique properties and reactivities.

Phosphine-stabilized iridium (V) hydrides have been known since the early 1970's[1] and were shown somewhat later to catalyze H/D exchange with deuterated solvents at elevated temperatures.[2] Recently, Maitlis and coworkers demonstrated the accessibility of pentamethylcyclopentadienyl-substituted organoiridium (V)[3] and organorhodium (V)[4] complexes, noting intriguing products upon pyrolysis of the remarkably stable compound $(C_5(CH_3)_5)Ir(CH_3)_4$.[3] However, examples of this type of complex are still relatively rare.

As part of our studies of the synthesis and reactivity of iridium hydride complexes, we report the synthesis of the photoactive complex $(C_5(CH_3)_5)IrH_4$ (2, Scheme 1). This material represents an unusual example of an iridium (V) organometallic polyhydride, and exhibits several interesting thermal and photochemical reactions.

Experimental

General. Experimental and characterization methods were described in Chapter 1. Dimethyl ether was vacuum distilled from sodium benzophenone ketyl. The photolysis apparatus was described by Janowicz and Bergman.[5] UV spectra were recorded on a Hewlett-Packard 8450A UV-VIS spectrophotometer.

$(C_5(CH_3)_5)IrH_4$, (2). A slurry of $[(C_5(CH_3)_5)Ir]_2(\mu\text{-}H)_3PF_6$ ($1\cdot PF_6$, Chapter 1) (2.01 g, 2.50 mmol) in hexane (200 mL) was cooled to -40 °C, then treated dropwise with $LiEt_3BH$ (15 mmol) from which most of the THF had been removed and replaced with an equivalent volume of toluene. Overnight stirring at room temperature resulted in a deep orange, homogeneous solution which was cooled to -40 °C, then filtered through hexane-wetted alumina III packed in a frit. The alumina was washed with benzene to give a pale yellow solution. Removal of the solvent from the combined solutions and two sublimations of the yellow-white residue (30-40 °C, 100 mtorr) gave 1.23 g (3.71 mmol, 74%) of pure white crystals.

^1H NMR (C_6D_6): δ 1.99 (s, 15H, C_5Me_5); -15.43 (s, 4H, Ir-H). $^{13}C\{^1H\}$ NMR (C_6D_6): δ 96.5 (s, $\underline{C}_5Me_5$); 10.0 (s, $C_5\underline{Me}_5$). IR (KBr): ν_{Ir-H} 2150 cm^{-1}. UV (C_6H_{12}): λ_{max}=215 nm (ε=5000). EIMS (25 °C, 30 eV): 332, 330, 328, 326, 324, 322. MW (Signer[6] method, CH_3OCH_3, 25 °C): calcd 331, found 327 ± 15. Anal. Calcd for $C_{10}H_{19}Ir$: C, 36.24; H, 5.78. Found: C, 35.98; H, 5.83. Solid state decomposition temperature: 50-100 °C.

Thermal Reaction of 2 with $P(CH_3)_3$. Trimethylphosphine (0.54 mmol) was condensed at liquid nitrogen temperature into a toluene-d_8

solution of **2** (6.5 mg, 0.020 mmol) in an NMR tube. The tube was flame sealed, warmed carefully to room temperature, then heated to 60 °C for 13 h. At this point, no reaction was observed by ^{1}H NMR spectroscopy. The sample was then heated to 110 °C for 44 h, at which point inspection of the ^{1}H NMR spectrum demonstrated $(C_5(CH_3)_5)Ir(P(CH_3)_3)H_2$[5] to be the sole product.

Photochemical Reaction with $P(CH_3)_3$. The reaction solution was prepared in an NMR tube as above. Irradiation for 1 h resulted in a pale yellow solution. Inspection of the ^{1}H NMR spectrum of this solution demonstrated complete loss of starting material and sole production of $(C_5(CH_3)_5)Ir(P(CH_3)_3)H_2$.

Thermal Reaction of 2 with CO. Carbon monoxide (0.16 mmol) was expanded onto a frozen toluene-d_8 solution of **2** (6.6 mg, 0.020 mmol) in an NMR tube. The tube was sealed, warmed carefully to room temperature, and stored in the dark. Inspection of the ^{1}H NMR spectrum after 24 h demonstrated nearly complete conversion of starting material to $(C_5(CH_3)_5)Ir(CO)H_2$.[7] After 72 h, inspection of the ^{1}H NMR spectrum demonstrated complete conversion to the dicarbonyl $(C_5(CH_3)_5)Ir(CO)_2$.[8] This was confirmed by IR spectroscopy.

Photochemical Reaction with CO. The reaction solution was prepared in an NMR tube as above. Irradiation for 30 min resulted in approximately 30% conversion of tetrahydride to $(C_5(CH_3)_5)Ir(CO)H_2$. Irradiation continued for an additional 2 h, at which point ^{1}H NMR and IR spectroscopies demonstrated sole production of $(C_5(CH_3)_5)Ir(CO)_2$.

Reaction of 2 with CCl_4. CCl_4 (1 mL) was vacuum transferred onto a benzene solution of **2** (73.7 mg, 0.222 mmol). Upon warming, the solution immediately became deep blue/purple, indicating the production of $[(C_5(CH_3)_5)IrCl]_2(\mu\text{-}H)_2$[9] and $[(C_5(CH_3)_5)IrCl]_2(\mu\text{-}H)(\mu\text{-}Cl)$.[10] The presence of these materials was confirmed by ^1H NMR spectroscopy in a separate experiment. The solution was heated to 60 °C for 17 h, at which point the reaction had become orange and orange solid had precipitated. The solvent was evaporated, and the residue recrystallized from hot methanol. Two crops of orange solid were filtered, washed with ether, and dried to give 82 mg (0.10 mmol, 92%) of $[(C_5(CH_3)_5)IrCl_2]_2$,[8a] shown to be pure by ^1H NMR spectroscopy.

Thermal Reaction of 2 with D_2. A toluene solution of **2** (66.3 mg, 0.200 mmol) was degassed with three freeze/pump/thaw cycles, then treated with D_2 (1.56 mmol). The reaction mixture was warmed to 60 °C for 25 h, then cooled to ambient temperature. The solvent was evaporated and the residue sublimed as for **2** to give extensively deuterated **2-d_x** in chemically pure form (54 mg, 0.16 mmol, 80%). This material was shown to be 83% deuterated by integration of the hydride resonance against the $C_5(CH_3)_5$ resonance in the ^1H NMR spectrum; lack of deuteration on the ring was confirmed by ^2H NMR and IR spectroscopies. ^1H NMR (C_6D_6): δ 1.99 (s). ^2H NMR (C_6H_6): δ -15.34 (br s). IR (KBr): ν_{Ir-D} 1555 (s), 1545 (sh) cm^{-1}; ν_H/ν_D = 1.38.

Photochemical Reaction with D_2. A reaction solution was prepared as above, except that the amount of D_2 (3.6 mmol) was

increased. The sample was irradiated for 20 min, after which the D_2 was removed and additional D_2 (5.2 mmol) was added. Irradiation continued for an additional 30 min, giving an orange-red solution. Volatile materials were evaporated, and the residue was sublimed as for **2** to give white product (51 mg, 0.15 mmol, 76%). Integration of the hydride resonance against the $C_5(CH_3)_5$ resonance in the ^1H NMR spectrum demonstrated the product to be 57% deuterated; lack of deuteration on the ring was confirmed by ^2H NMR and IR spectroscopies.

Reaction of 2 with CD_3OD. A CD_3OD solution of **2** (6.6 mg, 0.020 mmol) in an NMR tube was stored in the dark. Inspection of the ^1H NMR spectrum after four days showed complete disappearance of the hydride resonance, whereas the $C_5(CH_3)_5$ resonance was unaffected. The solvent was evaporated and the residue sublimed to give **8**. This material was shown to be > 95% deuterated solely at the hydride positions by ^1H and ^2H NMR spectroscopies.

Single Crystal X-ray Diffraction Study of 2. Large clear colorless crystals of the compound were obtained by slow sublimation in vacuo. Fragments cleaved from some of these crystals were mounted in capillaries in air, as decomposition was slow. The crystals were imbedded in Apiezon grease in one end of the capillary, which was then flushed with nitrogen gas and flame sealed. Initial examination of the crystals via photographs was performed at room temperature. All diffractometer work was performed at -150 ± 2 °C.[11] Preliminary precession photographs indicated some problems with pseudo-orthorhombic twinning, true monoclinic Laue symmetry, and yielded

preliminary cell dimensions. Systematic absences were consistent only with space group $P2_1/n$. Inspection of the Niggli values revealed no conventional cells of higher symmetry.

Each crystal used for data collection was mounted as described above and centered in the beam of the Enraf-Nonius CAD-4 diffractometer.[12] Automatic peak search and indexing procedures yielded the monoclinic reduced primitive cell, except for those samples of poor quality. All data were collected using the same diffractometer parameters and standards (Table 1). The cell parameters given in the table are those appropriate to the final refinement.

During the process of data collection it was noted that the intensity of the standards changed with time, that the widths of the peaks systematically increased, and that those reflections with high k increased more rapidly in width than those with low k. Due to this decay, it was necessary to use two crystals to obtain a complete unique set of data. The first crystal, used to collect data for $2\theta < 45°$, evidently suffered some exposure to air, for it became intensely colored just before becoming unsuitable for data collection. The second crystal, used first to collect data for $45° < 2\theta < 55°$ and then to resume the low angle data collection, remained colorless during its decay. Under optical examination at the end of data collection it displayed numerous striations aligned normal to the b axis. Further attempts to collect data were cancelled for monetary reasons.

Table 1. Crystal and Data Collection Parameters

Compound: $H_4Ir(C_5Me_5)$

A) Crystal Parameters @ -150°C [a)b)]

a = 16.7466(25)Å	Space Group: $P2_1/n$
b = 7.6224(15)Å	Formula weight: 331.46 amu
c = 17.0821(30)Å	Z = 8
β = 101.406(13)°	d (calc.) = 2.060 gcm^{-3}
V = 2137.5(12)$Å^3$	μ (calc.) = 123.9 cm^{-1}

Size: 0.25 x 0.28 x 0.45 mm

B) Data Measurement Parameters

Diffractometer: Enraf-Nonius CAD-4

Radiation: Mo Kα (λ=0.71073Å)

Monochrometer: Highly-oriented graphite ($2\theta_m$=12.2)
Perpendicular mode, assumed 50% perfect.

Detector: Crystal scintillation counter, with PHA.

Aperture → crystal = 173 mm. Vertical aperture = 3.0 mm.

Horizontal Aperture = 2 + 1 tan (θ) mm (variable).

Reflections measured: -H +K ±L

2θ Range: 45° → 55° Scan type: θ -2θ

Scan speed: 0.80 → 6.7 (θ, deg./min)

Scan width: Δθ = 0.6 + .347 tan (θ)

Background: Measured over an additional 0.25 (Δθ) added to each end of the scan.

No. of unique reflections: 2103 (1446 $F^2 > 3\sigma(F^2)$)

Intensity standards: 6 1 -11, 0 5 -2, 9 0 3; measured every 2 hours of x-ray exposure time.. Over the period of data collection complex decay in intensity was observed.

Orientation: 3 reflections were checked after every 150 measurements. Crystal orientation was redetermined if any of the reflections were offset from their predicted positions by more than 0.13°. Reorientation was needed several times during data collection.

---

a) Unit cell parameters and their esd's were derived by a least-squares fit to the setting angles of the unresolved Mo $K\bar{\alpha}$ components of 24 reflections with 2θ between 27° → 29°.

b) In this and all subsequent tables the esd's of all parameters are given in parentheses, right-justified to the least significant digit(s) given.

The raw intensity data were converted to structure factor amplitudes and their esds by correction for scan speed, background, and Lorentz and polarization effects. Inspection of the intensities of the standards showed a complex, non-linear pattern of decay for each of the two data crystals. The data were corrected isotropically for this decay. In addition, recollection of some portions of the data sets was necessary due to the loss of orientation of the crystal. These redundant data were used to check the decay correction. Inspection of the azimuthal scan data[13] showed a variation I_{min}/I_{max} = 0.70 (first crystal) and 0.48 (second crystal) for the average curve. Comparison of the azimuthal scan data taken before and after data collection on the second crystal showed that a qualitative change had taken place in the shape of the curve I_{rel} vs psi. Attempts to correct the data from the second crystal for absorption using either an average curve or the two individual curves led consistently to poorer agreement of equivalent and redundant reflections than did averaging of the uncorrected structure factors (But see below).

The structure was solved by Patterson methods using the first (low angle) data set, and refined via standard least squares and Fourier techniques while the second data set was being collected. Attempts to refine the atoms with anisotropic thermal parameters, however, led to non-positive-definite tensors for many of the carbon atoms. This data set was abandoned as useless for further refinement.

The data for the second crystal were then used to continue the

refinement, corrected for decay, but not for absorption. Indications that the low angle data were of poor quality, and the strange variation in the absorption curve from the beginning to the end of the data collection finally led to abandonment of the low angle data from the second crystal. The final refinement was performed on the 2103 unique high angle reflections from the second data set, corrected for decay and empirically corrected for absorption. The absorption correction was performed after refinement of all atoms with anisotropic thermal parameters. After correction (T_{min} = 0.51), refinement converged to the final residuals.

The quantity minimized by the least-squares program was $\Sigma w(F_o - F_c)^2$, where w is the weight of a given observation. The p factor, used to reduce the weight of intense reflections, was set to 0.05 during the high angle data refinement. The analytical forms of the scattering factor tables were used and all non-hydrogen scattering factors were corrected for both the real and imaginary components of anomalous dispersion.

The largest peak in the final difference Fourier map had an electron density of 1.46 e-/$\mathring{A}^3$ and was located near Ir2. The second largest peak (1.15 e-/$\mathring{A}^3$) was located near Ir1. There was no indication of hydrogen atoms attached to either the iridium atoms or the methyl carbons in the map.

The final residuals for 199 variables refined against the 1446 data for which $F^2 > 3\sigma(F^2)$ were R = 3.65%, R_w = 4.63%, R_{all} = 7.59%, GOF = 1.446.

Inspection of the residuals ordered in the ranges of sin θ/λ ,

F_o, and parity of the individual indexes showed no unusual features or trends. However, the value of the residuals ordered on the value of h (or data collection time; essentially the same thing given the method of collection) showed a dramatic increase for h = -3, -2, -1, and 0 (i.e. the last 300 reflections collected). Residuals calculated for the 1267 reflections with $F^2 > 3\sigma(F^2)$ and $|h| > 2$ were R = 3.02%, R_w = 3.83%, and GOF = 1.216.

Positional and thermal parameters for the refined atoms are given in Table 2.

Table 2.

Table of Positional Parameters and Their Estimated Standard Deviations

Atom	x	y	z	$B(Å^2)$
IR1	Ø.Ø8539(2)	Ø.Ø3646(5)	Ø.13955(2)	1.337(6)
IR2	Ø.36113(2)	-Ø.Ø4626(5)	-Ø.Ø8976(2)	1.353(6)
C1	Ø.Ø769(7)	-Ø.255(1)	Ø.1382(7)	1.4(2)
C2	Ø.Ø924(6)	-Ø.2Ø2(2)	Ø.22Ø3(7)	1.4(2)
C3	Ø.17Ø1(6)	-Ø.114(2)	Ø.2354(7)	1.5(2)
C4	Ø.2Ø28(6)	-Ø.119(1)	Ø.1644(7)	1.3(1)
C5	Ø.1454(6)	-Ø.2Ø6(1)	Ø.1Ø36(7)	1.1(1)
C6	Ø.ØØ69(7)	-Ø.366(2)	Ø.Ø968(7)	1.7(2)
C7	Ø.Ø4ØØ(7)	-Ø.24Ø(2)	Ø.2786(8)	1.9(2)
C8	Ø.2135(7)	-Ø.Ø52(2)	Ø.3158(7)	1.6(2)
C9	Ø.2864(6)	-Ø.Ø59(2)	Ø.1564(8)	1.8(2)
C1Ø	Ø.1564(9)	-Ø.255(2)	Ø.ØØ8(9)	2.3(2)
C11	Ø.2629(7)	Ø.1Ø4(1)	-Ø.17Ø1(7)	1.5(2)
C12	Ø.3352(7)	Ø.111(2)	-Ø.2Ø36(7)	1.6(2)
C13	Ø.3968(7)	Ø.195(2)	-Ø.1461(7)	1.6(2)
C14	Ø.3624(8)	Ø.245(2)	-Ø.Ø791(8)	1.8(2)
C15	Ø.2789(6)	Ø.189(2)	-Ø.Ø937(6)	1.4(2)
C16	Ø.1823(8)	Ø.Ø46(2)	-Ø.2151(9)	2.2(2)
C17	Ø.3419(9)	Ø.Ø63(2)	-Ø.2876(8)	2.4(2)
C18	Ø.48Ø3(8)	Ø.252(2)	-Ø.158(1)	2.8(3)
C19	Ø.4Ø14(9)	Ø.357(2)	-Ø.ØØ8Ø(9)	2.5(2)
C2Ø	Ø.2178(8)	Ø.222(2)	-Ø.Ø431(9)	2.5(2)

Anisotropically refined atoms are given in the form of the isotropic equivalent thermal parameter defined as:

$$(4/3) * [a^2 * B(1,1) + b^2 * B(2,2) + c^2 * B(3,3) + ab(\cos \text{gamma}) * B(1,2) + ac(\cos \text{beta}) * B(1,3) + bc(\cos \text{alpha}) * B(2,3)]$$

C2Ø	Ø.2178(8)	Ø.222(2)	-Ø.Ø431(9)	2.5(2)

Results and Discussion.

A search of the available literature indicated that no neutral iridium compounds containing only pentamethylcyclopentadienyl and hydride ligands were known. In 1973, however, White, Oliver and Maitlis[14] reported the synthesis of the cationic salt $[(C_5(CH_3)_5)Ir]_2H_3PF_6$, **1**, which seemed a viable precursor for a neutral complex of the proper formula. Accordingly, we treated a hexane slurry of the cation with six equivalents of $LiEt_3BH$ (Scheme 1) and allowed the resulting orange-red solution to stir overnight. Rapid chromatography through alumina III, followed by removal of solvent and sublimation of the residue gave the neutral iridium (V) tetrahydride $(C_5(CH_3)_5)IrH_4$, **2**, in good yield.

The polyhydride **2** is highly soluble in most common solvents, which hampered the isolation of single crystals. However, extremely slow sublimation (5 mtorr) on a warmed surface in a Pyrex NMR tube yielded crystals suitable for structure determination.

The single crystal X-ray diffraction study was performed at -150 °C. Even at this temperature, complex decomposition was observed in the X-ray beam over the data collection period. Three data sets were collected. An initial low angle set was discarded during refinement due to difficulties caused by the decomposition. Both a high angle and low angle set were collected on a second crystal; of these, the high angle set proved most amenable to a reasonable solution of the structure.

The tetrahydride crystallizes with two well-separated molecules in the asymmetric unit (Figure 1). The average Ir-C (ring) distance

Scheme I

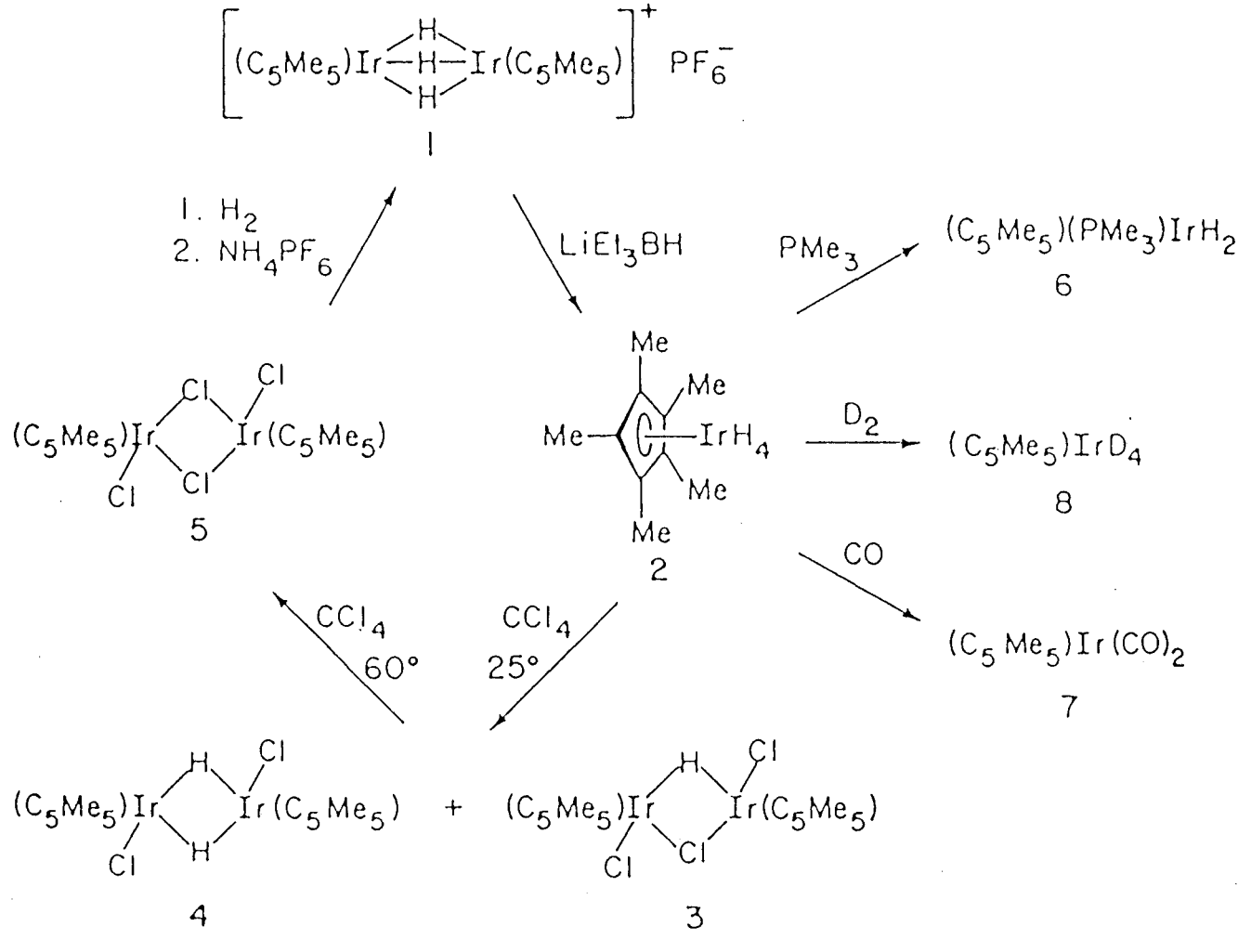
[(C5Me5)Ir(H)2Ir(C5Me5)]+ PF6−
1
1. H2
2. NH4PF6
LiEt3BH
PMe3
(C5Me5)(PMe3)IrH2
6
(C5Me5)Ir(Cl)2Ir(C5Me5)
5
IrH4
D2
(C5Me5)IrD4
8
2
CO
(C5Me5)Ir(CO)2
7
CCl4
60°
CCl4
25°
(C5Me5)Ir(H)(Cl)Ir(C5Me5)
4
+
(C5Me5)Ir(H)(Cl)Ir(C5Me5)
3

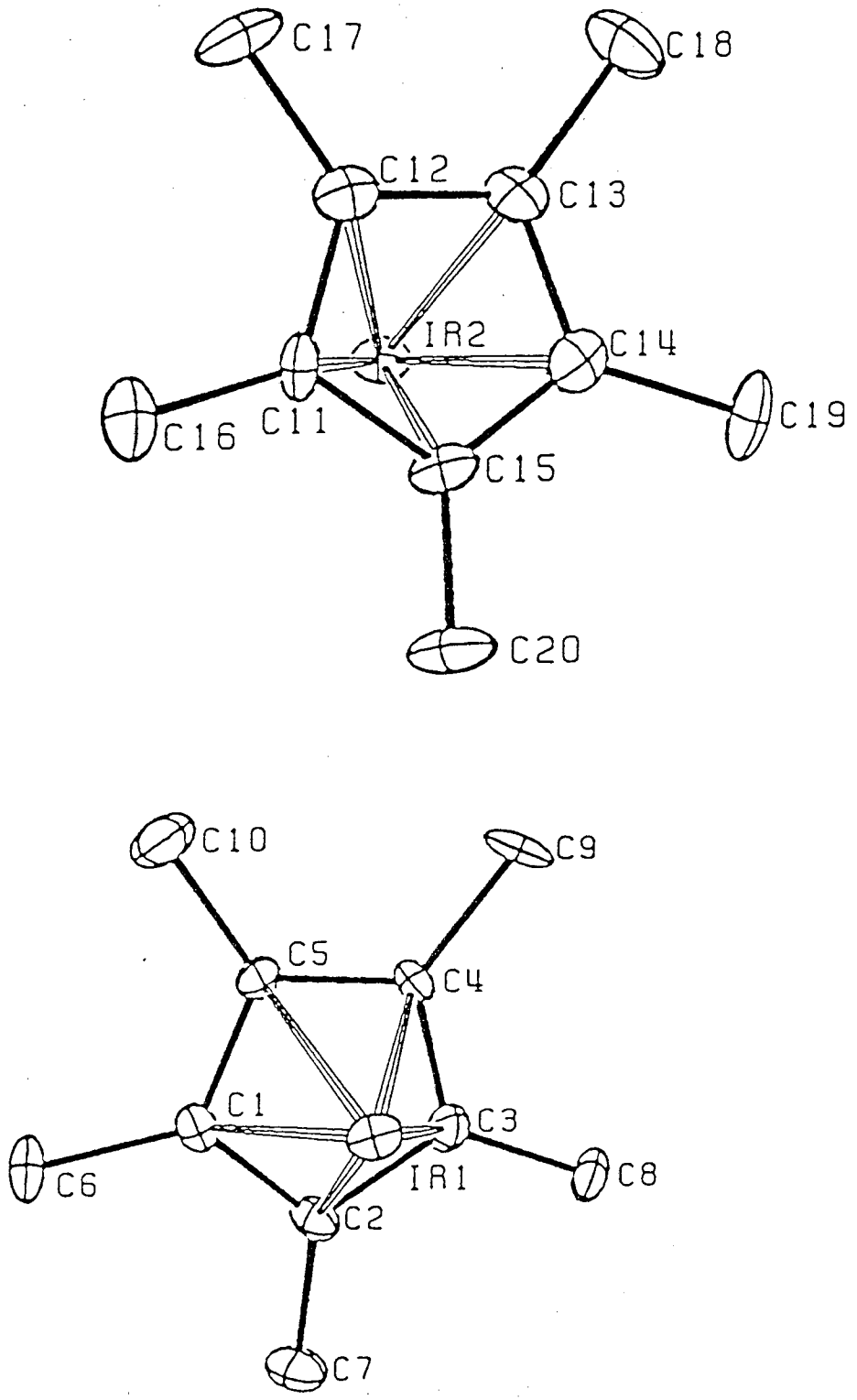

Figure 1. ORTEP drawing of $(C_5(CH_3)_5)IrH_4$, 2.

is 2.244[19] Å (range 2.224(10) - 2.271(11) Å), with the average iridium to ring centroid distance being 1.884 Å (Table 3). The carbon-carbon distances within the ring (1.443[5] Å) are normal, as are the methyl carbon-ring carbon distances (1.501[14] Å). The rings are planar to within one esd of an individual atomic distance, while the methyl carbons lie 0.10 to 0.21 Å out of the ring plane away from the iridium center.

Although the decomposition problems mentioned above prevented our locating the hydride hydrogen ligands directly, it is clear they must lie on the "open" side of the iridium atoms. The most likely arrangement is that of the four-legged piano stool, which has been shown to obtain for the closely analogous iridium (V) complex $(C_5(CH_3)_5)Ir(CH_3)_4$.[3] The closest intermolecular contacts to the iridium atoms are in the range 4.4 - 4.6 Å to the methyl groups of neighboring molecules.

Treatment of a benzene solution of **2** with excess CCl_4 at ambient temperature immediately caused the colorless solution to become bright purple; analysis of the ^1H NMR spectrum of the reaction mixture demonstrated that the compounds **3**[9] and **4**[10] were present. Heating the mixture to 60 °C for 14 h gave the well-known dimer **5**,[8a] which was isolated in 92% yield and characterized by ^1H NMR spectroscopy. This susceptibility to radical attack bears out the known sensitivity of **2** to oxygen.

The tetrahydride shows high photoactivity under reaction conditions similar to those described by Janowicz and Bergman.[5] Irradiation ($\lambda > 275$ nm; high-pressure Hg lamp, Pyrex filter) of **2** in

Table 3. Intramolecular Distances for 2.

ATOM 1	ATOM 2	DISTANCE
IR1	C1	2.224(10)
IR1	C2	2.271(11)
IR1	C3	2.256(11)
IR1	C4	2.264(10)
IR1	C5	2.244(8)
IR1	Cp1 *	1.893
IR2	C11	2.239(10)
IR2	C12	2.254(11)
IR2	C13	2.209(10)
IR2	C14	2.228(10)
IR2	C15	2.253(10)
IR2	Cp2 *	1.875
C1	C2	1.433(14)
C2	C3	1.440(12)
C3	C4	1.427(13)
C4	C5	1.428(12)
C5	C1	1.439(12)
C11	C12	1.439(13)
C12	C13	1.426(15)
C13	C14	1.432(16)
C14	C15	1.435(15)
C15	C11	1.433(14)
C1	C6	1.506(13)
C2	C7	1.480(13)
C3	C8	1.499(13)
C4	C9	1.505(11)
C5	C10	1.510(15)
C11	C16	1.483(13)
C12	C17	1.509(15)
C13	C18	1.512(16)
C14	C19	1.522(16)
C15	C20	1.485(14)

* Cp1 and Cp2 are the centroids of the cyclopentadiene rings.

the presence of $P(CH_3)_3$ in toluene smoothly generates **6** in quantitative ^1H NMR yield. Continued irradiation results in extrusion of dihydrogen and insertion of the intermediate into the carbon-hydrogen bonds of the solvent.[5] A similar irradiation of **2** in the presence of CO leads to $(C_5(CH_3)_5)Ir(CO)H_2$,[7] and then to $(C_5(CH_3)_5)Ir(CO)_2$,[8] as demonstrated by ^1H NMR and IR spectroscopies. These two experiments suggest that complex **2** extrudes dihydrogen upon irradiation, leading to the intermediate "$(C_5(CH_3)_5)IrH_2$", which is then trapped by the dative ligand.

Both of these photoreactions may be reproduced thermally at different temperatures. Surprisingly, exposure of a solution of **2** to CO at room temperature in the dark slowly leads to $(C_5(CH_3)_5)Ir(CO)H_2$ and then to $(C_5(CH_3)_5)Ir(CO)_2$ over 72 h. This reaction is unprecedented in our experience with the tetrahydride; we have been unable to duplicate this thermal ligand exchange with alkenes or isocyanides. While we cannot rule out the possibility of catalysis by a minor impurity in the CO, different sources of gas yield the same result.

In contrast, no reaction occurs between **2** and the dative ligand $P(CH_3)_3$ under these conditions; only upon elevation of the temperature to 110 °C and heating for 44 h is conversion of tetrahydride **2** to **6** observed.

The complex is capable of undergoing H/D exchange under photolysis and thermolysis conditions. Irradiation of **2** in toluene under 5 atm of D_2 for 2 H, followed by removal of solvent and sublimation of the reaction mixture led to a partially deuterated

analogue of 2 in 76% yield. Spectral analysis indicates 57% deuteration of the hydride ligands, and no deuteration of the ring methyl groups.[15] The extent of deuteration is limited by competitive formation of a burgundy complex during irradiation; this material seems to be a hydride-deficient iridium cluster but as yet has defied isolation due to its extreme solubility.

A more highly deuterated analogue of 2 may be prepared through thermal H/D exchange. Heating 2 at 60 °C in toluene for 26 h under D_2 (1.5 atm), followed by the workup described above, led to 8 in 80% yield. Complex 8 in this case was shown to be 83% deuterated at the hydride ligand positions. The fact that phosphine addition requires much higher temperatures indicates that the thermal hydrogen exchange reaction must take place by some mechanism (e.g. partial detachment of the Cp ligand; loss of hydrogen atoms in a radical chain process) other than simple reductive elimination of H_2 followed by oxidative addition of D_2.

The most efficient method for preparing 8 is also the most surprising: tetrahydride 2 exchanges hydride ligands with protic solvents such as D_2O and deuterated alcohols. Since this reaction occurs in the dark at ambient temperature, we believe that the exchange is not radical in nature. An intriguing possibility is protonation at the iridium center, giving rise to a cationic (pentahydrido)iridium (VII) intermediate, which does not reductively eliminate H_2, but instead loses a proton to the solvent. No iridium (VII) complexes have ever been unambiguously observed, although Crabtree recently reported the possible observation of IrH_6(P(c-

$C_6H_{11})_3)_2^+$ at low temperature.[16]

Irradiation of **2** in alkane solvents does not lead to isolable trihydrido(alkyl)iridium complexes analogous to those prepared by Janowicz.[5] Instead, the solution becomes burgundy, and inspection of the ^1H NMR spectrum at various times demonstrates the presence of numerous species. These apparently are hydride-deficient clusters, indicating either that the desired complexes are unstable, or that the intermediate prefers to react with other iridium species.

Conclusion.

The tetrahydride **2**, like most polyhydride complexes,[17] has demonstrated facile loss or exchange of hydrogen ligands as the predominant chemistry. Unlike the related $(C_5(CH_3)_5)Ir(CH_3)_4$,[3] the polyhydride undergoes thermolysis at fairly low temperatures, suggesting that a rich thermal chemistry is more likely for this complex. However, we chose to explore the less well-known synthetic chemistry of polyhydrides employing compound **2**; this work is discussed in Chapter 4.

References.

(1) Mann, B. E.; Masters, C.; Shaw, B. L. J. Inorg. Nucl. Chem. **1971**, 33, 2195.

(2) Parshall, G. W. Acc. Chem. Res. **1975**, 8, 113.

(3) Isobe, K.; Vasquez de Miguel, A.; Nutton, A.; Maitlis, P. M. J. Chem. Soc., Dalton Trans. **1984**, 929, and references therein.

(4) Fernandez, M. J.; Maitlis, P. M. J. Chem. Soc., Chem. Commun. **1982**, 310.

(5) (a) Janowicz, A. H.; Bergman, R. G. J. Am. Chem. Soc. **1982**, 104, 351. (b) Janowicz, A. H.; Bergman, R. G. J. Am. Chem. Soc. **1983**, 105, 3929.

(6) Clark, E. P. Ind. Eng. Chem., Anal. Ed. **1941**, 13, 820.

(7) Hoyano, J. K.; Graham, W. A. G., personal communication. Spectral data for $(C_5(CH_3)_5)Ir(CO)H_2$: ^1H NMR (C_6D_6): δ 1.89 (s, C_5Me_5); -15.75 (s, Ir-H). IR: ν_{Ir-H} 2150 cm^{-1}; ν_{CO} 1998 cm^{-1}.

(8) (a) Kang, J. W.; Moseley, K.; Maitlis, P. M. J. Am. Chem. Soc. **1969**, 91, 5970. (b) Graham, W. A. G.; Hoyano, J. K. J. Am. Chem. Soc. **1982**, 104, 3722.

(9) White, C.; Oliver, A. J.; Maitlis, P. M. J. Chem. Soc., Dalton Trans. **1973**, 3322.

(10) Gill, D. S.; Maitlis, P. M. J. Organomet. Chem. **1975**, 87, 359.

(11) Crystals were maintained at -150 °C by means of a cold stream of dry nitrogen gas, the temperature of which was monitored just upstream of the tube exit. Calibration of the temperature to that of the sample was acheived by mounting another thermocouple in the cold stream and monitoring both thermocouples. The

temperature was unregulated, but measurements of the upstream temperature taken at various times during data collection revealed that it was steady to ± 2 °C. The physical apparatus used was the commercial Enraf-Nonius Universal Low Temperature device as modified for the UCB CHEXRAY system.

(12) The instrumentation, methods of data collection, computer programs, and formulae for data reduction and structure solution have been described: Theopold, K. H.; Bergman, R. G. J. Am. Chem. Soc. 1983, 105, 464.

(13) Reflections used for azimuthal scans were located near $\chi = 90°$ and the intensities were measured at 10° increments of rotation of the crystal about the diffraction vector.

(14) White, C.; Oliver, A. J.; Maitlis, P. M. J. Chem. Soc., Dalton Trans. 1973, 1901.

(15) More recent experiments demonstrated that deuterium was incorporated into the $C_5(CH_3)_5$ when higher D_2 pressures or longer reaction times were employed. This may indicate that some component of both the thermal and photochemical exchange reactions is radical in nature. However, attack of the intermediate on the ring methyl carbon-hydrogen bond to give a dimer (as in "titanocene", for example), followed by addition of D_2 across the metal-carbon bond could also explain these results.

(16) Crabtree, R. H.; Hlatky, G. G.; Parnell, C. P.; Segmuller, B. E.; Uriarte, R. J. Inorg. Chem. 1984, 23, 354.

(17) (a) "Transition Metal Hydrides", Muetterties, E. L., Ed. Marcel Dekker: New York, 1971. (b) "Transition Metal Hydrides", Bau, R., Ed. Adv. Chem. Ser., No. 167. Marcel Dekker: New York, 1978. (c) Soloveichik, G. L.; Bulychev, B. M. Russian Chem. Rev. **1982**, 51, 286. (d) Moore, D. S.; Robinson, S. D. Chem. Soc. Rev. **1983**, 12, 415.

Chapter 4. (Pentamethylcyclopentadienyl)iridium Polyhydride Complexes: Synthesis of Intermediates in the Mechanism of Formation of $(C_5(CH_3)_5)IrH_4$, and the Preparation of Several Iridium (V) Compounds.

Introduction.

The hydride ligand is important in organometallic chemistry: metal hydrides are implicated in various homogeneous and heterogeneous catalytic processes,[1] and polyhydride complexes are known to be active catalysts for H/D exchange.[2] From a structural standpoint, the small van der Waals volume of hydrogen atoms and the ability of hydride ligands to move from bridging to terminal sites (similar to CO) make polyhydride complexes worthy of study;[3] the difficulty inherent in determining hydride positions by NMR or X-ray study presents a fascinating challenge. Of greatest interest to us is the well-documented ability of hydride ligands to stabilize the higher formal oxidation states of transition metals;[4] no other ligand forms as many high-oxidation state complexes as the hydrogen atom.

In general, little is known of the mechanism of preparing organometallic hydride species from organometallic halides and hydridic reducing agents, in spite of the fact that no method is more commonly used.[3c,d] In addition, one aspect of this chemistry is the well-documented result that oxidation of the metal center often occurs,[3c,d] even though the medium should be considered reducing. Studies have not yet definitively established the mechanisms of such oxidations.[5]

In Chapter 3, we described the synthesis of $(C_5(CH_3)_5)IrH_4$,[6a] one of the few organometallic iridium (V) complexes,[6b] starting with the iridium (III) dimer $[(C_5(CH_3)_5)Ir]_2(\mu\text{-}H)_3PF_6$ and the reducing agent $LiEt_3BH$. In addition to the question of the source of each iridium-bound hydrogen, we were perplexed by the formal oxidation of

the iridium atoms in what one presumed would be a reducing medium. The high yields of tetrahydride demonstrated that one possibility, oxidation of half the iridium and reduction of the other half, did not obtain.

In order to study the mechanism of the formation of $(C_5(CH_3)_5)IrH_4$, we drew upon our data for trimethylphosphine(pentamethylcyclopentadienyl)iridium polyhydrides and undertook to synthesize potential intermediates in the transformation. In addition, we attempted to expand the range of iridium (V) complexes known in order to increase the data for high-oxidation state species. Our results are described in this Chapter.

Experimental

General. Experimental and characterization methods were described in Chapter 1. ^{11}B and $^{1}H\{^{11}B\}$ NMR spectra were recorded on the 180 MHz instrument at the UCB NMR facility, and are reported as ppm downfield of TMS (^{1}H) or saturated $NaBF_4$ in methanol (^{11}B).

$[(C_5(CH_3)_5)Ir]_2H_3BH_4$, (2). A slurry of $LiBH_4$ (77 mg, 3.6 mmol) and $[(C_5(CH_3)_5)Ir](\mu\text{-}H)_3PF_6$ (**1·PF_6**, Chapter 1 and Ref. 7a) (408 mg, 0.508 mmol) in 10% THF/pentane (both freshly distilled) was stirred for 3 h at ambient temperature. Removal of the solvent in vacuo without heating yielded orange-yellow solid, which was extracted with pentane (3 x 15 mL). The extracts were filtered through celite packed in a frit, whereupon approximately half the pentane was evaporated from the filtrate. Upon cooling the solution to -40 °C, bright yellow-orange material crystallized, and was collected by filtration and washed with cold pentane. Successive evaporations and crystallizations of the mother liquor gave two additional crops of product indistinguishable from the first by ^{1}H NMR spectroscopy, for a total yield of 216 mg (0.321 mmol, 63%) of **2**. The compound is quite thermally sensitive; solutions of **2** decompose at 60 °C within 5 min and at 23 °C over 48 h. ^{1}H NMR (C_6D_6): δ 1.92 (s, 30H, C_5Me_5); -14.18 (br, 2H, Ir-H_{bridg}-B); -17.51 (s, 1H, Ir-H_{bridg}-Ir); -17.78 (s, 2H, Ir-H_t). $^{1}H\{^{11}B\}$ NMR (toluene-d_8, -50 °C): δ 5.52 (br, 2H, BH_2); 1.91 (s, 30H, C_5Me_5); -14.10 (br, 2H, Ir-H_{bridg}-B); -17.46 (s, 1H, Ir-H_{bridg}-Ir); -17.69 (s, 2H, Ir-H_t). $^{11}B\{^{1}H\}$ NMR (toluene-d_8, -50 °C): δ 5.5 (br s). $^{13}C\{^{1}H\}$ NMR (C_6D_6): δ 94.1 (s, $\underline{C}_5Me_5$); 10.5 (s, $C_5\underline{Me}_5$). IR (KBr): ν 2430, 2360, 2290 (all s, B-H) cm^{-1}; 2115 (s,

Ir-H_t), 2040 (sh), 1155 (s, Ir-H_{bridg}) cm^{-1}. EIMS (20 eV, 23 °C): m/e 672, 671, 670, 669, 668, 667. Anal. Calcd for $C_{20}H_{37}Ir_2B$: C, 35.71; H, 5.54. Found: C, 35.88; H, 5.66.

$[(C_5(CH_3)_5)IrH_3]_2$, (3). Trihydride dimer **1**·PF_6 (401 mg, 0.500 mmol) and $LiBH_4$ (65.3 mg, 3.00 mmol) were slurried in 2% THF in hexane (50 mL). After stirring overnight, the homogeneous solution containing 2 was filtered through hexane-wetted alumina III packed in a frit, after which the alumina was washed with benzene to give an orange solution. The solutions were combined, the solvent removed and the residue recrystallized from pentane to give deep orange-burgundy crystals (116 mg, 0.176 mmol, 35%). A somewhat impure second crop could be obtained. ^1H NMR (C_6D_6, RT): δ 1.97 (s, 30H, C_5Me_5); -14.76 (s, 6H, Ir-H). ^1H NMR (3:2 THF-d_8/toluene-d_8, -120 °C): δ 1.94 (s, 30H, C_5Me_5); -10.70 (br s, 2H, Ir-H_{bridg}); -17.11 (br s, 4H, Ir-H_t). $^{13}C\{^1H\}$ NMR (C_6D_6): δ 93.0 (s, $\underline{C}_5Me_5$); 10.2(s, $C_5\underline{Me}_5$). IR (C_6H_6): ν_{Ir-H} 2110; (KBr): 2120(terminal hydride), 1190, 1120(both br, bridging hydride) cm^{-1}. EIMS (15 eV, RT): m/e 659, 658, 657, 656, 654. Anal. Calcd for $C_{20}H_{36}Ir_2$: C, 36.35; H, 5.49. Found: C, 36.30; H, 5.32. Solid state decomposition temperature: 60-80 °C.

In a separate experiment, the reaction mixture was hydrolyzed by the addition of methanol (125 mmol) at 0 °C, giving a yellow orange solution. After evaporation of solvent, the resulting residue was extracted with toluene (12 mL). The filtered extracts were layered with hexane and cooled to -40 °C, ultimately yielding orange crystals of **3** identical by ^1H NMR spectroscopy to those from the procedure

above (128 mg, 0.194 mmol, 38%).

Reaction of 3 with $P(CH_3)_3$. $P(CH_3)_3$ (0.200 mmol) was vacuum transferred into a C_6D_6 solution of **3** (33 mg, 0.050 mmol) in an NMR tube. The yellow solution was warmed to 55 °C for 6 h, at which point the solution was colorless. Inspection of the ^1H NMR spectrum demonstrated clean conversion of starting material to $(C_5(CH_3)_5)Ir(P(CH_3)_3)H_2$,[8] **4** (0.073 mmol by integration against internal $(Me_3Si)_2O$, 73%).

Generation and Reactions of $(C_5(CH_3)_5)IrH_3[Li(THF)_x]$, (5). $LiEt_3BH$ (1.0 mmol) was added dropwise to a slurry of **1**·PF_6 (240 mg, 0.299 mmol) in 1:1 toluene/hexane (6 mL). After stirring for 3 h, the homogeneous solution was cooled to -40 °C. Deep red-orange crystals precipitated; these were filtered, washed with hexane and dried to yield 215 mg of material. At this point, ^1H NMR spectroscopy showed a great deal of THF and BEt_3/BEt_3H^- present in the product. High vacuum could not completely remove the solvent; it was noted that the solubility of the material decreased dramatically as the THF was removed (see compound **7** below). As discussed in the text, spectral and chemical evidence strongly suggests that this material is $(C_5(CH_3)_5)IrH_3[Li(THF)_x]$, by analogy with **8**. ^1H NMR (C_6D_6): δ 2.18 (br s, 15H, C_5Me_5); 3.55, 1.40 (THF); 1.45, 1.27 (BEt_3/BEt_3H^-); -19.22 (br s, 3H, Ir-H). $^{13}C\{^1H\}$ NMR (C_6D_6): δ 87.4 (s, $\underline{C}_5Me_5$); 67.3, 24.4 (THF); 16.0, 11.0 (BEt_3/BEt_3H^-); 11.3 (s, $C_5\underline{Me}_5$). IR (C_6H_6): ν_{Ir-H} 2019 (br) cm^{-1}.

In a second experiment designed to characterize **5** chemically, a hexane slurry of **1**·BF_4 (186 mg, 0.250 mmol) and pmdeta (430 mg, 2.5

mmol) was treated dropwise with $LiEt_3BH$ (1.5 mmol) from which most of the THF had been evaporated and replaced with toluene. The solution slowly became homogeneous during 20 h of stirring. The solvent was removed in vacuo, and the oily residue extracted with hexane followed by benzene. The solvent was removed from the filtered extracts and the burgundy residue dissolved in hexane. Cooling to -40 °C gave 26 mg of an unidentified BEt_3/pmdeta adduct as shown by ^1H NMR spectroscopy. Filtration and refrigeration of the mother liquor gave two crops of $(C_5(CH_3)_5)IrH_3[Li(pmdeta)]$, **8**, shown to be >85% pure by ^1H NMR spectroscopy (70 mg, 0.14 mmol, 27%). The BEt_3/BEt_3H^--containing impurity could not be removed by crystallization.

In a third experiment, a sample of 5 was treated with methanol (50 μL). The orange solution decolorized as black solid precipitated. Inspection of the ^1H NMR spectrum of the sample demonstrated the presence of THF and only one organometallic product, $(C_5(CH_3)_5)IrH_4$, **6**.

Finally, adding 5 (70 mg) in 1:1 toluene/hexane to a hexane slurry of Ph_3SnBr (35 mg, 0.081 mmol) at -78 °C, stirring 2 h at this temperature, warming to room temperature and evaporating the solvent gave a brown-white semisolid. Recrystallization from ether/pentane gave two crops of colorless crystals of **9c** (30 mg, 0.044 mmol, 18% based on $\mathbf{1 \cdot PF_6}$), shown to be pure by ^1H NMR spectroscopy.

$(C_5(CH_3)_5)IrH_3Li$, (7). A pentane solution of tetrahydride **6** (410 mg, 1.24 mmol) was treated dropwise with t-BuLi (1.50 mmol). White solid precipitated instantly from the solution. After stirring 30 min, the powdery material was filtered and washed with pentane to

give 371 mg (1.10 mmol, 89%) of slightly pyrophoric material. Methanol hydrolysis of this material in an NMR tube reaction instantly generated **6** as the only product by ^{1}H NMR spectroscopy.

The total insolubility of the compound in inert solvents precluded most spectral characterizations. IR (KBr): ν_{Ir-H} 2060 (br) cm^{-1}. Anal. Calcd for $C_{10}H_{18}IrLi$: C, 35.60; H, 5.38. Found: C, 35.98; H, 5.62.

$(C_5(CH_3)_5)IrH_3[Li(pmdeta)]$, (8). At -78 °C (dry ice/acetone), a pentane solution of **6** (680 mg, 2.05 mmol) and pmdeta (1.40 ml, 8.08 mmol) was treated dropwise over 15 min with t-BuLi (3.40 mmol) in 10 mL pentane. After 1.5 h stirring at this temperature, the pale yellow-white solid was filtered and dried to give highly air-sensitive **8**, (295 mg, 0.578 mmol, 28%). ^{1}H NMR (C_6D_6): δ 2.52 (br s, 15H, C_5Me_5); 2.16 (s, 3H, internal amine $-CH_3$); 2.05 (s, 12H, terminal amine $-CH_3$); -19.21 (br s, 3H, Ir-H). $^{13}C\{^1H\}$ NMR (C_6D_6): δ 85.0 (s, $\underline{C}_5Me_5$); 56.1, 52.9 (s, amine methylenes); 45.9 (s, terminal amine $-CH_3$); 45.1 (s, internal amine $-CH_3$); 12.2 (s, $C_5\underline{Me}_5$). IR (C_6H_6): ν_{Ir-H} 2020 (br) cm^{-1}. Signer[9] molecular weight (C_6H_6, 25 °C, slight decomposition noted during equilibration): calcd 511, found 445. Anal. Calcd for $C_{19}H_{41}N_3IrLi$: C, 44.68; H, 8.09; N, 8.23. Found: C, 44.31; H, 8.27; N, 8.16.

A sample of **8** (15.0 mg, 0.0294 mmol) slurried in pentane was treated with isopropanol (250 μL). After stirring 5 min, the solvent was evaporated and the residue taken into C_6D_6. Inspection of the ^{1}H NMR spectrum demonstrated free pmdeta and **6** (0.0250 mmol by integration vs. internal $(Me_3Si)_2O$, 85%) to be the only ^{1}H NMR-active

species present in the solvent.

$(C_5(CH_3)_5)IrH_3(SiMe_3)$, (9a). A toluene solution of **8** (51 mg, 0.10 mmol) was added dropwise to a pentane solution of $Me_3SiO_3SCF_3$ (27 mg, 0.12 mmol) at -78 °C. The pale yellow solution was stirred 5 h, then allowed to warm slowly to room temperature. Following removal of solvent, the residue was dissolved in benzene, filtered through celite to remove insoluble material, and the benzene evaporated to yield a yellow-white solid. Sublimation (5 mtorr, 45 °C) gave pure white product (31 mg, 0.077 mmol, 76%). ^1H NMR (toluene-d_8, RT): δ 1.91 (s, 15H, C_5Me_5); 0.61 (s, 9H, $SiMe_3$); -16.20 (s, 3H, Ir-H). ^1H NMR (toluene-d_8, -80 °C): δ 1.79 (s, 15H, C_5Me_5); 0.80 (s, 9H, $SiMe_3$); -15.83 (t, J_{HH}=5.6, 1H, Ir-H_{tr}); -16.00 (d, J_{HH}=5.6, 2H, Ir-H_{cis}). $^{13}C\{^1H\}$ NMR (toluene-d_8): δ 96.9 (s, $\underline{C}_5Me_5$); 10.6 (s, $C_5\underline{Me}_5$); 9.95 (s, $Si\underline{Me}_3$). IR (KBr): ν_{Ir-H} 2195, 2160 cm^{-1}. EIMS (13 eV, RT): m/e 404, 402. Anal. Calcd for $C_{13}H_{27}IrSi$: C, 38.68; H, 6.74. Found: C, 38.39; H, 6.57. Solid state decomposition temperature: 110-120 °C.

$(C_5(CH_3)_5)IrH_3(SnMe_3)$, (9b). A toluene solution of **8** (51 mg, 0.10 mmol) was added dropwise to a pentane solution of Me_3SnCl (30 mg, 0.15 mmol) at 0 °C. After stirring 4 h at this temperature, the solvent was removed and the resulting oil taken up in pentane. The pentane solution was filtered through celite and the solvent evaporated. Sublimation of the resultant oily residue (30 mtorr, 30 °C, LN_2-cooled cold finger) gave greasy white crystals of **9b** (16 mg, 0.032 mmol, 33%).

^1H NMR (toluene-d_8, RT): δ 1.94 (s, J_{Sn-H}<1, 15H, C_5Me_5); 0.50

(J_{Sn-H}=47.8, 9H, $SnMe_3$); -16.32 (J_{Sn-H}=23.6, 3H, Ir-H). ^1H NMR (toluene-d_8, -80 °C): δ 1.81 (s, J_{Sn-H}<1, 15H, C_5Me_5); 0.68 (J_{Sn-H}=48.0, 9H, $SnMe_3$); -15.87 (t, J_{HH}=6.5, 1H, Ir-H_{tr}); -16.15 (d, J_{HH}=6.5, 2H, Ir-H_{cis}). $^{13}C\{^1H\}$ NMR (toluene-d_8): δ 95.8 (s, $\underline{C}_5Me_5$); 10.9 (s, $C_5\underline{Me}_5$); -5.0 (broad s, $Sn\underline{Me}_3$). IR (thin film): ν_{Ir-H} 2160(sh), 2120(s) cm^{-1}. EIMS (70 eV, RT): envelopes centered around m/e 479, 461, 443. Anal. Calcd for $C_{13}H_{27}IrSn$: C, 31.59; H, 5.51. Found: C, 31.80; H, 5.36.

$(C_5(CH_3)_5)IrH_3(SnPh_3)$, (9c). A toluene slurry of anion 7 (84.4 mg, 0.250 mmol) was treated dropwise with Ph_3SnBr (140 mg, 0.324 mmol) dissolved in toluene. After stirring five days, filtration of the solution, removal of the solvent and recrystallization from ether/hexane gave white crystals (112 mg, 0.165 mmol, 66%) of product. The crystal used in the X-ray diffraction study crystallized from a saturated pentane solution.

^1H NMR (toluene-d_8, 80 °C): δ 7.8-7.1 (complex, 15H, $SnPh_3$); 1.84 (br s, J_{SnH}<1, 15H, C_5Me_5); -15.69 (J_{SnH}=28.2, 3H, Ir-H). ^1H NMR (toluene-d_8, -65 °C): δ 7.9-7.1 (complex, 15H, $SnPh_3$); 1.70 (br s, J_{SnH}<1, 15H, C_5Me_5); -15.36 (d, J_{HH}=8.1, 2H, Ir-H_{cis}); -15.58 (t, J_{HH}=8.1, 1H, Ir-H_{tr}). $^{13}C\{^1H\}$ NMR (acetone-d_6): δ 144.1 (s, Ph); 137.4 (J_{SnC}=37.8, Ph); 128.5 (overlapping, Ph); 97.7 (s, $\underline{C}_5Me_5$); 10.8 (s, $C_5\underline{Me}_5$). IR (KBr): ν_{Ir-H} 2190, 2105 cm^{-1}. EIMS: m/e 680, 600, 524, 442. MP: 150-160 °C dec. Anal. Calcd for $C_{28}H_{33}IrSn$: C, 49.42; H, 4.89. Found: C, 49.96; H, 5.09. Repeated crystallization did not result in improved analyses.

This compound was also prepared from the pmdeta-sequestered

lithium salt 8 at -78 °C in 88% recrystallized yield, shown to be pure by ^{1}H NMR spectroscopy.

$(C_5(CH_3)_5)IrH_3((C_5H_5)_2ZrCl)$, (10). A homogeneous solution of 8 was prepared by addition of t-BuLi (0.360 mmol) to a toluene solution of tetrahydride **6** (100 mg, 0.302 mmol) and pmdeta (63 mg, 0.36 mmol) at -40 °C. After 18 h, addition of this reagent to $(C_5H_5)_2ZrCl_2$ (105 mg, 0.360 mmol) in toluene at 0 °C gave a cloudy orange solution. This was stirred 2 h, then warmed to ambient temperature and stirred 18 h. The solvent was removed, and the residue extracted with a minimum amount of toluene. The extracts were filtered and treated with hexane. Cooling to -40 °C precipitated bright orange solid; this was filtered, washed with hexane and dried to give the product pure by ^{1}H NMR spectroscopy (105 mg, 0.179 mmol, 59%). ^{1}H NMR (toluene-d_8, 21 °C, 300 MHz): δ 6.04 (s, 10H, Cp); 1.96 (s, 15H, C_5Me_5); -14.27 (s, 3H, Ir-H). ^{1}H NMR (3:2 THF-d_8/methylcyclohexane-d_{14}, -120 °C, 500 MHz): δ 6.25 (s, 10H, Cp); 2.12 (s, 15H, C_5Me_5); -12.46 (br s, fwhh ~ 40 Hz, 2H, Ir-H); -16.92 (br s, fwhh ~ 70 Hz, 1H, Ir-H). $^{13}C\{^1H\}$ NMR (toluene-d_8, 21 °C): δ 112.8 (s, Cp); 91.6 (s, $\underline{C}_5Me_5$); 10.9 (s, $C_5\underline{Me}_5$). IR (C_6D_6): ν_{Ir-H} 2070 cm^{-1}. EIMS (30 eV, RT): m/e 586. Anal. Calcd for $C_{20}H_{28}ClIrZr$: C, 40.90; H, 4.81; Cl, 6.04. Found: C, 42.90; H, 4.75; Cl, 6.28. Repeated crystallization did not result in improved analyses.

Single Crystal X-ray Diffraction Study of $\underline{2}\cdot 1/3\ C_5H_{12}$. Single crystals of **2** suitable for diffraction study were grown from cold pentane solution as partial pentane solvates. Elemental analysis for boron using these crystals gave acceptable values. Assuming a

stoichiometry of $[(C_5(CH_3)_5)Ir]_2H_3BH_4 \cdot 1/3\ C_5H_{12}$, anal. calcd for $C_{21.67}H_{41}Ir_2B$: B, 1.55. Found: B, 1.5.

A cleaved single crystal of **2·1/3 C_5H_{12}** was mounted on a glass fiber and then coated with polycyanoacrylate cement. The crystal was mounted on the UCB CHEXRAY Enraf-Nonius CAD-4 diffractometer,[10] centered in the beam and cooled to -90 ± 3 °C by a stream of cold nitrogen gas. Automatic peak search and indexing procedures yielded a rhombohedral reduced primitive cell with systematic absences consistent with the space groups R3c or R$\bar{3}$c. Final cell parameters and specific data collection parameters are given in Table 1. Three intensity standards were checked every two hours of X-ray exposure time. Three orientation standards were checked every 250 reflections, and the crystal orientation redetermined if any of the reflections were offset more than 0.1° from their predicted positions; reorientation was needed twice during data collection.

The 3258 raw intensity data were converted to structure factor amplitudes and their esds by correction for scan speed, background, and Lorentz and polarization effects. Inspection of the intensity standards showed a monotonic isotropic decrease to 0.92 of the original intensity; the data were corrected for this decay. Inspection of azimuthal scan data[11] showed a variation of I_{min}/I_{max} = 0.77 for the average curve; an empirical absorption correction based on these data was applied to the intensities. Removal of systematically absent and averaging of redundant data (R(I)=3.1%) left 1570 unique data.

Table I. Cell Constants and Data Collection Parameters for the X-ray Diffraction Experiments

	$2 \cdot {}^1/_3 C_5H_{12}$ (−90 °C)	9c (25 °C)
	(A) Crystal Parameters	
a, Å	15.466 (3)[a]	9.7438 (9)[b]
b, Å		11.1893 (10)
c, Å		11.1364 (12)
α, deg	81.941 (12)	101.382 (6)
β, deg		98.282 (9)
γ, deg		94.786 (8)
V, Å^3	3599 (2)	1275.1 (4)
space group	$R\bar{3}c$	$P\bar{1}$
Z	6	2
d_{calcd}, g/cm^3	1.86	1.77
μ_{calcd}, cm^{-1}	110.4	61.89
size, mm	0.25 × 0.28 × 0.30	0.18 × 0.23 × 0.25
	(B) Data Measurement Parameters	
radiation	Mo Kα (λ = 0.71073 Å)	
monochromator	highly oriented graphite (2θ = 12.2°)	
detector	crystal scintillation counter, with PHA	
reflcns measd	$+h,+k,\pm l$ (in hexagonal cell)	$+h,\pm k,\pm l$
2θ range, deg	3–45	3–55
scan type	θ–2θ	θ–2θ
scan speed	0.8 → 6.7 (θ, deg/min)	1.2 → 6.7 (θ, deg/min)
scan width	$\Delta\theta$ = 0.7 + 0.347 tan θ	$\Delta\theta$ = 0.5 + 0.347 tan θ
background	0.25 ($\Delta\theta$) at each end	0.25 ($\Delta\theta$) at each end
aperture → crystal, mm	173	173
vertical aperture, mm	3.0	3.0
horizontal aperture, mm	2.5 + 1.0 tan θ (var)	2.0 + 1.0 tan θ (var)
reflcns collected	3528	6630
unique reflcns	1570	5857

[a] Unit cell parameters and their esds were derived by a least-squares fit to the setting angles of the unresolved Mo Kα components of 24 reflections with 2θ near 28°. [b] Unit cell parameters and their esds were derived by a least-squares fit to the setting angles of the unresolved Mo Kα components of 24 reflections with 2θ between 25° and 32°.

The structure was solved by Patterson methods and refined via standard least-squares and Fourier techniques. The assumption that the space group was R$\bar{3}$c was confirmed by the successful solution and refinement of the structure. In a difference Fourier map calculated following refinement of all non-hydrogen atoms with anisotropic thermal parameters, peaks corresponding to the expected positions of most of the hydrogen atoms were found. In addition a set of moderately large peaks was found near the position of 32 symmetry at (1/4,1/4,1/4). These peaks were assumed to be due to a highly disordered partial molecule of pentane. Three positions (CP11, CP12, CP13) were refined with carbon scattering factors, isotropic thermal parameters and with occupancies constrained to represent equivalent amounts of electron density for each site. The refinement of the occupancy converged well to a value of 0.50 for the carbons in general positions (CP12 and CP13), and 0.167 for the carbon located on a crystallographic three-fold axis (CP11). Adding the occupancies and summing to calculate electron density gives approximately 42 electrons per site. Pentane, C_5H_{12}, has 42 electrons per molecule, including the hydrogen atoms. Thus the results of the refinement are consistent with one disordered pentane molecule occupying each site, giving a stoichiometric ratio of one molecule of pentane for every three iridium dimers, or equally, one-third molecule of pentane per iridium dimer.

The hydrogen atoms on the pentamethylcyclopentadiene ligand were fixed during the first cycles of refinement, but were later allowed to refine. The terminal hydrogen atoms attached to the iridium (H1

and H2) were immediately obvious in difference Fourier maps and refined well. The bridging hydrogen (H3) and the boron-bound hydrogen (H4) were less obvious, so various models were tried before settling on the final one. Obvious correlation existed between the placement of atoms on the crystallographic two-fold axis and the refinement of the "pentane" atoms.

In the final cycles of refinement the (222) and (021) reflections were removed from the data set as being adversely affected by extinction. There was no other evidence of effects of extinction. Inspection of the final residuals ordered in ranges of $\sin \theta/\lambda$, F_{obs}, parity, and hkl values showed no unusual features.

The quantity minimized by the least-squares program was $\Sigma w(F_{obs} - F_{calc})^2$, where w is the weight of a given reflection. The p-factor, used to reduce the weight of intense reflections, was set to 0.02 throughout the refinement. The analytical forms of the scattering factor tables for the neutral atoms were used, and all non-hydrogen scattering factors were corrected for both the real and imaginary components of anomalous dispersion.

The largest peak in the final difference Fourier map had an electron density of 0.86 e-/$\mathring{A}^3$. All peaks larger than 0.5 e-/$\mathring{A}^3$ were located near iridium atoms except peak 2, near H3.

The final residuals for 190 variables refined against the 1143 data for which $F^2 > 3\sigma F^2$ were R=2.00%, R_w=2.08%, R_{all}=3.89%, with GOF=0.897.

Positional and thermal parameters for the refined atoms are given in Table 2.

Table 2. Positional Parameters and Their Estimated Standard Deviations for 2·1/3 C_5H_{12}.

Atom	x	y	z	$B(Å^2)$
IR1	0.11771(2)	0.44681(2)	0.66326(1)	3.192(5)
C1	0.1798(4)	0.5147(4)	0.5442(4)	4.2(2)
C2	0.2437(4)	0.4944(4)	0.6032(4)	4.1(2)
C3	0.2148(4)	0.5391(4)	0.6765(4)	3.4(1)
C4	0.1327(4)	0.5897(4)	0.6631(4)	3.7(2)
C5	0.1116(4)	0.5764(4)	0.5793(5)	4.4(2)
C6	0.1865(6)	0.4918(5)	0.4530(5)	8.0(2)
C7	0.3299(5)	0.4369(5)	0.5871(6)	6.8(2)
C8	0.2651(5)	0.5373(5)	0.7530(5)	6.0(2)
C9	0.0810(5)	0.6502(5)	0.7229(6)	7.1(2)
C10	0.0370(5)	0.6250(5)	0.5364(6)	8.4(2)
CP11	0.319(2)	0.319	0.319	17(2)*
CP12	0.240(2)	0.286(2)	0.342(2)	17(1)*
CP13	0.213(3)	0.194(2)	0.319(2)	21(1)*
B1	0.1695(6)	0.330	0.750	5.0(2)
H1	0.048(4)	0.489(4)	0.630(4)	6(2)*
H2	0.133(4)	0.346(4)	0.645(4)	7(2)*
H3	0.050(7)	0.450	0.750	17(5)*
H4	0.158(4)	0.260(4)	0.737(4)	6(2)*
H61	0.219(4)	0.526(4)	0.410(4)	6(2)*
H62	0.214(5)	0.442(5)	0.450(5)	9(2)*
H63	0.145(4)	0.471(4)	0.432(4)	6(2)*
H71	0.373(3)	0.465(3)	0.551(3)	5(1)*
H72	0.364(8)	0.443(7)	0.642(8)	22(5)*
H73	0.325(4)	0.396(4)	0.555(4)	7(2)*
H81	0.293(3)	0.508(3)	0.743(3)	4(1)*
H82	0.234(5)	0.543(5)	0.800(5)	9(2)*
H83	0.306(5)	0.466(4)	0.769(5)	9(2)*
H91	0.098(4)	0.698(4)	0.712(4)	8(2)*
H92	-0.000(4)	0.669(5)	0.716(5)	10(2)*
H93	0.079(5)	0.631(5)	0.768(5)	9(2)*
H101	0.042(4)	0.695(4)	0.526(4)	7(2)*
H102	0.029(4)	0.595(4)	0.496(4)	6(2)*
H103	0.001(4)	0.626(4)	0.552(4)	5(2)*

* -- Atoms refined with isotropic thermal parameters.

Anisotropically refined atoms are given in the form of the isotropic equivalent thermal parameter defined as:

$(4/3) * [a^2*B(1,1) + b^2*B(2,2) + c^2*B(3,3) + ab(\cos gamma)*B(1,2) + ac(\cos beta)*B(1,3) + bc(\cos alpha)*B(2,3)]$

Single Crystal X-ray Diffraction Study of 9c. Two colorless single crystals of **9c** grown from pentane were mounted on glass fibers with polycyanoacrylate cement. Preliminary study and alignment on the diffractometer closely paralleled the procedures for **2**. The first data crystal was placed on the diffractometer and automatic peak search and indexing procedures used to yield a triclinic reduced primitive cell. Data collection proceeded for the hemisphere h<0; significant decay was noted in the intensity standards as the cell dimensions gradually changed. After collection of the first hemisphere, the second crystal was placed on the diffractometer and collection proceeded for the hemisphere h>0. The structure was solved using the data from the first crystal, but the iridium-bound hydrogen atoms could not be located using those data. The structure as reported is based on data from the second crystal only, and the final cell parameters and data collection parameters given in Table 1 are for that crystal. Intensity and orientation standards were checked as noted above; reorientation was needed twice during data collection for the second crystal.

The raw intensity data were converted to structure factor amplitudes as for **2**. Inspection of the intensity standards showed a monotonic, slightly anisotropic decay to 0.70 of the original intensity (second crystal); the data were corrected for this decay. An absorption correction based on the measured shape and size of the crystal and an 8x8x10 Gaussian grid of internal points was applied to the data after solution of the structure confirmed the unit cell contents (T_{max} = 0.396, T_{min} = 0.301). Removal of a series of badly

measured data which had been remeasured left 5857 unique data.

The structure was solved by Patterson methods. The assumption that the space group was $P\bar{1}$ was confirmed by successful solution and refinement. Refinement of the data on the first crystal led to the location of the hydrogen atoms on the organic ligands but not the iridium-bound hydrogen atoms.

At this point the data set from the second crystal was reduced and refinement continued using those data. In a difference Fourier map calculated following refinement of all non-hydrogen atoms with anisotropic thermal parameters, and with all organic hydrogen atoms included in fixed positions, peaks corresponding to the expected positions of the three iridium-bound hydrogen atoms were found as three of the top four peaks on the map. The three hydrogen atoms were refined with isotropic thermal parameters, keeping all other hydrogen atoms fixed in idealized geometries with assigned thermal parameters 1-2 $\AA^2$ larger than the equivalent B_{iso} of the carbon to which they were attached. Refinement converged rapidly and cleanly. A secondary extinction coefficient[12] was included in the least squares refinement after inspection of the low-angle high-intensity data indicated a necessity for such a correction.

Sources of scattering factors, etc. were as given for **2**. The p-factor was set to 0.02.

The largest peak in the final difference Fourier map had an electron density of 0.87 e-/$\AA^3$ and was located near the iridium atom.

The final residuals for 284 variables refined against the 4989 data for which $F^2 > 3\sigma(F^2)$ were R=1.91%, R_w=2.41%, R_{all}=2.93%, and

GOF=1.391.

Positional and thermal parameters of the refined atoms are given in Table 3.

Table 3. Positional Parameters and Their Estimated Standard Deviations for 9C.

Atom	x	y	z	$B(Å^2)$
IR1	0.09033(1)	0.42880(1)	0.21483(1)	3.486(2)
SN1	0.12530(2)	0.66442(2)	0.28023(2)	3.314(4)
C1	0.2797(3)	0.3554(3)	0.1528(3)	4.47(7)
C2	0.1664(4)	0.2614(3)	0.1254(3)	4.48(7)
C3	0.1298(4)	0.2485(3)	0.2314(3)	5.09(8)
C4	0.2208(4)	0.3233(3)	0.3216(3)	4.90(7)
C5	0.3135(3)	0.3940(3)	0.2732(3)	4.63(7)
C6	0.3633(4)	0.3977(4)	0.0702(3)	6.6(1)
C7	0.1068(5)	0.1869(4)	0.0077(4)	6.8(1)
C8	0.0232(5)	0.1406(3)	0.2416(4)	7.7(1)
C9	0.2257(5)	0.3273(4)	0.4466(3)	7.8(1)
C10	0.4344(4)	0.4828(4)	0.3381(4)	7.2(1)
C11	-0.0666(3)	0.7447(3)	0.3014(2)	3.78(6)
C12	-0.1949(4)	0.6806(3)	0.2510(3)	4.82(8)
C13	-0.3164(4)	0.7375(4)	0.2516(3)	5.89(9)
C14	-0.3107(4)	0.8573(4)	0.3049(4)	6.10(9)
C15	-0.1863(4)	0.9224(3)	0.3586(4)	6.6(1)
C16	-0.0659(4)	0.8664(3)	0.3557(3)	5.10(8)
C17	0.2458(3)	0.7237(3)	0.4579(2)	3.71(6)
C18	0.1978(3)	0.6844(3)	0.5474(3)	4.46(7)
C19	0.2696(4)	0.7203(4)	0.6574(3)	5.37(9)
C20	0.3915(4)	0.7954(4)	0.6794(3)	5.58(9)
C21	0.4438(4)	0.8359(3)	0.5920(3)	5.39(9)
C22	0.3712(4)	0.7994(3)	0.4812(3)	4.52(7)
C23	0.2288(3)	0.7654(3)	0.1827(2)	3.83(6)
C24	0.2486(4)	0.7076(3)	0.0752(3)	4.93(8)
C25	0.3034(4)	0.7723(4)	0.0023(3)	6.08(9)
C26	0.3383(4)	0.8983(4)	0.0366(3)	6.64(9)
C27	0.3192(4)	0.9573(3)	0.1422(3)	6.5(1)
*C28	0.2653(4)	0.8915(3)	0.2148(3)	4.86(8)
H1	0.055(3)	0.494(3)	0.119(3)	5.4(8)*
H2	-0.060(4)	0.485(3)	0.170(3)	6.1(9)*
H3	0.007(3)	0.477(3)	0.317(3)	6.0(9)*

* -- Atoms refined with isotropic thermal parameters.

Anisotropically refined atoms are given in the form of the isotropic equivalent thermal parameter defined as:

$$(4/3) * [a^2*B(1,1) + b^2*B(2,2) + c^2*B(3,3) + ab(\cos\ \text{gamma})*B(1,2) + ac(\cos\ \text{beta})*B(1,3) + bc(\cos\ \text{alpha})*B(2,3)]$$

Results and Discussion

Metathesis of $[(C_5(CH_3)_5)Ir]_2(\mu\text{-}H)_3A$ (A = PF_6 or BF_4), **1**, with $LiBH_4$ yields the novel borohydride dimer $[(C_5(CH_3)_5)Ir]_2H_3BH_4$, **2**, as orange-yellow crystals (Scheme 1). Initial characterization of **2** proved ambiguous, as the compound is quite thermally sensitive and difficult to purify. The hydride region of the ^1H NMR spectrum suggested **2** to be a dimer with two sets of two terminal iridium-bound hydrogens (δ -14.2, -17.7), with the lower field set probably coupled to a non-hydrogen nucleus as the resonance appeared quite broad, and one hydrogen bridging the iridium atoms (δ -17.5) which was not coupled to the non-hydrogen nucleus. Variable temperature ^1H NMR experiments demonstrated the low (-80 °C) temperature pattern to be equivalent to the room temperature pattern, indicating that the hydride ligand site exchange barrier must be large. Rapid decomposition of **2** occurred at higher temperatures, thus removing the possibility of finding the value of the barrier. Surprisingly, the hydrogen-hydrogen couplings could not be resolved at any temperature, indicating that the coupling constants must be small.

The first suggestion that the non-hydrogen nucleus present was boron resulted from the IR spectrum. In addition to the expected bands due to the $C_5(CH_3)_5$ ligands, strong bands were observed at 2430, 2360, 2290, 2115, 2040, and 1155 cm^{-1}. The 2115 and 2040 cm^{-1} bands clearly result from terminal Ir-H stretching modes, by analogy with numerous examples from our laboratory.[6a,8] The band at 1155 cm^{-1} we tentatively assign to a mode related to a hydrogen bridging the iridium atoms, based on the broadness of the peak, comparison

Scheme I

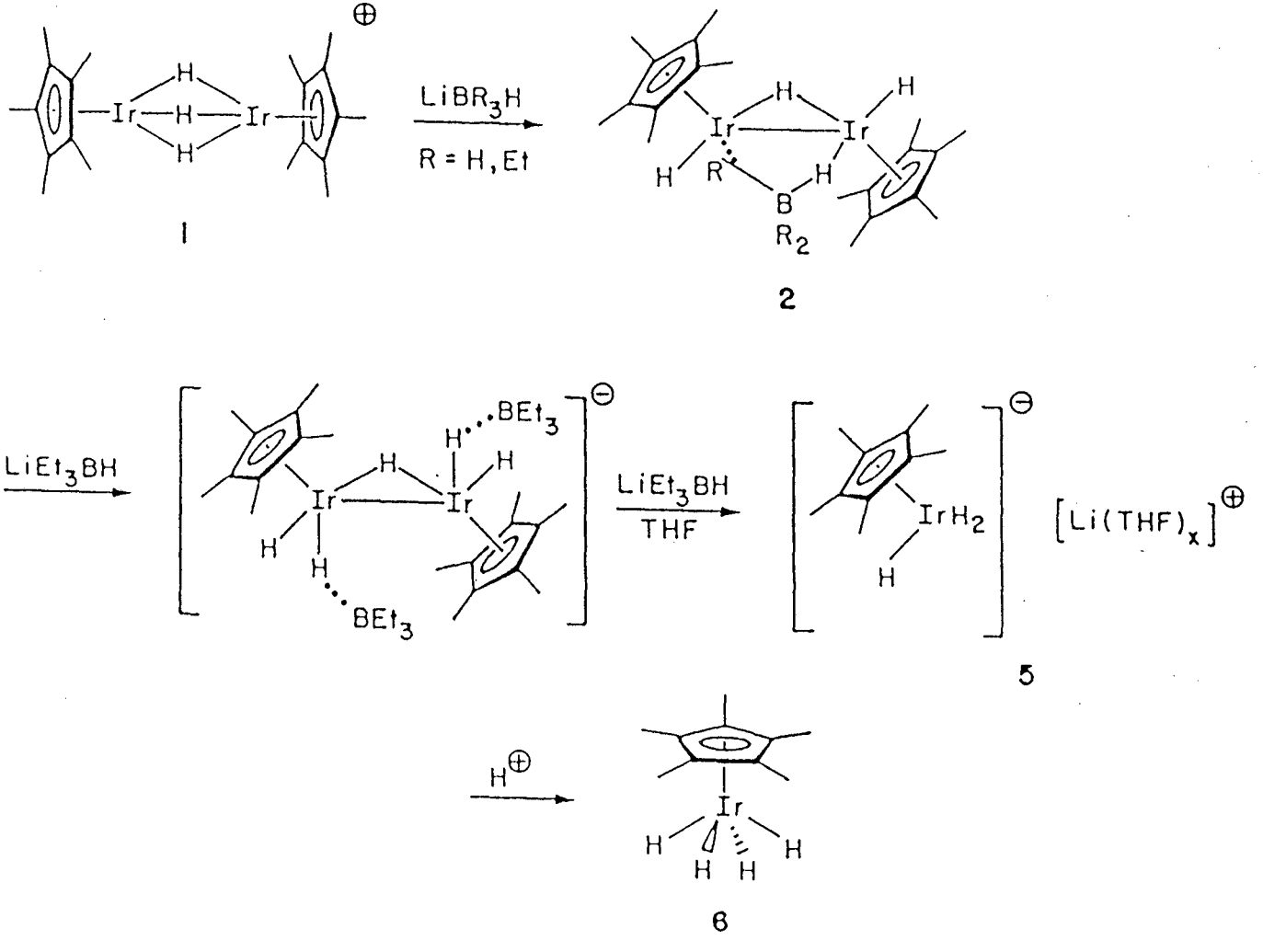

1

2

5

6

with the IR spectrum of **3**, and literature data.[7] The very strong bands at 2430, 2360, and 2290 cm^{-1} appear in a region characteristic of B-H stretching frequencies,[13] and little else,[14] strongly suggesting that **2** is a borohydride adduct. Elemental analysis and the $^{11}B\{^1H\}$ NMR experiment confirmed this hypothesis, and an additional resonance (δ 5.5) in the $^1H\{^{11}B\}$ NMR spectrum not visible in the undecoupled ^1H NMR spectrum proved that the complex was indeed an iridium borohydride dimer.

However, certain questions remained unanswered at this point. The appearance of <u>two</u> resonances in the ^1H NMR spectrum (δ 5.5, -14.2) for the borohydride hydrogens implied that the different hydrogens do not rapidly exchange sites, a very uncommon result for the BH_4 ligand.[15] The barriers for such exchanges are known to be low.[13,15] Also, the IR spectra of metal-bound borohydride ligands have been thought to be diagnostic;[13] we were unable to relate the IR bands for **2** to a particular borohydride bonding type.

Because of the ambiguous characterization of **2** and the strong probability of our locating the iridium-bound hydrides crystallographically, we performed a single crystal X-ray diffraction study. Experimental difficulties and the presence of disordered molecules of pentane in the crystal lattice lowered the experimental accuracy, but overall a reasonable model of **2** was obtained and shows a surprising bonding mode for the borohydride fragment.

Figure 1 depicts an ORTEP drawing of **2**. A crystallographic two fold axis passes through B1 and H3, relating the two halves of the dimer. Each iridium atom is bound to a terminal hydrogen, and a

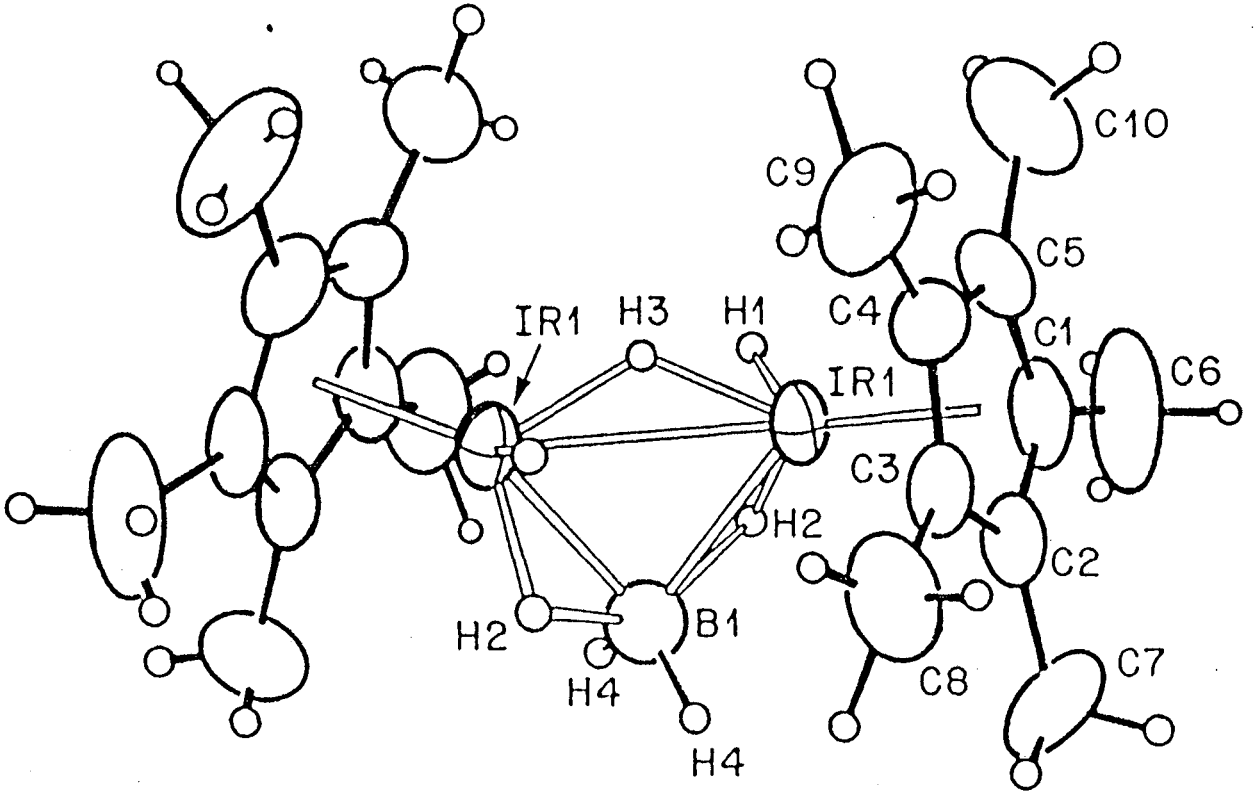

Figure 1. ORTEP drawing of 2 (disordered solvent not shown) viewing approximately normal to the Ir - Ir bond vector.

third hydrogen bridges the metals, in agreement with the above predictions. Remarkably, the borohydride ligand bridges both metals as well, a mode well known for carboxylate ligands,[16] but virtually unknown for borohydride. Only one case has been identified and crystallographically characterized previously,[17,18] in which two borohydrides each donate three hydrogens to a cobalt dimer. While the positions of the hydrogen atoms in our model are somewhat inaccurate due to the nature of the X-ray diffraction experiment and to the experimental difficulties, the general atomic locations seem sufficient for tentative conclusions to be drawn.

As may be seen from Table 4, the bond lengths and angles for the $(C_5(CH_3)_5)Ir$ fragments of the molecule lie within the expected ranges for such species; the Ir-Ir distance of 2.823(1) Å clearly indicates the presence of a metal-metal bond. Bond lengths and angles for the borohydride fragment, however, present problems in defining the exact nature of the molecular interactions. While the average B1-H4 distance (1.18(8) Å) lies well within expected values, the average B1-H2 distance (1.77(8) Å) is very long, much longer than the sum of the covalent bonding radii (1.27 Å) for these atoms.[19] However, this value lies well within the sum of the van der Waals contact radii (ca. 2.8 Å)[20] for boron and hydrogen, clearly suggestive of some significant interaction between the atoms. Related to this observation, the Ir-B1 distance (2.214(6) Å), while on the longer side of the range of iridium-boron bond lengths,[21] indicates a strong iridium-boron interaction, probably mediated by the presence of the bridging hydrogen. This effect has been remarked on previously.[15b]

Table 4. Selected Bond Distances (Å) and Angles (°) for 2·1/3 C_5H_{12}.

ATOM 1	ATOM 2	DISTANCE
IR1	IR1	2.823(1)
IR1	H1	1.47(8)
IR1	H2	1.61(8)
IR1	H3	1.59(7)
IR1	B1	2.214(4)
IR1	C1	2.160(7)
IR1	C2	2.215(7)
IR1	C3	2.259(6)
IR1	C4	2.253(7)
IR1	C5	2.228(8)
IR1	CENT[a]	1.869
B1	H2	1.77(8)
B1	H4	1.18(8)

ATOM 1	ATOM 2	ATOM 3	ANGLE
IR1	IR1	CENT	134.3
IR1	IR1	H1	89.9(30)
IR1	IR1	H2	86.1(33)
IR1	IR1	B1	50.4(2)
CENT	IR1	H1	128.8
CENT	IR1	H2	131.2
CENT	IR1	H3	121.9
CENT	IR1	B1	126.9
H1	IR1	H2	60.4(39)
H1	IR1	H3	84.2(50)
H1	IR1	B1	99.7(30)
H2	IR1	H3	106.0(34)
H3	IR1	B1	77.5(23)
IR1	H3	IR1	125.8(57)
IR1	B1	IR1	79.21(24)
IR1	B1	H4	118.8(40)
IR1	B1	H4	107.5(40)
H4	B1	H4	118.9(80)
IR1	B1	H2	45.9(27)
IR1	B1	H2	104.0(30)
H2	B1	H2	145.6(56)
H2	B1	H4	74.6(45)
H2	B1	H4	124.4(49)
IR1	H2	B1	81.8(38)

(a) CENT is the calculated centroid of the pentamethylcyclopentadienyl ring

While other workers have found bond variations between boron centers and terminal hydrogen atoms and boron centers and bridging hydrogen atoms in transition metal complexes,[22] the B1-H2 distance here is by far the longest reported and nearly eight standard deviations longer than the B1-H4 distance. Also, the small H2-B1-H4 angle (74.7(4.5)°) and the large H2-B1-H4 (124(5)°) angle are quite different from the expected value of 109.5°. Therefore we consider the "BH_4" moiety to be strongly distorted from a tetrahedral geometry (Figure 2), and view **2** conceptually as a complex in which a hydrogen atom has been nearly transferred from boron to iridium. Presumably the fact that the borohydride fragment bridges two metal centers contributes to the distortion as well.

Reaction of a sample of pure **2** with excess $LiEt_3BH$ generates $(C_5(CH_3)_5)IrH_3[Li(THF)_x]$ (see below) as the major product by ^1H NMR spectroscopy. Apparently the borohydride dimer, while unreactive toward excess $LiBH_4$, does react with the more nucleophilic $LiEt_3BH$.

Hydrolysis of a solution of **2**, either by reaction with methanol or by filtration through alumina III, yields the neutral, formally iridium (IV) polyhydride dimer $[(C_5(CH_3)_5)IrH_3]_2$, **3** (Scheme 2). This yellow-orange, air-sensitive complex proved much easier to handle and purify than **2**, being less soluble in pentane and more thermally robust, although it too decomposes on continued heating.

Complex **3** may also be isolated, although in low yield, upon column chromatographic hydrolysis of the reaction mixture when dimer **1** reacts with two equivalents of $LiEt_3BH$. The major product of this reaction is $(C_5(CH_3)_5)IrH_4$, **6**. In order for any quantity of **3** to be

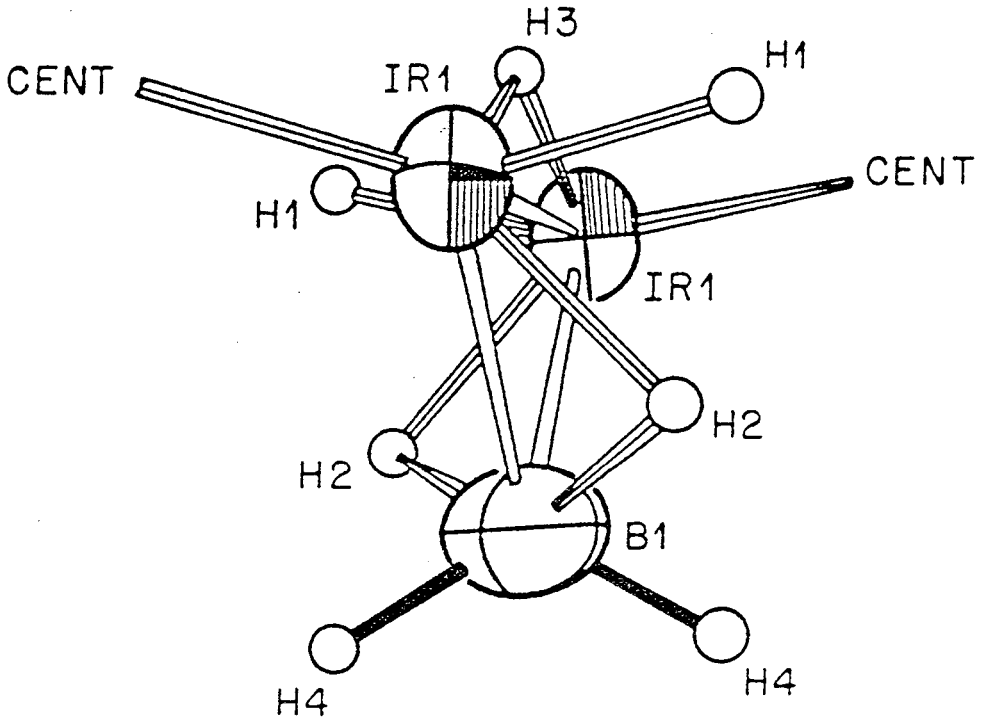

Figure 2. ORTEP drawing of 2 viewing approximately along the Ir - Ir bond vector. CENT represents the calculated centroid of the pentamethylcyclopentadienyl ring.

Scheme 2

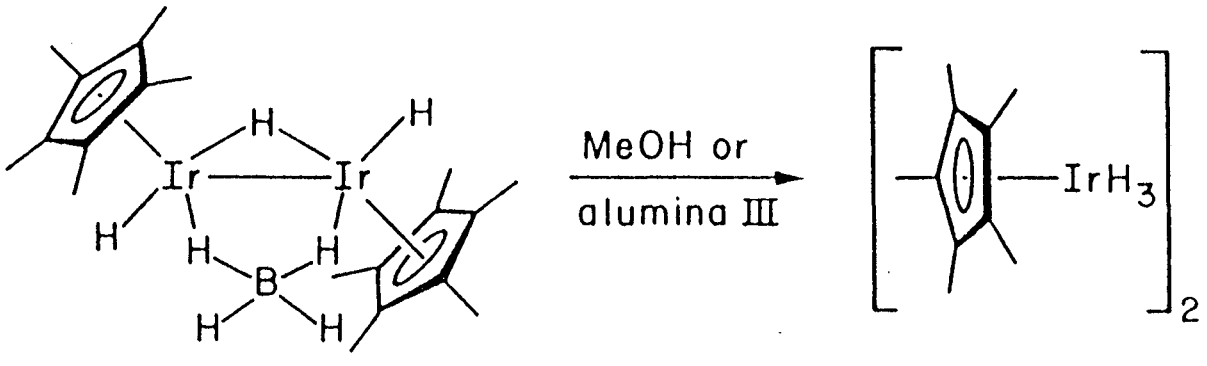

2

3

observed in this reaction, no more than two equivalents of $LiEt_3BH$ can be used; amounts in excess of this value yield only **6**. However, dimer **3** does not appear to be an intermediate in the production of **6**, as pure **3** is unreactive toward $LiEt_3BH$ in benzene solution; the dimer is produced intact upon alumina III hydrolysis of this reaction mixture.

Dimer **3**, in addition to the usual spectroscopic techniques, was characterized by reaction with $P(CH_3)_3$, yielding two equivalents of $(C_5(CH_3)_5)Ir(P(CH_3)_3)H_2$.[8] This reaction proved surprisingly slow at ambient temperature, suggesting a fairly large barrier to nucleophilic attack by phosphine for this system.

Variable temperature ^1H NMR and IR spectroscopies indicate that the dimer probably adopts a structure with four terminal iridium-bound hydrogens and two hydrogens bridging the metals. The solid state IR spectrum shows, in addition to the stretches due to the $C_5(CH_3)_5$ ligand, bands at 2120, 1190, and 1120 cm^{-1}. The 2120 cm^{-1} band should be assigned to a terminal iridium-hydride stretching mode. Tentatively, we assign the lower frequency bands to modes related to hydrogen atoms bridging the metals based on the broadness of the peaks and by analogy to previous work.[7]

Clearer characterization resulted from the variable temperature ^1H NMR experiment. At room temperature, only one resonance (δ -14.8) appears in the ^1H NMR spectrum in the upfield hydride region, indicating rapid site exchange. Upon cooling to -80 °C, the resonance broadens into the baseline, while the $C_5(CH_3)_5$ resonance remains unaffected. At -120 °C, with a field strength of 500 MHz,

two new resonances appear, a broad downfield singlet (δ -10.7) and a broad upfield singlet (δ -17.1). Presumably, the hydrogens couple to some extent, but the broadness of each resonance (ca. 35 Hz at half height) removes the possibility of resolving this coupling. The relative peak areas are 30:2:4 with the $C_5(CH_3)_5$ peak the largest, suggesting that the downfield resonance corresponds to one type of iridium-bound hydrogen, and the upfield resonance to another type. Based upon van der Waals radii arguments and literature data,[23] we believe that the larger, upfield resonance corresponds to four terminally-bound hydrogens, and the smaller, downfield resonance to two hydrogens bridging the two metals. Line shape analysis of the variable temperature ^1H NMR data (see Appendix, Chapter 1), assuming that equivalence of the hydrogen atoms obtains as the atoms move from terminal to bridging to terminal positions, that no more than three hydrogen atoms bridge the metal centers at any one time, and that at no time does an iridium have more than two terminal hydrogen ligands, for a total of eight exchange permutations, allows calculation of the activation parameters $\Delta H^{\ddagger}$ = 7.35(7) kcal, $\Delta S^{\ddagger}$ = 0.2(0.3) e.u., k_{298} (extrapolated) = 3.6(6) x 10^6 s^{-1}, and $\Delta G^{\ddagger}_{298}$ = 7.26(3) kcal. The smallness of this value of $\Delta G^{\ddagger}$ is in keeping with the difficulty in reaching a static limit.

Reaction of $\mathbf{1}\cdot PF_6$ or $\mathbf{1}\cdot BF_4$ with the more nucleophilic trialkylborohydride reducing agent $LiEt_3BH$ yields a dark solution from which the lithium salt of a trihydride anion, $(C_5(CH_3)_5)IrH_3[Li(THF)_x]$, **5**, can be isolated as a strongly THF-solvated material (Scheme 1). The deep red-orange complex, while

impossible to purify, proved reasonably soluble in hydrocarbon solvents due to the presence of THF. The presence of pentamethyldiethylenetriamine, pmdeta, in the reaction mixture leads to $(C_5(CH_3)_5)IrH_3[Li(pmdeta)]$, **8**, in impure form and mediocre yield, due in part to the formation and persistence of an unknown pmdeta/triethylborohydride adduct. Both **8** and **5** react with Ph_3SnBr to give $(C_5(CH_3)_5)IrH_3SnPh_3$, in fair yield.

Spectral characterization of **5** took the form of comparison with the well-characterized salt $(C_5(CH_3)_5)IrH_3[Li(pmdeta)]$, **8**, formed by treatment of $(C_5(CH_3)_5)IrH_4$, **6**, with t-BuLi and pmdeta (see below); we are quite certain of the formulation of **5** based on these comparisons. The ^1H and $^{13}C\{^1H\}$ NMR experiments provided the most telling comparisons, so we shall discuss the spectra of both compounds here.

In the ^1H NMR spectrum of **8**, in addition to the resonances due to sequestering ligand, resonances due to the $C_5(CH_3)_5$ ligand (δ 2.52) and the iridium-bound hydrogen atoms (δ -19.2) appear as broad singlets. Of note is the significant downfield shift of the $C_5(CH_3)_5$ resonance from that of its neutral precursor $(C_5(CH_3)_5)IrH_4$, **6** (δ 1.99). In addition, the hydride resonance shifts upfield nearly four ppm from that in **6** (δ -15.4). In fact, the resonances for **8** are each well shifted from any of the neutral polyhydride complexes we have characterized containing the $(C_5(CH_3)_5)Ir$ fragment, whether monomeric or dimeric. We suggest this result indicates the presence of a very electron-rich (basic) metal center in **8** (cf. $(C_5(CH_3)_5)Ir(P(CH_3)_3)H_2$,[8] ^1H NMR: δ 2.11 (C_5Me_5); -17.4 (Ir-H); and

$(C_5(CH_3)_5)Ir(P(CH_3)_3)_2HBF_4$, (Chapter 2) ^1H NMR: δ 2.09 (C_5Me_5); -17.8 (Ir-H)). For complex 5, the corresponding resonances occur at δ 2.18 and -19.2 respectively, predicting that complexes 5 and 8 are similar in structure and metal basicity.

A similar, and possibly more indicative, result arises from the $^{13}C\{^1H\}$ NMR spectra of 5 and 8. For 8, the $C_5(CH_3)_5$ ring carbon resonance appears at δ 85.0, a full 11.5 ppm shift upfield from that of tetrahydride 6, and the only previous example in our experience (Chapters 1-3 and Refs. 6a and 8) with these compounds of this resonance lying upfield of δ 90. For 5, the corresponding resonance appears at δ 87.4, strongly suggesting that 5 is a salt of the trihydride anion. The IR spectra of both complexes are consistent with this assignment as well; the band corresponding to the iridium-terminal hydrogen stretch (2019 cm^{-1}) shifts strongly to lower frequency compared to that for tetrahydride 6, a result noted previously.[24,25]

Compound 5, like its analogues 7 and 8, will scavenge a proton from a number of sources to yield tetrahydride 6, a formal oxidation of an iridium (III) species to an iridium (V) species (Scheme 1). It is clear that in the original preparation of 6, anion 5 was formed in the reaction mixture and converted to 6 when the reaction mixture was filtered through a short column of alumina (III). This explains a previously puzzling result: when we attempted to isolate 6 by merely evaporating the solvent from the reaction mixture and subliming the residue, no product ever appeared.

Tetrahydride **6** reacts with t-BuLi, either with or without the sequestering agent pmdeta, to cleanly generate the anionic trihydride complexes $(C_5(CH_3)_5)IrH_3Li$, **7**, and $(C_5(CH_3)_5)IrH_3[Li(pmdeta)]$, **8**, in good yield and analytical purity (Scheme 3). Compound **7** is a somewhat pyrophoric white salt, completely insoluble in inert solvents at ambient temperature, although the isolation of **5** indicates that **7** might be stable in THF solution; so far, our attempts at dissolution have proved unsuccessful.

Complex **8** has the advantage of far greater solubility than **7**, and shows no tendency to burn in air. The yellow-white salt decomposes instantly in air to black material, but may be easily handled under an inert atmosphere. Determination of the molecular weight indicates that the complex is monomeric in solution at ambient temperature, presumably due to the sequestering of the lithium cation by pmdeta. The salt dissolves easily in toluene, benzene and hexane at ambient temperature without decomposition or loss of the sequestering agent, allowing homogeneous quenching with stannylating and silylating agents to give new iridium (V) complexes.

Quenching anion **8** (or **7**) with Ph_3SnBr allows the isolation of the stable iridium (V) trihydride $(C_5(CH_3)_5)IrH_3SnPh_3$, **9c** (Scheme 4). The compound decomposes upon heating to 150 °C in the solid state, and seems to be air stable both as a solid and in solution. The ^1H NMR spectrum of **9c** shows dynamic behavior over the temperature range -65 to 80 °C, allowing the prediction of the molecular structure in solution. At 80 °C, the resonance resulting from the iridium-bound hydrogens (δ -15.7) appears as a sharp singlet, with satellite peaks

Scheme 3

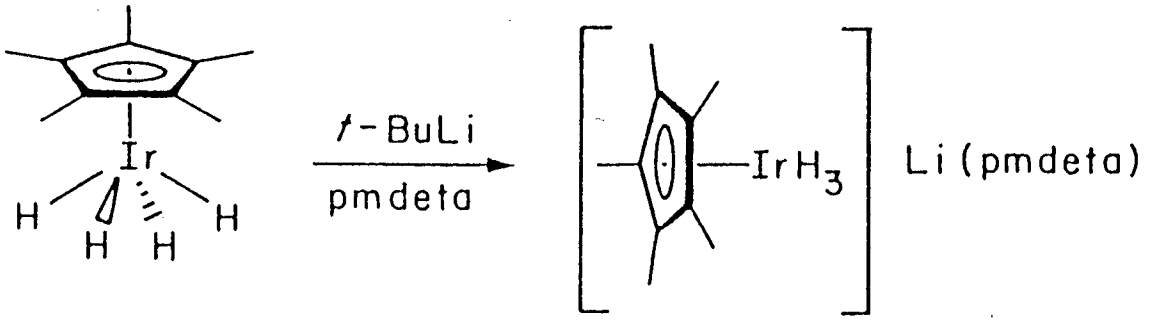

6 8

Scheme 4

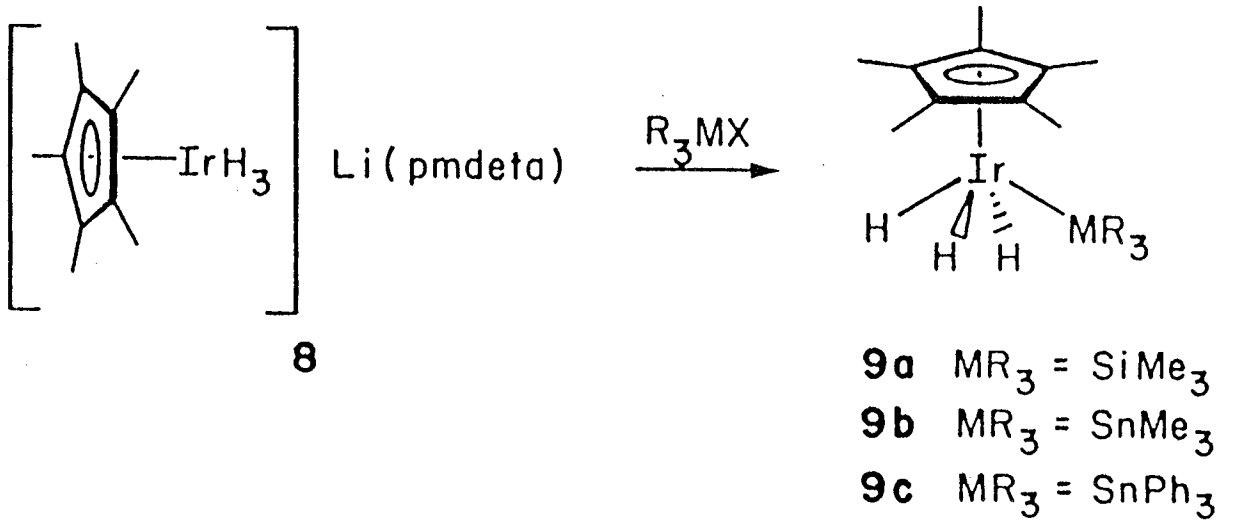

8

9a $MR_3 = SiMe_3$

9b $MR_3 = SnMe_3$

9c $MR_3 = SnPh_3$

due to the presence of tin (^{117}Sn, abundance 7.61%; ^{119}Sn, abundance 8.58%; for both isotopes, s=1/2), although the two sets of satellites are unresolved. Near room temperature, the hydride resonance broadens to near the baseline, with the tin satellites no longer visible. Decoalescence of the signal occurs at -10 °C; upon cooling to -65 °C, two resonances appear, a downfield doublet (δ -15.4) integrating as two hydrogens, and an upfield triplet (δ -15.6) integrating as one hydrogen. The equivalence of the coupling constants demonstrates that the two sets of hydrogens couple to each other. Although the tin satellites could not be resolved, the most reasonable structure consistent with the data is the "four-legged piano stool", with the $SnPh_3$ ligand occupying one "leg" site and the hydrogen atoms the other three, giving one hydrogen trans to the tin atom and two hydrogens cis. Such a structure has been predicted previously for $(C_5(CH_3)_5)Os(CO)H_3$,[26] and observed crystallographically for $(C_5(CH_3)_4(C_2H_5))Ru(CO)Br_3$.[27]

Line shape analysis of the variable temperature ^1H NMR data (Figures 3 and 4), using two exchange permutations (representing each of the cis hydrogens exchanging with the trans hydrogen, but not with each other), yielded activation parameters $\Delta H^{\ddagger}$ = 10.6(5) kcal, $\Delta S^{\ddagger}$ = -10.3(1.9) e.u., k_{298} (extrapolated) = 297(15) s^{-1}, and $\Delta G^{\ddagger}_{298}$ = 13.69(3) kcal. The large negative entropy of activation seems to correlate with the steric bulk of the non-hydrogen ligand (see below).

In order to test the "piano-stool" hypothesis, we performed a single crystal X-ray diffraction study of **9c**. Experimental data are

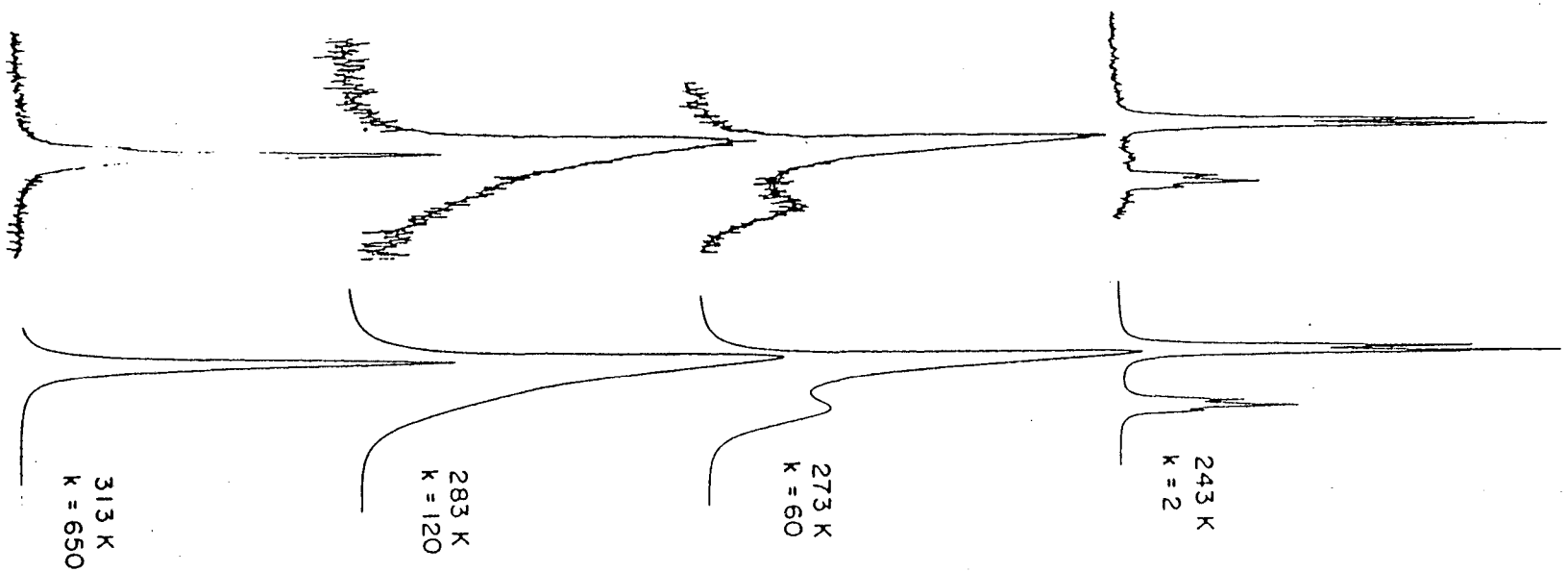

Figure 3. Experimental and calculated ^{1}H NMR spectra (300 MHz) for **9c** at various temperatures. The region shown is that between δ -14 and -17.3.

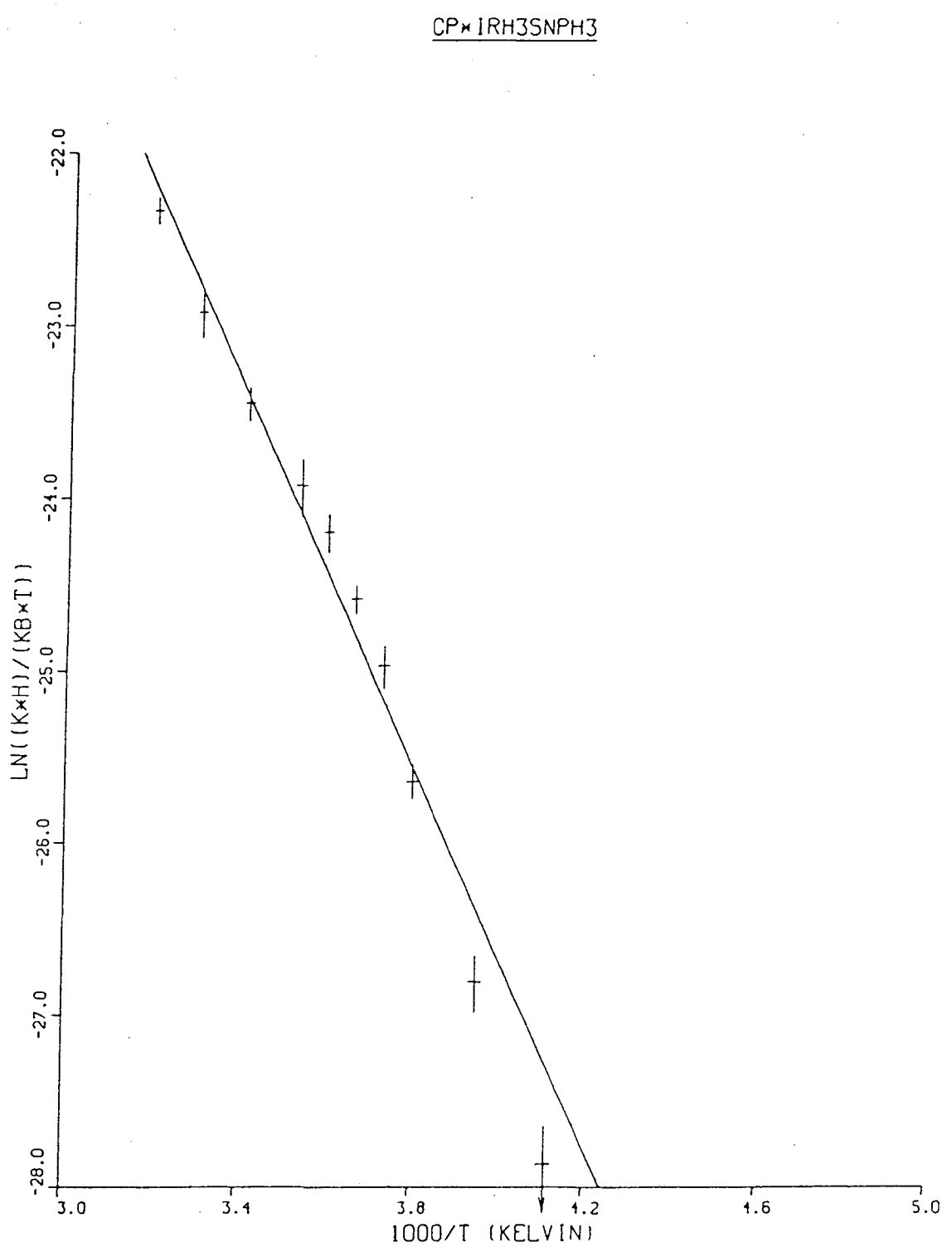

Figure 4. Eyring plot (from ACTPAR) for **9c**.

given in Table 1; an ORTEP view of the molecule appears in Figure 5.

The solid state result confirms the interpretation of the ^1H NMR data. The molecule adopts a nearly perfect piano stool configuration (given the difference in bonding radii between tin and hydrogen), minimizing steric contacts between the $C_5(CH_3)_5$ ring and the ligands. In general, the bond lengths and angles lie in the expected ranges (Table 5); within experimental error, the Ir, Sn, and H2 atoms and the Cp centroid lie in a molecular (not crystallographic) pseudo mirror plane. Interestingly, a real variation in bond distances from the iridium atom to the $C_5(CH_3)_5$ ring carbon atoms exists; this effect may be interpreted as either a ring slippage toward the tin atom, or a ring tilt away from the tin atom.

The use of $Me_3SiO_3SCF_3$ or Me_3SnCl as quenching agents for **8** yields the new complexes $(C_5(CH_3)_5)IrH_3SiMe_3$, **9a**, and $(C_5(CH_3)_5)IrH_3SnMe_3$, **9b**, as white, crystalline solids which may be sublimed from the reaction mixture. Variable temperature ^1H NMR experiments indicate that **9a** and **9b** adopt molecular structures isomorphous to that of **9c**; in both cases the low temperature pattern appears as a doublet integrating as two hydrogens and a triplet integrating as one hydrogen. Interestingly, for these complexes the more upfield resonance is the doublet, whereas for **9c** the more upfield resonance is the triplet. For **9a**, line shape analysis as described above for **9c** yields $\Delta H^{\ddagger}$ = 13.9(6) kcal, $\Delta S^{\ddagger}$ = 8.6(2.4) e.u., k_{298} (extrapolated) = 1.5(4) x 10^4 s^{-1}, and $\Delta G^{\ddagger}_{298}$ = 11.35(14) kcal, while for **9b**, $\Delta H^{\ddagger}$ = 10.7(2) kcal, $\Delta S^{\ddagger}$ = -6.0(1.0) e.u., k_{298} (extrapolated) = 2.2(3) x 10^3 s^{-1}, and $\Delta G^{\ddagger}_{298}$ = 12.48(9) kcal. We

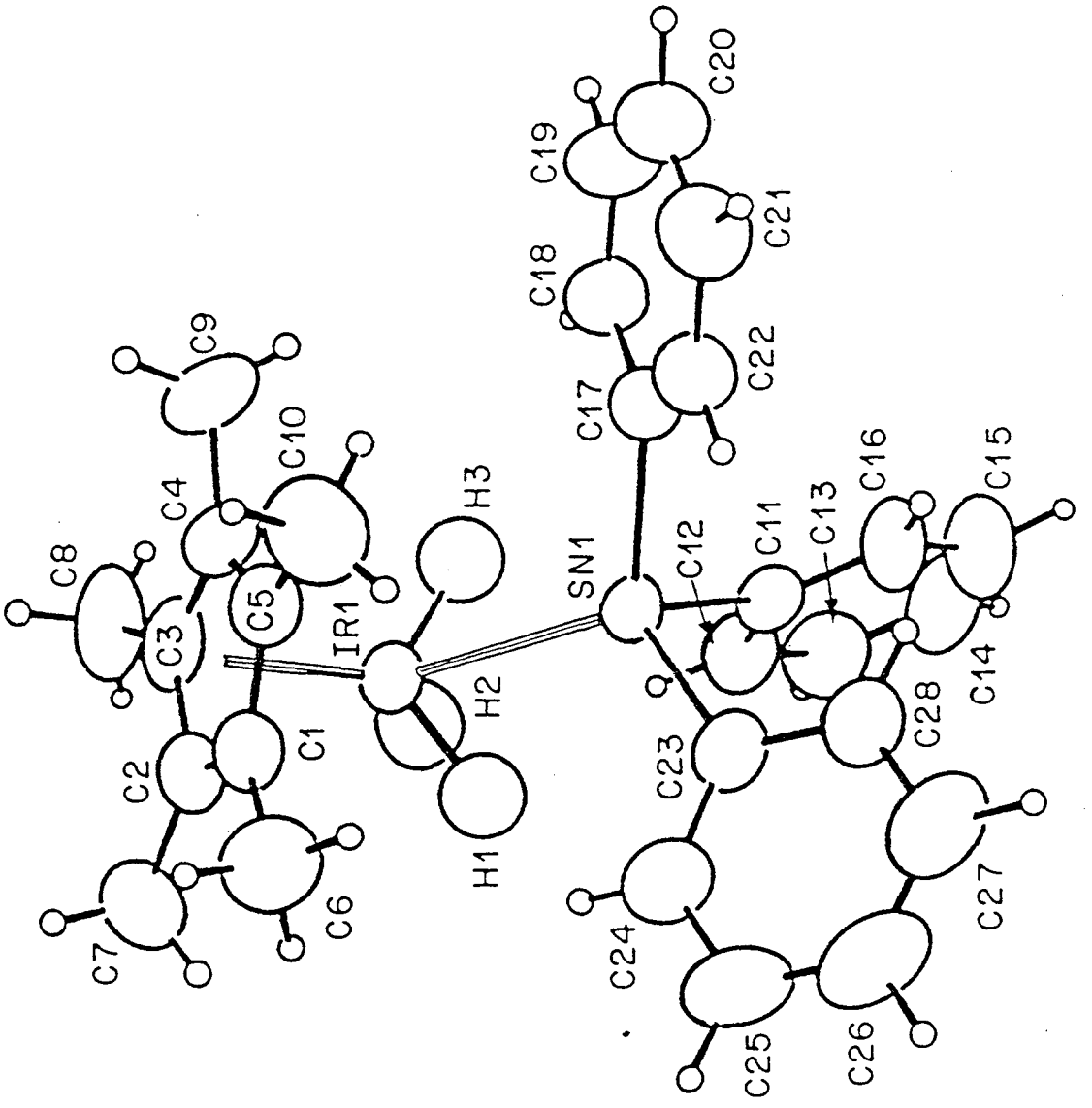

Figure 5. ORTEP drawing of **9c**.

Table 5. Selected Bond Distances (Å) and Angles (°) for 9c.

ATOM 1	ATOM 2	DISTANCE
IR1	SN1	2.588(1)
IR1	H1	1.50(3)
IR1	H2	1.47(3)
IR1	H3	1.61(3)
IR1	C1	2.248(3)
IR1	C2	2.213(3)
IR1	C3	2.216(3)
IR1	C4	2.251(3)
IR1	C5	2.278(3)
IR1	CP1[a]	1.890
SN1	C11	2.154(3)
SN1	C17	2.166(2)
SN1	C23	2.165(3)

ATOM 1	ATOM 2	ATOM 3	ANGLE
CP1	IR1	SN1	128.94
CP1	IR1	H1	126.6
CP1	IR1	H2	128.5
CP1	IR1	H3	122.9
SN1	IR1	H1	68.9(11)
SN1	IR1	H2	102.5(12)
SN1	IR1	H3	65.8(11)
H1	IR1	H2	69.7(15)
H1	IR1	H3	110.4(15)
H2	IR1	H3	71.9(16)
IR1	SN1	C11	113.80(7)
IR1	SN1	C17	113.86(7)
IR1	SN1	C23	114.57(7)
C11	SN1	C17	103.79(10)
C11	SN1	C23	104.28(9)
C17	SN1	C23	105.41(10)

(a) CP1 is the calculated centroid of the pentamethylcyclopentadienyl ring

note the general decrease in $\Delta S^{\ddagger}$ and the resulting increase in $\Delta G^{\ddagger}$ as the presumed steric bulk of the silyl/stannyl group increases from $SiMe_3$ through $SnMe_3$ to $SnPh_3$. Further confirmation of this effect is provided by the even less sterically hindered[28] complex $(C_5(CH_3)_5)Ir(P(CH_3)_3)H_3BF_4$ (Chapter 1), for which $\Delta S^{\ddagger} = 3.7(1.6)$ e.u. and $\Delta G^{\ddagger}_{298} = 10.84(8)$ kcal.

As this synthetic method had worked so well for preparing iridium-main group metal dimers, we attempted to prepare an iridium-transition metal dimer. Upon reaction with one equivalent of Cp_2ZrCl_2, the heteronuclear dimer $(C_5(CH_3)_5)IrH_3((Cp_2)ZrCl)$ may be isolated in good yield from the reaction mixture as a crystalline orange solid. This material is rather air-sensitive, and surprisingly thermally unstable as well. Dimer **10** decomposes completely to $(C_5(CH_3)_5)IrH_4$ and an unknown complex containing the Cp_2Zr fragment in benzene solution over a few days at room temperature, in contrast to **9a**, **9b**, and **9c**, which appear indefinitely stable under similar conditions. The complex appears to be stable in the solid state for longer periods, however.

The structure of **10** is of interest, particularly in light of recent work by Caulton and coworkers.[29] Unfortunately, we have not yet been successful in growing crystals suitable for X-ray diffraction studies. Low temperature ^1H NMR studies indicate that complex **10** probably adopts a different structure than the electronically analogous $Cp_2ZrCl(\mu\text{-}H)_3Os(PR_3)_3$.[29] At ambient temperature, one sharp upfield signal appears in the ^1H NMR spectrum, but at -120 °C, the signal splits into a broad downfield resonance

(δ -12.46) integrating as two hydrogens, and a broad upfield resonance (δ -16.92) integrating as one hydrogen. These are only slightly above the baseline at this temperature and field strength, indicating a coalescence temperature of approximately -100 °C (173 K), and therefore a free energy at this temperature $\Delta G^{\ddagger}_{173} \sim 8$ kcal. This value, and the difficulty in obtaining it, are reminiscent of those for dimer 3, suggesting that the exchange process probably interconverts bridging and terminal hydride ligands.

Throughout the temperature region studied, the resonances appearing in the downfield alkyl region of the ^{1}H NMR spectrum remain singlets, indicating in particular that the cyclopentadienyl rings of the zirconium fragment are equivalent on the NMR time scale. However, this does not necessarily require that these rings be equivalent at the true (i.e. solid state) static limit. We cannot determine whether one or two hydrogens bridge at the NMR static limit, or whether perhaps the chlorine ligand occupies a bridging site; the only provable statement is that there are clearly different types of hydride ligands, in contrast to $Cp_2ZrCl(\mu\text{-}H)_3Os(PR_3)_3$. Structures consistent with the available data are given in Figure 6; only a diffraction study will answer all the structural questions.

Conclusion

On the basis of the results outlined in this paper, we propose that the conversion of $[(C_5(CH_3)_5)Ir]_2(\mu\text{-}H)_3^+$ **(1)** to two equivalents of $(C_5(CH_3)_5)IrH_4$ **(6)** upon reaction with excess $LiEt_3BH$ occurs according to the mechanism outlined in Scheme 1. Specific features of this hypothesis follow.

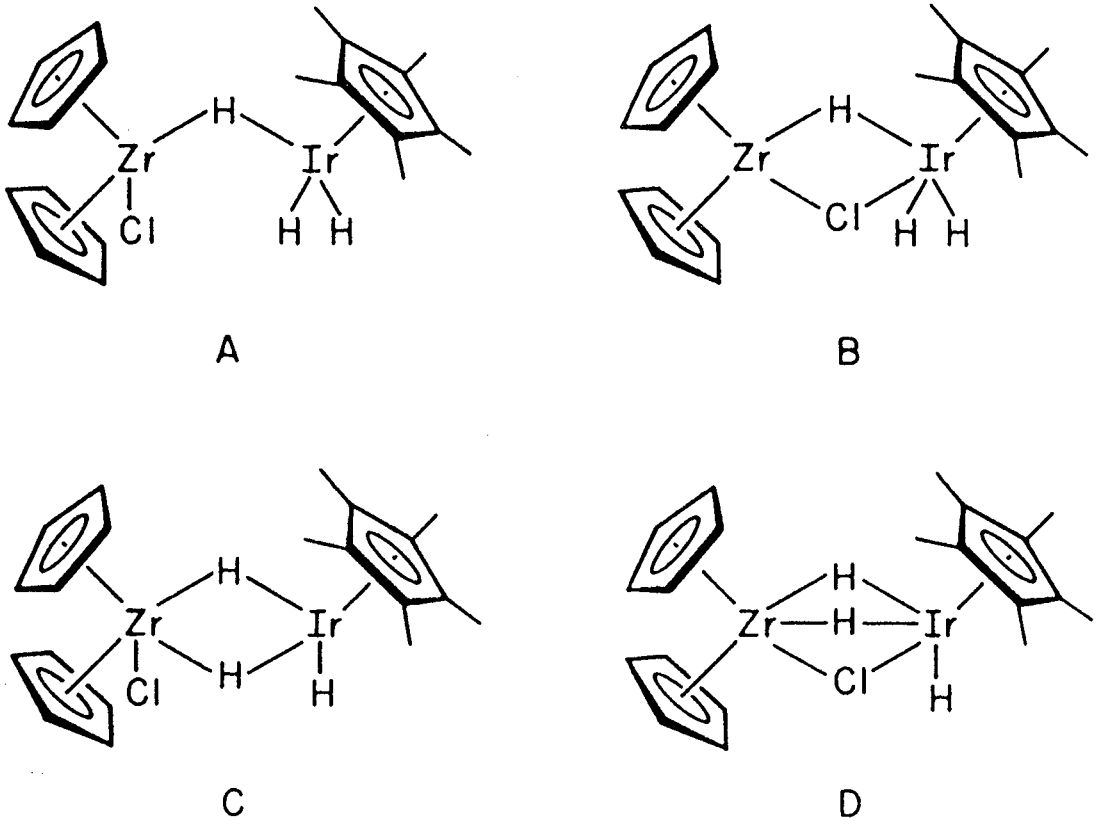

Figure 6. Possible structures for complex 10

Upon reaction of 1 with the first equivalent of borohydride reducing agent ($LiBH_4$ or $LiEt_3BH$), the neutral, dimeric borohydride complex **2** is produced. When $LiBH_4$ (R = H, Scheme 1) acts as the reducing agent, dimer **2** is unreactive toward further attack by $LiBH_4$ (it will react further with $LiEt_3BH$, however). In this instance, the BH_4 fragment "swings around" and coordinates to both iridium centers, giving the isolated complex studied by X-ray diffraction. When $LiEt_3BH$ (R = Et, Scheme 1) acts as the reducing agent, the borohydride fragment probably does not bridge both metals in the neutral complex 2, since it is unlikely that the ethyl group can form such a bridge. Instead, the triethyl borohydride anion either fully transfers its hydride to the iridium dimer, yielding transient $[(C_5(CH_3)_5)IrH_2]_2$ and free triethylborane, or possibly a complex is formed with a hydrogen bridging the iridium and boron centers and the ethyl groups uncoordinated. In any event, with either borohydride reducing agent, a neutral iridium dimer with at least four coordinated hydrogen atoms is formed.

Hydrolysis of the reaction mixture at this point (R = H, Et) by treatment with methanol or chromatography through alumina III generates the polyhydride dimer **3**, presumably by oxidation of the boron center to $B(OH)_3$ or $B(OCH_3)_3$ (Scheme 2). This dimer represents a dead end in the reaction; **6** cannot be generated by reaction of **3** with $LiEt_3BH$.

Further reduction of **2** occurs when $LiEt_3BH$ acts as the reducing agent (assuming that excess $LiEt_3BH$ is used), presumably yielding the anionic dimer shown in the Scheme. The BEt_3 fragments do not

necessarily coordinate as shown; however, no a priori reason exists why they should not, and the presence of boron in **2** and of boron-containing impurities in isolated **5** suggests that "BEt_3" species are not simply inert.

At this point, a third equivalent of $LiEt_3BH$ splits the anionic dimer into two equivalents (based on **1**) of monomeric $(C_5(CH_3)_5)IrH_3[Li(THF)_x]$, **5**, which we isolated and characterized. This step of the process represents the last in which $LiEt_3BH$ takes part; thus the formation of **5** from **1** requires three equivalents of hydride. Experience has shown, however, that somewhat more reducing agent results in higher yields of tetrahydride **6**, probably due to the increased bimolecular reaction rate brought on by larger reactant concentration.

Oxidation of **5** to $(C_5(CH_3)_5)IrH_4$, **6**, then, occurs not in the reaction vessel, but in the purification procedure. When the reaction mixture is poured through alumina III, impurities and excess $LiEt_3BH$ are removed; the anionic iridium (III) trihydride monomer **5** is protonated by surface water leading to the neutral iridium (V) tetrahydride **6**. Therefore **6** cannot be isolated from the unhydrolyzed reaction mixture.

The mechanism in Scheme 1 is very similar to that illustrated in Scheme 1 in Chapter 1. In fact, the molecules in each Scheme are isomorphous, with the substitution of H^- for $P(CH_3)_3$. Thus the unisolable monophosphine dimer cation $[(C_5(CH_3)_5)Ir]_2(P(CH_3)_3)H_3^+$ maps onto borohydride dimer $[(C_5(CH_3)_5)Ir]_2H_3(BH_4)$, **2**; the bisphosphine dimer cation $[(C_5(CH_3)_5)Ir(P(CH_3)_3)(H)]_2(\mu\text{-}H)^+$ maps onto

the proposed anionic dimer $[(C_5(CH_3)_5)Ir]_2H_5^-$, and $(C_5(CH_3)_5)Ir(P(CH_3)_3)H_2$ maps onto $[(C_5(CH_3)_5)IrH_3]^-$, **5**. Protonation of each of the latter leads to the iridium (V) complexes $(C_5(CH_3)_5)Ir(P(CH_3)_3)H_3^+$ and $(C_5(CH_3)_5)IrH_4$, **6**, completing the analogy.

We consider this work to be a particularly detailed study of a hydride-induced reaction which, overall, results in formal oxidation of the metal center.[5] Workers in the field know that hydrolysis is often a necessary step after borohydride reduction, and that protonation of hydride anions yields polyhydride complexes in which formal oxidation has occurred at the metal center, but this seems to be the first demonstration of the combination of the two concepts in a reaction mechanism.[30] As workers often report hydrolysis or column chromatography of reaction mixtures to destroy the hydridic reducing agent, the potential exists that processes such as described here are general features of polyhydride oxidation chemistry.

Similar potential exists for the formal substitution of hydride anion for phosphine ligands to lead to future chemistry. For example, the stability of the well-studied ReH_9^{2-} dianion complex[31] might have been expected based on the many complexes of the general form $ReH_7(PR_3)_2$, and in fact the formal hydride/phosphine substitution has been applied to this rhenium system.[32] Similarly, applying this substitution to the series $FeH_2(PR_3)_4$[33] predicts the stability of FeH_6^{4-}, an example of which has been described.[34] We hope that future work in this area will help to develop (or negate) the reasonableness of this phosphine/hydride analogy; one interesting

series of complexes which would provide evidence for the hypothesis is the WH_{6+x}^{x-} group, based on the known $WH_6(PR_3)_x$ series.[35]

Clearly, the use of $LiEt_3BH$ is important in the reaction; the nucleophilicity of this reagent must play a role in the formation of **5** (and therefore **6**) from **1**, since different results obtain when $LiBH_4$ is used. Possibly the inability of the Et_3BH^- moiety to form stable bridging networks analogous to those of BH_4^- is a factor as well; however, as **2** reacts with $LiEt_3BH$ to generate **5**, this factor is of only slight importance. Other workers[36] have commented upon cleaner reactions and higher yields of polyhydrides using $LiEt_3BH$; thus the difference observed here appears to be general.

Of importance to the development of iridium (V) chemistry is the synthesis of complexes **9a**, **9b**, and **9c** by the method described. Green and coworkers[24,25] first employed alkyllithium reagents to deprotonate organometallic polyhydrides, and were able to prepare numerous interesting alkyl, aryl, and acyl hydrides from the anionic species; however, this method has not until now enjoyed widespread use. We have not yet prepared an iridium (V) alkyl hydride, but the syntheses of **9a**, **9b**, and **9c** give hope that such complexes may be isolable. In any event, the work described herein may lead to a general route for the preparation of heteronuclear organometallic polyhydride dimers, including the important early-to-late transition metal complexes.

As noted in Chapter 1, few activation parameter data exist regarding hydride site exchange in organometallic polyhydride species,[37] particularly when the populations of the sites are

unequal. For the iridium (V) complexes described, apparently a correlation exists between the values of $\Delta S^{\ddagger}$ (and since the enthalpies of activation are similar, of $\Delta G^{\ddagger}$) and the steric bulk of the non-hydrogen ligand. The results show that when the ligand is bulky, a strong increase in molecular ordering occurs as the transition state is approached; the hydrogen ligands "see" the substituents attached to the silicon or tin as they exchange with one another. How the increase in ordering is actually manifested is unclear; we hope future studies will address this question.

References.

(1) "Transition Metal Hydrides"; Muetterties, E. L., Ed.; Marcel Dekker: New York, 1971.

(2) Parshall, G. W. Acc. Chem. Res. **1975**, 8, 113.

(3) For recent reviews, see (a) "Transition Metal Hydrides"; Bau, R., Ed.; Adv. Chem. Ser., No. 167; Marcel Dekker: New York, 1978. (b) Teller, R. G.; Bau, R. Struc. Bonding (Berlin), **1981**, 44, 1. (c) Soloveichik, G. L.; Bulychev, B. M. Russian Chem. Rev. **1982**, 51, 286. (d) Moore, D. S.; Robinson, S. D. Chem. Soc. Rev. **1983**, 12, 415.

(4) Reference to high oxidation states is meant in a formal electron-counting sense when applied to organometallic polyhydride species; a deficiency of electron density at the metal center is not necessarily implied. See Crabtree, R. H. Acc. Chem. Res. **1979**, 12, 331.

(5) Labinger, J. A.; Wong, K. S. J. Organomet. Chem. **1979**, 170, 373.

(6) (a) Gilbert, T. M.; Bergman, R. G. Organometallics **1983**, 2, 1458. (b) Isobe, K.; Vasquez de Miguel, A.; Nutton, A.; Maitlis, P. M. J. Chem. Soc., Dalton Trans. **1984**, 929, and references therein.

(7) (a) White, C.; Oliver, A. J.; Maitlis, P. M. J. Chem. Soc., Dalton Trans. **1973**, 1901. (b) Gill, D. S.; Maitlis, P. M. J. Organomet. Chem. **1975**, 87, 359.

(8) (a) Janowicz, A. H.; Bergman, R. G. J. Am. Chem. Soc. **1982**, 104, 351. (b) Janowicz, A. H.; Bergman, R. G. J. Am. Chem. Soc. **1983**, 105, 3929.

(9) Clark, E. P. Ind. Eng. Chem., Anal. Ed. **1941**, 13, 820.

(10) The instrumentation, methods of data collection, computer programs, and formulae for data reduction and structure solution have been described: Theopold, K. H.; Bergman, R. G. J. Am. Chem. Soc. **1983**, 105, 464.

(11) Reflections used for azimuthal scans were located near $\chi = 90°$ and the intensities were measured at 10° increments of rotation of the crystal about the diffraction vector.

(12) Zachariesen, W. H. Acta Cryst. **1963**, 16, 1139.

(13) Marks, T. J.; Kolb, J. R. Chem. Rev. **1977**, 77, 263.

(14) Streitweiser, A.; Heathcock, C. H. "Introduction to Organic Chemistry"; MacMillan: New York, 1976.

(15) (a) Letts, J. B.; Mazanec, T. J.; Meek, D. W. J. Am. Chem. Soc. 1982, 104, 3898 and references therein. (b) Takusagawa, F.; Fumagilli, A.; Koetzle, T. F.; Shore, S. G.; Schmitkons, T.; Fratini, A. V.; Morse, K. W.; Wei, C-Y.; Bau, R. J. Am. Chem. Soc. **1981**, 103, 5165 and references therein. (c) Wink, D. J.; Cooper, N. J. J. Chem. Soc., Dalton Trans. **1984**, 1257, and references therein.

(16) Cotton, F. A.; Wilkinson, G. "Advanced Inorganic Chemistry, 4th Edition"; Wiley and Sons: New York, 1980.

(17) Holah, D. G.; Hughes, A. N.; Maciasek, S.; Magnuson, V. R. J. Chem. Soc., Chem. Commun. **1983**, 1308.

(18) Holah, D. G.; Hughes, A. N.; Hui, B. C.; Wright, K. Can. J. Chem. **1974**, 52, 2990.; Holah, D. G.; Hughes, A. N.; Hui, B. C.; Kan, C-T. Can. J. Chem. **1978**, 56, 2552.

(19) Huheey, J. E. "Inorganic Chemistry"; Harper and Row: New York, 1978.

(20) Bondi, A. J. Phys. Chem. **1964**, 68, 441.

(21) Bould, J.; Greenwood, N. N.; Kennedy, J. D.; McDonald, W. S. J. Chem. Soc., Chem. Commun. **1982**, 465; Bould, J.; Crook, J. E.; Greenwood, N. N.; Kennedy, J. D.; McDonald, W. S. Ibid, **1982**, 346; Crook, J. E.; Greenwood, N. N.; Kennedy, J. D.; McDonald, W. S. Ibid **1981**, 933.

(22) Corey, E. J.; Cooper, N. J.; Canning, W. M.; Lipscomb, W. N.; Koetzle, T. F. Inorg. Chem. **1982**, 21, 192, and references therein.

(23) (a) Only one example of a quadruply hydrogen-bridged metal-metal dimer is known,[23b] which contains sterically undemanding terminal phosphine and hydride ligands; the $C_5(CH_3)_5$ ligands in complex **3** should be much more sterically demanding and should "push" hydrogens to terminal sites. We are attempting to confirm this by growing suitably sized crystals for a neutron diffraction study. (b) Bau, R.; Carroll, W. E.; Teller, R. G.; Koetzle, T. F. J. Am. Chem. Soc. **1977**, 99, 3872. (c) The dimer $[(Me_2PhP)_2IrH_3]_2$ has been determined to have two bridging and four terminal hydrogen ligands by X-ray diffraction; Robertson, G. B.; Tucker, G. A. Aust. J. Chem. **1984**, 37, 257.

(24) $Cp_2MoH_2/(Cp_2MoHLi)_4$: D'Aniello, M. J.; Barefield, E. K. J. Organomet. Chem. **1974**, 76, C50.; Francis, B. R.; Green, M. L. H.; Luong-Thi, T.; Moser, G. A. J. Chem. Soc., Dalton Trans. **1976**, 1339.

(25) Cp_2WH_2/$[Cp_2WHLi(pmdeta)]_x$: Cooper, R. L.; Green, M. L. H.; Moelwyn-Hughes, J. T. J. Organomet. Chem. 1965, 3, 261.; Johnson, M. D.; Shriver, D. F. J. Am. Chem. Soc. 1966, 88, 301.; Mink, R. I. Ph. D. Dissertation, University of Illinois, Champaign-Urbana, Ill., 1977.

(26) Graham, W. A. G.; Hoyano, J. K. J. Am. Chem. Soc. 1982, 104, 3722.

(27) Nowell, I. W.; Tabatabaian, K.; White, C. J. Chem. Soc., Chem. Commun. 1979, 547.

(28) Tolman, C. A. Chem. Rev. 1977, 313.

(29) Bruno, J. W.; Huffman, J. C.; Green, M.A.; Caulton, K. G. J. Am. Chem. Soc. 1984, 106, 8310.

(30) Davies, S. G.; Moon, S. D.; Simpson, S. J. J. Chem. Soc., Chem. Commun. 1983, 1278.

(31) Abrahams, S. C.; Ginsberg, A. P.; Knox, K. Inorg. Chem. 1964, 3, 558.

(32) Chatt, J.; Coffey, R. S. J. Chem. Soc. (A) 1969, 1963.

(33) Gerlach, D. H.; Peet, W. G.; Muetterties, E. L. J. Am. Chem. Soc. 1972, 94, 4545.

(34) Bau, R.; Ho, D. M.; Gibbins, S. G. J. Am. Chem. Soc. 1981, 103, 4960.

(35) Borisov, A. P.; Makhaev, V. D.; Semenenko, K. N. Sov. J. Coord. Chem. 1980, 6, 549.

(36) Crabtree, R. H.; Hlatky, G. G. Inorg. Chem. 1982, 21, 1273.

(37) (a) Meakin, P.; Guggenberger, L. J.; Peet, W. G.; Muetterties, E. L.; Jesson, J. P. J. Am. Chem. Soc. 1973, 95, 1467. (b) Muetterties, E. L.; Jesson, J. P. in "Dynamic Nuclear Magnetic Resonance Spectra", L. M. Jackman and F. A. Cotton, Eds. Academic Press: New York, 1975.

Chapter 5. NMR Spectra of $(C_5(CH_3)_5)IrH_2SiMe_3Li(pmdeta)$ and $(C_5(CH_3)_5)IrH_3Li(pmdeta)$: The First Direct Observation of Resolved ^7Li-^1H Coupling.

Introduction.

Observation of scalar spin-spin coupling between ^{7}Li and ^{13}C in the nuclear magnetic resonance spectra of these nuclei has been critical in determining degrees of oligomerisation for organolithium species in solution.[1] Recently, coupling between ^{7}Li and ^{31}P was reported for a series of phosphido-lithium dimers $[LiPR_2]_2$, R = Ph[2], $CH(SiMe_3)_2$[3]. Surprisingly, however, coupling between ^{7}Li and ^{1}H nuclei has not been resolved in simple alkyl- and aryl lithium complexes, although labeling and decoupling experiments strongly suggest such couplings exist.[4,5]

We report the observation of significant ^{7}Li-^{1}H spin-spin coupling between the hydrogen and lithium ligands in the complexes $(C_5(CH_3)_5)IrH_2SiMe_3Li(pmdeta)$, **1** (pmdeta = pentamethyldiethylenetriamine), and $(C_5(CH_3)_5)IrH_3Li(pmdeta)$, **2**, as well as temperature dependence studies which bear upon the novelty of these results.

Experimental.

General. Experimental and characterization methods were described in Chapter 1. ^{7}Li and $^{1}H\{^{7}Li\}$ NMR spectra were obtained on the 300 MHz instrument at the UCB NMR facility, and are reported as ppm downfield of TMS (^{1}H) and LiCl in MeOH (^{7}Li).

$(C_5(CH_3)_5)IrH_2SiMe_3Li(pmdeta)$, (1). Addition of t-BuLi (0.210 mmol) to a solution of $(C_5(CH_3)_5)IrH_3SiMe_3$ (Chapter 4) (81 mg, 0.20 mmol) and pmdeta (36 mg, 0.21 mmol) in 1 mL hexane at -40 °C led to precipitation of yellow-white solid. The reaction mixture was maintained at this temperature for 24 h. The microcrystals were then filtered, washed with cold hexane and dried to give pure white **1** (37 mg, 0.063 mmol, 30%). Removal of solvent from the mother liquor and recrystallization of the residue from hexane gave an additional 30% of pure material. ^{1}H NMR (C_6D_6, 20 °C, 300 MHz): δ 2.34 (s, 15H, C_5Me_5); 2.04 (s, 3H, internal amine methyl); 1.98 (s, 12H, terminal amine methyl); 1.7 (br, 8H, amine methylenes); 0.81 (s, 9H, $SiMe_3$); -20.15 (1:1:1:1 quartet, J_{LiH} = 8.4 Hz, 2H, Ir-H). $^{1}H\{^{7}Li\}$ NMR (C_6D_6, 20 °C, 300 MHz, hydride resonance only): δ -20.15 (s, 2H, Ir-H). ^{7}Li NMR (C_6D_6, 20 °C, 116 MHz): δ 3.2 (t, J_{LiH} = 8.4 Hz). $^{7}Li\{^{1}H\}$ NMR (C_6D_6, 20 °C, 116 MHz): δ 3.2 (s). $^{13}C\{^{1}H\}$ NMR (C_6D_6, 20 °C, 75 MHz): δ 88.6 (s, $\underline{C}_5Me_5$); 58.3, 57.0, 46.0, 43.2 (all br s, pmdeta); 12.5 (s, $C_5\underline{Me}_5$); 11.7 (s, $SiMe_3$). IR (C_6D_6): ν_{Ir-H} 2069 cm^{-1} (very br). Anal. Calcd for $C_{20}H_{50}N_3LiSiIr$: C, 45.26; H, 8.63; N, 7.20. Found: C, 44.88; H, 8.37; N, 7.20.

$(C_5(CH_3)_5)IrH_3Li(pmdeta)$, (2). The synthesis and characterization of this complex was reported in Chapter 4. ^1H NMR (toluene-d_8, -20 °C, 300 MHz, hydride resonance only): δ -19.27 (1:1:1:1 quartet, J_{Li-H} = 6.4 Hz, 3H, Ir-H). $^1H\{^7Li\}$ NMR (toluene-d_8, -20 °C, 300 MHz, hydride resonance only): δ -19.27 (s, 3H, Ir-H). ^7Li NMR (toluene-d_8, -20 °C, 116 MHz): δ 5.0 (q, J_{Li-H} = 6.4 Hz). $^7Li\{^1H\}$ NMR (toluene-d_8, -20 °C, 116 MHz): δ 5.0 (s).

Results and Discussion.

As a test of the generality of the deprotonation of (pentamethylcyclopentadienyl)iridium polyhydride compounds by t-BuLi/pmdeta (Chapter 4), we treated a mixture of $(C_5(CH_3)_5)IrH_3SiMe_3$ and pmdeta with t-BuLi in a minimum amount of n-hexane at -40 °C. The pale yellow solution deposited white microcrystals over 24 h, and ultimately we isolated the desired salt **1** in 60% yield. The material is surprisingly soluble in non-polar solvents such as hexane, probably due to the "greasy" $SiMe_3$ and pmdeta ligands.

The ^1H NMR spectrum of a sufficiently dilute (ca. 0.01 M) solution of pure **1** shows an upfield resonance (δ -20.15) due to the iridium-bound hydrides, which appears as a 1:1:1:1 quartet (J = 8.4 Hz), with the outermost peaks slightly reduced in intensity due to the significant linewidth (fwhh ~ 6-7 Hz) (Figure 1, 20 °C spectrum). The structure of the resonance proved to be independent of magnetic field strength over the range 200 - 500 MHz. Suspecting that this feature was due to ^7Li - ^1H spin-spin coupling (^7Li has s = 3/2, 92.6% abundance), we performed a $^1H\{^7Li\}$ NMR experiment. Upon broadband decoupling of the ^7Li frequency, the quartet collapsed to a singlet, indicating loss of ^7Li-^1H coupling. No apparent difference between the downfield alkyl regions of the two spectra were noted.

Further confirmation of this coupling resolution resulted from the ^7Li spectrum. This showed a broad triplet resonance (δ 3.2, J = 8.4 Hz), which collapsed to a broad singlet (fwhh ~ 8-9 Hz) upon broadband irradiation of the proton frequency.

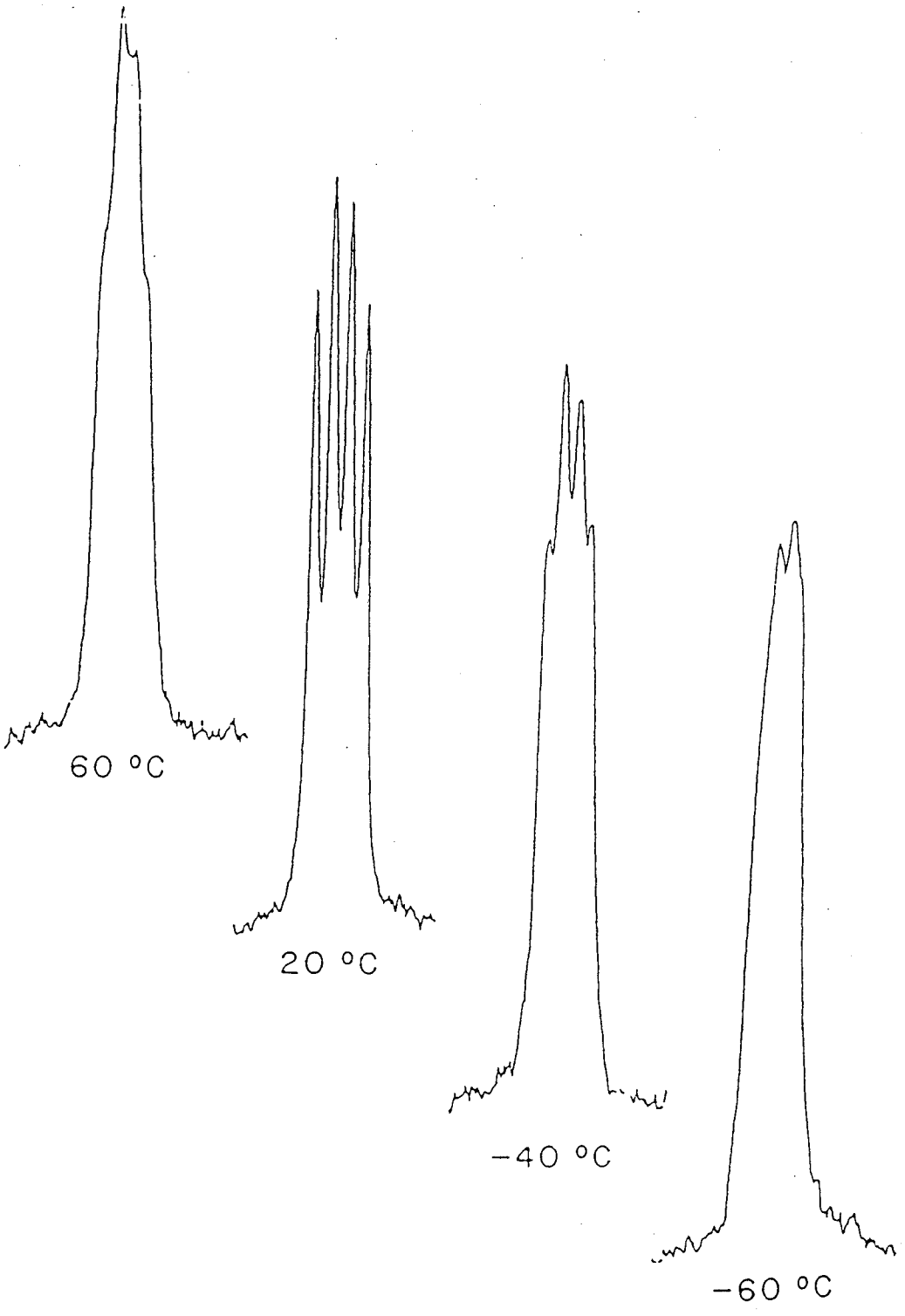

Figure 1. Experimental ^{1}H NMR spectra (300 MHz) of the hydride resonance (δ -20.15) for complex 1 at various temperatures.

During these experiments we noted that the ability to resolve the ^{7}Li-^{1}H coupling varied with temperature. In fact, resolution of the coupling for **1** is restricted to the temperature range -40 to +40 °C; outside this window the lines are broadened to the point where the quartet structure is lost (Figure 1).

Given this interesting result, we carefully reinvestigated the ^{1}H NMR spectrum of $(C_5(CH_3)_5)IrH_3Li(pmdeta)$ (2, Chapter 4), and found a similar window. Splitting of the hydride resonance could only be observed between -10 and -40 °C. The most well-resolved spectrum occurred at -20 °C, and showed essentially the same features as those for complex **1**. The coupling constant proved to be somewhat smaller for this compound than for **1**, and as the proper window covers a smaller temperature range, we were not surprised this feature had not been observed previously.

These results conclusively demonstrate the resolution of scalar spin-spin ^{7}Li-^{1}H coupling, with a coupling constant quite large compared to those observed in organic systems.

Although we do not know how many careful searches have been made for ^{7}Li-^{1}H coupling in other systems, complexes **1** and **2** appear at present to be unique. We suggest the following reasons for this situation:

(1) We believe that both complexes are monomeric in solution. Because the proton resonance appears as a quartet, and not some more complex pattern, the hydride ligands must "see" only one lithium atom on the NMR time scale. Also, a Signer molecular weight determination on $(C_5(CH_3)_5)IrH_3Li(pmdeta)$ indicated it to be monomeric in benzene

solution (Chapter 4). We presume this is due to the known ability of pmdeta to occupy three of four lithium coordination sites.[6]

(2) The ability to resolve the coupling seems quite sensitive to the concentration of **1**. As noted, the results described apply to 0.01 M solutions. While we have not explored this phenomenon in detail, at concentrations approaching 0.02 M, the hydride resonances broaden to doublet-like patterns with "fattening" of the peaks at the wings, and at concentrations > 0.05 M, the peaks appear as broad singlets.

(3) The couplings are large enough that the inherent linewidth plus the quadrupolar broadening due to ^{6}Li and ^{7}Li cannot obscure the fine structure. Even though the ^{7}Li resonances, for example, are 6–9 Hz wide at half height, the total wing separation of 16 Hz for **1** and 18 Hz for **2** are easily large enough to overcome the broadening and show the appropriate multiplet pattern.

(4) The ability to resolve the coupling is clearly temperature dependent. We cannot at this point determine whether the temperature windows observed are due to changes in viscosity of the solvent, changes in the molecular correlation time,[7] differences in rates of intra- or intermolecular ligand exchange, combinations of these factors or some completely different phenomenon. However, we believe that the paucity of variable temperature studies on organolithium complexes may be partly responsible for the novelty of our results.

We have attempted to prepare the phosphine-substituted analogue of complex **1** by deprotonation of $(C_5(CH_3)_5)Ir(P(CH_3)_3)(Si(CH_3)_3)(H)$ (Chapter 1). Possibly due to steric constraints, no reaction occurs

between this substrate and either n-BuLi, n-BuLi/pmdeta, t-BuLi, or t-BuLi/pmdeta. Upon reaction of the hydrido(silyl)iridium complex with n-BuLi/t-BuOK,[8] a yellow solid deposits from the reaction mixture; however, characterization and derivatization experiments lead to the conclusion that the solid is paramagnetic and <u>not</u> the desired salt $(C_5(CH_3)_5)Ir(P(CH_3)_3)(Si(CH_3)_3)K$.

In conclusion, we have observed the first examples of lithium-proton spin-spin coupling in two transition-metal lithium complexes. Attempts to understand the results on structural and chemical bases are continuing.

References.

(1) (a) Lindman, B.; Forsen, S. in "NMR and the Periodic Table", Harris, R. K. and Mann, B. E., Eds.; Academic Press: London, 1978, p. 166. (b) Wardell, J. L.; in "Comprehensive Organometallic Chemistry", Wilkinson, G.; Stone, F. G. A.; Abel, E. W., Eds.; Oxford: Pergamon Press, 1982, Section 2.4.2.3, and references therein. (c) Seebach, D.; Hassig, R.; Gabriel, J. Helv. Chim. Acta 1983, 66, 308.

(2) Colquhoun, I. J.; McFarlane, H. C. E.; McFarlane, W. J. Chem. Soc., Chem. Commun. 1982, 220.

(3) Hitchcock, P. B.; Lappert, M. F.; Power, P. P.; Smith, S. J. J. Chem. Soc., Chem. Commun. 1984, 1669.

(4) Brown T. L.; Ladd, J. A. J. Organomet. Chem., 1964, 2, 373. McGarrity, J. F.; Ogle, C. A. J. Am. Chem. Soc. 1985, 107, 1805.

(5) Oliver and coworkers suggest $J(^{7}Li-^{1}H) < 1$ Hz for ethyl-, propyl-, and trimethylsilyl lithium based on decoupling experiments. Oliver, J. A., personal communication.

(6) Lappert, M. F.; Engelhardt, L. M.; Raston, C. L.; White, A. H. J. Chem. Soc., Chem. Commun. 1982, 1323.

(7) Suzuki, M.; Kubo, R. Mol. Phys. 1963-64, 7(3), 201.

(8) Schlosser, M.; Hartmann, J. Angew. Chem., Intl. Ed. Engl. 1973, 12, 508.

This report was done with support from the Department of Energy. Any conclusions or opinions expressed in this report represent solely those of the author(s) and not necessarily those of The Regents of the University of California, the Lawrence Berkeley Laboratory or the Department of Energy.

Reference to a company or product name does not imply approval or recommendation of the product by the University of California or the U.S. Department of Energy to the exclusion of others that may be suitable.

LAWRENCE BERKELEY LABORATORY
TECHNICAL INFORMATION DEPARTMENT
UNIVERSITY OF CALIFORNIA
BERKELEY, CALIFORNIA 94720